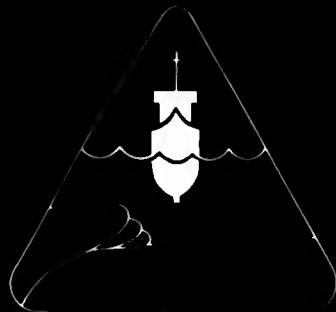


Geo-Marine Letters

An International Journal of Marine Geology

Editor-in-Chief: Arnold H. Bouma

Volume 8 Number 4 1988



Origin, Physical, and Mineralogical Nature of
Red Clays: The Pacific Ocean Basin as a Model



Springer International

Exploration of the Deep Continental Crust Through Drilling

A. Boden, Vällingby; K. G. Eriksson, Göteborg, Sweden (Eds.)

Deep Drilling in Crystalline Bedrock

Following two volumes present the results of the Third International Symposium on Observation of the Continental Crust Through Drilling held in Mora and Orsa, Sweden, September 7-10, 1987. The **first volume** summarizes the results of the Deep Gas Project in the Siljan impact structure, Sweden, including papers dealing with general aspects of astroblemes. It is of interest to all researchers working in the drilling industry and those interested in the problem of "deep gas".

The **second volume** reviews new and general information on geology, geophysics, rock mechanics, geochemistry, drilling techniques and drilling problems in very deep holes of the FRG, USA and the Soviet Union. The proceedings are invaluable for earth scientists as well as for exploiters of geoenergy and other natural resources in the crust.

Volume 2

Review of Deep Drilling Projects, Technology, Science and Prospects for the Future

1988. 283 figures. XI, 538 pages. Hard cover DM 168,-. ISBN 3-540-18996-3

Contents: Opening Remarks. - International Review of Deep Drilling Projects. - Technical Papers. - Scientific Papers. - Prospect for the Future of Deep Drilling.

Volume 1

The Deep Gas Drilling in the Siljan Impact Structure, Sweden, and Astroblemes

1988. 151 figures, 42 tables.

XIII, 364 pages. Hard cover DM 138,-. ISBN 3-540-18995-5

List of Contributors: A. A. AlDahan, K. Baker, A. J. Beswick, L. Bischoff, T. L. Brittenham, K. B. Broberg, P. E. Brown, J. R. Castano, B. Collini, T. Dahl-Jensen, D. Dyrelius, D. V. Ellis, T. Ericsson, F. Fish, T. Gold, J. A. Grau, A. W. Gorody, R. A. F. Grieve, G. Gustafson, M. M. Herron, A. W. A. Jeffrey, C. Juhlin, S. Jovanovic, I. R. Kaplan, D. Karlsson, P.-O. Karlsson, S. C. Komor, T. Laier, T. Lindbo, J. Lindgren, C. E. Lund, G. J. MacDonald, P. L. Moore, S. Morad, W. Oskierski, L. B. Pedersen, A. Raheim, K. Ramseyer, T. Rasmussen, G. W. Reed Jr., G. Rissler-Åkesson, R. G. Roberts, H. Sandstedt, J. S. Schweitzer, D. Stöfler, J. W. Valley, F. E. Wickman, B. Wiest, P. Zhang



Springer-Verlag Berlin
Heidelberg New York London
Paris Tokyo Hong Kong

Heidelberger Platz 3, D-1000 Berlin 33-175 Fifth Ave.,
New York, NY 10010, USA 28, Lurke Street, Bedford
MK40 3HU, England 26, rue des Carmes, F-75005 Paris
37-3, Hongo 3-chome, Bunkyo-ku, Tokyo 113, Japan
Citicorp Centre, Room 1603, 18 Whitfield Road,
Causeway Bay, Hong Kong

Forthcoming:
Proceedings of the Third International Symposium on Observation of the Continental Crust Through Drilling
Seeheim, Federal Republic of Germany

Springer

For the latest in
marine geology . . .

Geo-Marine Letters

Order Card

(For North American Subscribers Only)

Please enter my 1989 subscription to volume 9 (4 issues):

ISSN 0276-0460

Title No. 367

\$130.00 (Institutional rate)

\$71.00 (Personal rate)*

Check enclosed, made payable to Springer-Verlag New York Inc.

Charge my MasterCard VISA American Express

Card No _____ Exp. Date _____

Signature _____

Name _____

Address _____

City/State/Zip _____

*Personal rate is applicable only in North America and when paid by personal check or charge. Prices include postage and handling. Subscriptions are entered with prepayment only and are filled as issues are published.

Return orders to **Springer-Verlag New York Inc.**,
Journal Fulfillment Services
44 Hartz Way, Secaucus, NJ 07094, USA

 **Springer-Verlag New York Publishers**

Order Card

(For All Subscribers Outside North America)

Please order through your bookseller or: Springer Verlag
Heidelberger Platz
D 1000 Berlin 33, Germany

Geo-Marine Letters

ISSN 0276-0460

Title No. 367

Please enter my 1989 subscription to **Geo-Marine Letters**, Volume 9 (4 issues)
DM 293 plus postage and handling

Name _____

Address _____

Signature _____ Date _____

Please note: I realize that I may cancel this order within ten days by writing to Springer Verlag, Heidelberger Platz 3, D 1000, Berlin 33, whereby the postmark date will suffice as proof that the cancellation has been made within the deadline. I confirm my understanding of this with my second signature.

 **Springer-Verlag New York Publishers**

Does your library subscribe?

To recommend **Geo-Marine Letters** for acquisition, complete this card and submit it to your librarian or department head.

Attention: Librarian/Department Head

I have examined **Geo-Marine Letters** and would like to recommend the journal for acquisition.

Signature _____ Date _____

Name _____

Department _____

Geo-Marine Letters

ISSN 0276-0460 Title No. 367

1989, Volume 9 (4 issues) \$130.00

Sample copies available upon request

Write to **Springer-Verlag New York Inc.**

175 Fifth Avenue

New York, NY 10010, USA



NO POSTAGE
NECESSARY
IF MAILED
IN THE
UNITED STATES

BUSINESS REPLY MAIL

FIRST CLASS PERMIT NO. 119 SECAUCUS, N.J.

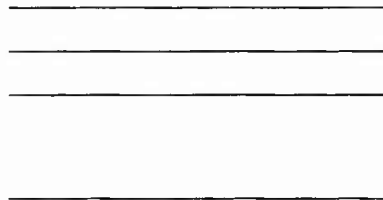
POSTAGE WILL BE PAID BY ADDRESSEE

Springer-Verlag New York Inc.

Journal Fulfillment Services

P. O. Box 2485

Secaucus, NJ 07094, USA



Geo-Marine Letters

An International Journal of Marine Geology

Editor-in-Chief:
A.H. Bouma,
Baton Rouge, Louisiana, USA

By publishing only short communications, **Geo-Marine Letters** allows researchers access to important findings very soon after they occur. Topics in this international journal include:

- marine geophysics, marine geochemistry, and marine geotechniques
- directly related dynamics, processes, stratigraphy
- environmental issues and economic applications

While covering the world's oceans, the journal also emphasizes the continental margin and concentrates on the interaction between pure and applied science. Its large paper size and high-quality paper permit excellent reproduction of seismic records, side-scan records, and photographs.

REPORT DOCUMENTATION PAGE				Form Approved OMB No. 0704-0188
1a. REPORT SECURITY CLASSIFICATION Unclassified		1b. RESTRICTIVE MARKINGS		
2a. SECURITY CLASSIFICATION AUTHORITY		3. DISTRIBUTION/AVAILABILITY OF REPORT Approved for public release; distribution unlimited		
2b. DECLASSIFICATION/DOWNGRADING SCHEDULE				
4. PERFORMING ORGANIZATION REPORT NUMBER(S) JA 360:083:88		5. MONITORING ORGANIZATION REPORT NUMBER(S)		
6a. NAME OF PERFORMING ORGANIZATION		6b. OFFICE SYMBOL (if applicable)	7a. NAME OF MONITORING ORGANIZATION Naval Ocean Research and Development Activity	
6c. ADDRESS (City, State, and ZIP Code)		7b. ADDRESS (City, State, and ZIP Code) Stennis Space Center, MS 39529-5004		
8a. NAME OF FUNDING/SPONSORING ORGANIZATION NORDA 6.1		8b. OFFICE SYMBOL (if applicable)	9. PROCUREMENT INSTRUMENT IDENTIFICATION NUMBER	
8c. ADDRESS (City, State, and ZIP Code) Stennis Space Center, MS 39529-5004		300	10. SOURCE OF FUNDING NUMBERS	
PROGRAM ELEMENT NO. 601153N	PROJECT NO. 03207	TASK NO. 330	WORK UNIT ACCESSION NO. 13609A	
11. TITLE (Include Security Classification) Origin, Physical, and Mineralogical Nature of Red Clays: The Pacific Ocean Basin as a Model				
12. PERSONAL AUTHORS William R. Bryant and Richard H. Bennett*				
13a. TYPE OF REPORT Journal Article	13b. TIME COVERED FROM _____ TO _____	14. DATE OF REPORT (Year, Month, Day) 1988		15. PAGE COUNT 60
16. SUPPLEMENTARY NOTATION				
17. COSATI CODES		18. SUBJECT TERMS (Continue on reverse if necessary and identify by block number) Microfabric; Sediment Transport; Clay; Shale; Red Clay; Geology; Clay		
FIELD	GROUP	SUB-GROUP		
19. ABSTRACT (Continue on reverse if necessary and identify by block number) Extensive examination of North Pacific Basin red clays by scanning and transmission electron microscopy reveals that the main constituent of the red clays are illite-rich argillaceous or shale clasts, quartz and authigenic smectite. The main source of the shale clasts and quartz are aeolian in nature and are derived mainly from African and Asian shales. Illite-rich argillaceous or shale clasts are identifiable by their morphology (high degree of roundness), selected area diffraction, and their unique fracture characteristics created by an ultra thin-sectioning process. This allows for the identification and differentiation of illite-rich shale clasts from other clays, including detrital illite, kaolinite, and smectite. Geotechnical examination of the red clays indicate that they are overconsolidated: the preconsolidation stress is in all cases larger than the vertical effective stress. The overconsolidation is attributed to the strong bonding of argillaceous or shale clasts, quartz and other particulate matter by x-ray amorphous and well developed crystalline sheets of authigenic smectite characterized by high surface activity.				
20. DISTRIBUTION/AVAILABILITY OF ABSTRACT <input checked="" type="checkbox"/> UNCLASSIFIED/UNLIMITED <input type="checkbox"/> SAME AS RPT. <input type="checkbox"/> DTIC USERS		21. ABSTRACT SECURITY CLASSIFICATION Unclassified		
22a. NAME OF RESPONSIBLE INDIVIDUAL Richard Bennett		22b. TELEPHONE (Include Area Code) 601-688-5460		22c. OFFICE SYMBOL 360

2

Special Issue

ORIGIN, PHYSICAL, AND MINERALOGICAL NATURE OF RED CLAYS: THE PACIFIC OCEAN BASIN AS A MODEL

DTIC
ELECTE
FEB 08 1988
S D
H

DISTRIBUTION STATEMENT A

Approved for public release
Distribution Unlimited

89 2 7 037

Geo-Marine Letters

An International Journal of Marine Geology

Editor-in-Chief

Arnold H. Bouma

Department of Geology and Geophysics, Louisiana State University, Baton Rouge, Louisiana 70803-4101, USA

Editorial Board

Neal E. Barnes

Missouri City, Texas, USA

David A. Cacchione

U.S. Geological Survey, Menlo Park, California, USA

Robert M. Carter

James Cook University of North Queensland, Townsville, Australia

James M. Coleman

Louisiana State University, Baton Rouge, Louisiana, USA

Joseph R. Curran

Scripps Institution of Oceanography, La Jolla, California, USA

Alberto G. de Figueiredo

Lab. Geologia Marinha, Universidade Federal Fluminense, Niteroi, Brazil

Larry J. Doyle

University of South Florida, St. Petersburg, Florida, USA

Robert W. Embrey

OSU Hatfield Marine Science Center, Newport, Oregon, USA

Burg W. Flemming

Institut für Meeresgeologie und Meeresbiologie

Wilhelmshaven, West Germany

Helios S. Gribidenko

Sakhalin Complex Scientific Research Institute, Yuzhno-Sakhalinsk, Sakhalin, USSR

Gary H. Greene

U.S. Geological Survey, Menlo Park, California, USA

Liu Guang-Ding

National Ocean Bureau, Beijing, People's Republic of China

Anthony D. Heathershaw

Admiralty Research Establishment, Dorset, UK

Hans-Rudi Katz

Lower Hutt, New Zealand

Keith A. Kvenvolden

U.S. Geological Survey, Menlo Park, California, USA

Andrés Maldonado

Instituto de Ciencias del Mar, C.S.I.C., Barcelona, Spain

Yossi Mart

National Oceanographic Institute, Haifa, Israel

S. Dijn Nio

Comparative Sedimentology Division, State University of Utrecht, Utrecht, The Netherlands

Harold D. Palmer

MRJ Inc., Oakton, Virginia, USA

David J. W. Piper

Bedford Institute of Oceanography, Dartmouth, Nova Scotia, Canada

David B. Prior

Louisiana State University, Baton Rouge, Louisiana, USA

Richard Rezak

Texas A & M University, College Station, Texas, USA

Nahum Schneidermann

Chevron Overseas Petroleum, Inc., San Ramon, California, USA

Roger M. Slatt

Arco Oil and Gas Co., Plano, Texas, USA

Daniel J. Stanley

Smithsonian Institution, Washington, D.C., USA

Donald L. Tiffin

Vancouver, British Columbia, Canada

Friedrich Werner

Geologisch-Palaeontologisches Institut, Universität Kiel, Kiel, West Germany

L. Donelson Wright

Virginia Institute of Marine Science, Gloucester Point, Virginia, USA



Springer International

Geo-Marine Letters

An International Journal of Marine Geology

Volume 8 Number 4 1988

Special Issue: Origin, Physical, and Mineralogical Nature of Red Clays: The Pacific Ocean Basin as a Model

Contents

Instructions to Authors vi

W. R. Bryant, R. H. Bennett

Origin, Physical, and Mineralogical Nature
of Red Clays: The Pacific Ocean Basin
as a Model

189

Volume Contents

Accession For	
NTIS	GRA&I <input checked="" type="checkbox"/>
DTIC TAB	<input type="checkbox"/>
Unannounced	<input type="checkbox"/>
Justification	
<i>Price \$39.00</i>	
By <i>per telecon</i>	
Distribution/	
Availability Codes	
Dist	Avail and/or Special
A-1	21

Sold by:
Springer Verlag
175 Fifth Avenue
New York, NY 10010
Price: \$39.00



Springer International



Geo-Marine Letters

An International Journal of Marine Geology

Subscription Information

Geo-Marine Letters is published quarterly. Volume 9 (4 issues) will appear in 1989.

North America: Institutional subscription price (per volume): \$130.00 including postage and handling. Subscriptions are entered with prepayment only. In North America a special rate is available for individual subscriptions for personal use only. Orders should be addressed to: Springer-Verlag New York Inc., Service Center Secaucus, 44 Hartz Way, Secaucus, NJ 07094, USA. Tel. (201)348-4033. Telex 12 59 94.

All Other Countries: Subscription rate (per volume): DM293.00 plus postage and handling. SAL delivery (surface airmail lifted) is mandatory for Japan, India, Australia and New Zealand. Customers should ask for the appropriate price list. Airmail delivery to all other countries is available upon request. Subscriptions can either be placed via a bookdealer or sent directly to: Springer-Verlag, Heidelberger Platz 3, D-1000 Berlin 33, W. Germany. Tel. (030)82 07 1, Telex 18 33 19.

Back Volumes and Microfilm Editions: Prices for back volumes are available on request. Microform editions are available from: University Microfilms International, 300 N. Zeeb Rd., Ann Arbor, MI 48106, USA.

Changes of Address: Allow six weeks for all changes to become effective. All communications should include both old and new addresses (with zip codes) and should be accompanied by a mailing label from a recent issue.

Copyright Information

Submission of a manuscript implies: that the work described has not been published before (except in the form of an abstract or as part of a published lecture, review, or thesis); that it is not under consideration for publication elsewhere; that its publication has been approved by all coauthors, if any, as well as by the responsible authorities at the institute where the work has been carried out; that, if and when the manuscript is accepted for publication, the authors agree to automatic transfer of the copyright to the publisher; and that the manuscript will not be published elsewhere in any language without the consent of the copyright holders.

All articles published in this journal are protected by copyright, which covers the exclusive rights to reproduce and distribute the article (e.g., as offprints), as well as all

translation rights. No material published in this journal may be reproduced photographically or stored on microfilm, in electronic data bases, video disks, etc., without first obtaining written permission from the publisher.

The use of general descriptive names, trade names, trademarks, etc., in this publication, even if not specifically identified, does not imply that these names are not protected by the relevant laws and regulations.

While the advice and information in this journal is believed to be true and accurate at the date of its going to press, neither the authors, the editors, nor the publisher can accept any legal responsibility for any errors or omissions that may be made. The publisher makes no warranty, express or implied, with respect to the material contained herein. Springer-Verlag publishes advertisements in this journal in reliance upon the responsibility of the advertiser to comply with all legal requirements relating to the marketing and sale of products or services advertised. Springer-Verlag and the editors are not responsible for claims made in the advertisements published in the journal. The appearance of advertisements in Springer-Verlag publications does not constitute endorsement, implied or intended, of the product advertised or the claims made for it by the advertiser.

Photocopies may be made for personal or in-house use beyond the limitations stipulated under Section 107 or 108 of U.S. Copyright Law, provided a fee is paid. This fee is US \$0.20 per page. All fees should be paid to the Copyright Clearance Center, Inc., 27 Congress Street, Salem, MA 01970, USA, stating the ISSN 0276-0460, the volume, and the first and last page numbers of each article copied. The copyright owner's consent does not include copying for general distribution, promotion, new works, or resale. In these cases, specific written permission must first be obtained from the publisher.

Office of Publication

Springer-Verlag New York Inc., 175 Fifth Avenue, New York, NY 10010, USA. Tel. (212)460-1500, Telex 23 22 35

Responsible for Advertisements

Springer-Verlag New York Inc., 175 Fifth Avenue, New York, NY 10010, USA.

Attention: Dieter Finkelmeier. Tel. (212)460-1612.
Advertising production: Marina Gonatas. Tel. (212)460-1627.

Springer-Verlag, Heidelberger Platz 3, D-1000 Berlin 33, W. Germany. Tel. (030)82 07 1, Telex 18 54 11

Aims and Scope

Geo-Marine Letters is an international journal for the publication of short, original studies and reviews dealing with all aspects of marine geology, marine geophysics, marine chemistry, marine geotechnique, and directly related dynamics, processes, stratigraphy, environmental problems,

techniques, and applications. The editorial board wishes to emphasize the continental margin in the broadest sense where the valuable interaction between pure and applied science can be demonstrated. A high level of scientific quality is ensured by using a peer review system. The quarterly publication, together with the brevity of each paper, assure rapid distribution of a large variety of topics in each volume.

Forthcoming Papers

M. H. Caralp

Abundance of *Bulimina exilis* and *Melonis barleeanum*: Relationship to the Quality of Marine Organic Matter

D.-D. Sheu, C. -Y. Huang

Carbonate and Organic Carbon
Sedimentation on the Continental Margin
off Southeastern Taiwan

T. L. Holcombe, C. G. Fisher,

F. A. Bowles

Gravity-Flow Deposits from the St. Croix
Ridge: Depositional History

D. A. V. Stow, J. R. Cochran

The Bengal Fan: Some Preliminary
Results from ODP Drilling

F. J. Hein, J. P. M. Syvitski

Sea Floor Gouges and Pits in Deep
Fjords, Baffin Island: Possible Mammalian
Feeding Traces

G. Evans, H. Erten, N. Alavi,

H. R. Von Gunten, M. Ergin
Superficial Deep-Water Sediments of the
Eastern Marmara Basin

K. M. Scanlon, H. J. Knebel

Pockmarks in the Floor of Penobscot
Bay, Maine

A. Cramp, C. J. Vitaliano, M. B. Collins

Identification and Dispersion of the
Campanian Ash Layer (Y-5) in the
Sediments of the Eastern Mediterranean

Instructions to Authors*

1. *Submission:* Three copies of the manuscript should be submitted to Dr. Arnold H. Bouma, Editor-in-Chief, Department of Geology and Geophysics, Louisiana State University, Baton Rouge, LA 70803-4011, USA. Telephone (504)388-6186. All manuscripts should be in English, neatly typed, double-spaced (including abstracts and references), and paginated.

2. *Length:* including abstract, illustrations, and references, should not exceed the equivalent of eight printed pages. Each printed page is equivalent to approximately 3 double-spaced manuscript pages; however, the space required for illustrations and tables must be subtracted.

3. *Abstracts:* should not exceed 100 words in which the author should briefly state the essence of the paper in an informative rather than a descriptive manner. The abstract should not be a listing of contents.

4. *Illustrations:* All line drawings and halftones (photographs, micrographs, shaded drawings, seismic sections, sonographs) are considered illustrations. All drawings and halftones should have a border of at least 1 in. (2¹/₂ cm) width for protection and for handling instructions. The width of each illustration should be either one column (8.1 cm or 3¹/₈ in.) or two columns (17 cm or 6⁷/₈ in.), and the maximum length, including the legend, should not be more than 23.2 cm (9¹/₁₆ in.). Illustrative material should be provided in final size.

Halftones should be clear and sharp and display good contrast. Halftones and photographs of drawings should be submitted on glossy paper. The author(s) and figure number should be shown on the back of each illustration. Use a stick-on label or taped label rather than a felt-tip pen to avoid imprint or tonal change on the front side.

5. *Tables:* If tables are necessary, they should be typed double-spaced using minimum space and submitted separately on white paper. Use either a Prestige Elite or a Letter Gothic typeface and a black carbon ribbon.

6. *Legends:* All legends (including table captions) should be typed double-spaced on separate sheets. Do not include them in the text.

7. *Footnotes* are discouraged.

8. *Acknowledgments* will appear immediately preceding the references.

9. *Dimensions:* The metric system should be used whenever possible in the text, legends, and all illustrations. The metric conversion should be given in parentheses if the English system is used for other than standard expression. Water depths may be given in fathoms.

10. *Format:* Unless otherwise indicated, style and manuscript preparation should follow the sixth edition of "Suggestions to Authors" published in 1978 by the U.S. Geological Survey. Only standard abbreviations are acceptable as recommended in the U.S.G.S. publication.

11. *Manuscript order:* Title, author(s), affiliation(s), address, abstract, body of text divided into sections as needed, acknowledgments, and references.

12. *References in the text* should give only the author's name and the year of publication. Multiple authors will be listed as (Smith and Jones 1980) or (Smith and others 1984). Please avoid the use of *et al.* If the reference is structurally part of a sentence, use parentheses around the date only; for example, "Jones (1981) believes that . . ." Written communication, personal communication, or unpublished data should be included in the text (including year), but should not appear again in the reference list. Authors may refer to published articles, reports, maps, and manuscripts accepted for publication, but not to papers in preparation or review.

13. *References* should be listed in alphabetical order. Initials for multiple-authored papers follow each last name. Punctuation is minimal. All journal names should be spelled out in full; do not use prepositions. Examples are:

Bouma AH, Pluenneke JL (1975) Structural and textural characteristics of debrites from the Philippine Sea. In: Karig DE, Ingle JC Jr, and others. *Initial Reports Deep Sea Drilling Project 31*. U.S. Government Printing Office, Washington, D.C., pp 497-505

Coleman JM, Prior DB, Adams Jr CE (1981) Erosional furrows on continental shelf edge, Mississippi Delta region. *Geo-Marine Letters* 1:11-15

Kuenen PH (1964) Deep-sea sands and ancient turbidites. In: Bouma AH, Brouwer A (eds) *Developments in Sedimentology* 3. Elsevier, Amsterdam, pp 3-33

Lacombe H, Tchernia P (1972) Caractères hydrologiques et circulation des eaux en Méditerranée. In: Stanley DJ (ed) *The Mediterranean Sea—A Natural Sedimentation Laboratory*. Dowden, Hutchinson & Ross, Stroudsburg, PA, pp 25-36

Moore DG (1961) Submarine slumps. *Journal Sedimentary Petrology* 31:342-357

Moore DG (1969) Reflection profiling studies of the California Continental Borderland: Structure and Quaternary basins. Geological Society America Special Paper 109, 142 pp

Shepard FP, Dill RF (1966) Submarine Canyons and Sea Valleys. Rand McNally, Chicago, 381 pp

Diacritical or foreign punctuation marks are the responsibility of the author(s). Please provide names and initials for all authors.

14. *Charges:* There are no page charges for articles published in *Geo-Marine Letters*. Oversize illustrations, color photographs, and any other nonstandard figures will be published only with the approval of the Editor-in-Chief and the publisher, and only if the extra expenses are borne by the author.

15. *Editorial procedure:* Two copies of each manuscript will be reviewed for scientific content and coherence. The third copy will be examined for length and consistency by the Editor-in-Chief. All three copies will be returned to the author unless no changes are required. The author should resubmit to the Editor-in-Chief one original and two copies of the revised and retypeset manuscript plus the three reviewed copies. Final copy editing, typesetting, and printing will be handled by the publisher. Page proofs will be mailed to the author and should be returned to:

Springer-Verlag New York Inc.
Journal Production/Geo-Marine Letters
175 Fifth Avenue
New York, New York 10010, USA

within forty-eight (48) hours of receipt. Changes other than those of typographical errors will not be accepted.

16. *Correspondence:* Unless other arrangements are made during the initial submission of the manuscript, correspondence and mailing of manuscripts will be directed to the senior author.

17. *Reprints (offprints):* Fifty offprints without covers will be supplied free of charge to the senior author. Additional offprints can be ordered from the publisher at the time proofs are returned, using the offprint order form provided with the page proofs. Reprints ordered after an issue has gone to press can be produced only with a minimum order of 300 copies. The cost of such reprints is substantially higher than offprints.

18. *Published manuscripts:* All manuscript materials will normally be destroyed after publication. Illustrations can be returned only if a request is made at the time that manuscripts are submitted for publication.

*Please note several important changes in format, especially with regard to reference style.

Origin, Physical, and Mineralogical Nature of Red Clays: The Pacific Ocean Basin as a Model

William R. Bryant¹ and Richard H. Bennett²

¹Department of Oceanography, Texas A&M University, College Station, Texas 77843, USA

²Seafloor Geosciences Division, Naval Ocean Research and Development Activity, John C. Stennis Space Center, Mississippi 39529, USA

Abstract

Extensive examination of North Pacific Basin red clays by scanning and transmission electron microscopy reveals that the mean constituent of the red clays are illite-rich argillaceous or shale clasts, quartz and authigenic smectite. The main source of the shale clasts and quartz are aeolian in nature and are derived mainly from African and Asian shales. Illite-rich argillaceous or shale clasts are identifiable by their morphology (high degree of roundness), selected area diffraction, and their unique fracture characteristics created by an ultra thin-sectioning process. This allows for the identification and differentiation of illite-rich shale clasts from other clays, including detrital illite, kaolinite, and smectite. Geotechnical examination of the red clays indicate that they are overconsolidated: the preconsolidation stress is in all cases larger than the vertical effective stress. The overconsolidation is attributed to the strong bonding of argillaceous or shale clasts, quartz and other particulate matter by x-ray amorphous and well developed crystalline sheets of authigenic smectite characterized by high surface activity.

Introduction

Pelagic sediments, especially red clays, have been an enigma from the dawn of geological ocean exploration. Red clays were discovered during the Challenger Expedition (1872–1875) when scientists found that deep ocean sediments consisted of either calcareous or siliceous biogenic ooze and extremely fine-grained material consisting of authigenic minerals, volcanogenic clastics, and biogenous particles. These two types of sediments, biogenic and inorganic, were both classified as pelagic sediments (Arrhenius 1963, Bramlette 1958). Despite the fact that red clays cover approximately 31 percent of the world's ocean basins or

about 20 percent of the total surface of the earth, very little knowledge exists concerning the origin, physical nature, the sources of the major mineralogical components, and the consolidation history of these soft clays of antiquity. The mystery of red clays has been complicated over the years by the elusive definitions of pelagic sediments as well as the direct misuse of red clays as a "type deposit" for pelagic sediments.

The Glossary of Oceanographic Terms (1966) defined pelagic-abyssal sediments as "Deep sea sediments that are free of terrestrial material except for a small portion of very fine clay." The first edition of the Glossary of Geology (Gray and McAfee 1972) defined pelagic sediments as "Deep-sea sediments without terrigenous material; they are either inorganic red clay or organic ooze" but the second edition defined red clays as "A pelagic deposit that is fine-grained and bright to reddish brown or chocolate-colored, formed by the slow accumulation of material a long distance from the continents and at depths generally greater than 3500 meters. It contains relatively large proportions of windblown particles, meteoric and volcanic dust, pumice, shark teeth, whale carbones, manganese nodules, and debris rafted by ice. The contents of CaCO_3 ranges from 0 to 30%."

Sverdrup and others (1942) classified red clays as inorganic pelagic deposits and clearly differentiated them from terrigenous deposits. These authors pointed out that the earlier work of Revelle (1936) and Mehl (1939) demonstrated the presence of clay minerals in seabed deposits and that "From this evidence it would appear that at least part of the clay fractions

are not formed on the sea bottom but represent the products of subaerial weathering carried into the sea with other terrigenous debris" (Sverdrup and others 1942). It also is interesting to note these author's foresight in regard to the possible significance of wind-blown source material to the sea in the following passage: "Although the present evidence does not preclude the formation of some clay minerals from volcanic debris on the sea bottom, there is considerable evidence which indicates that much of the clay fraction found in marine deposits, both nearshore and pelagic, is of terrigenous origin. The detection of this finely divided material in the water and the determination of its distribution in the ocean waters will be the conclusive argument in deciding upon the source of the red clay and the nonorganic fraction of the pelagic oozes."

In an extensive article on deep-sea sediments by Emiliani and Milliman (1966), pelagic sedimentation was defined as deposition consisting almost entirely of inorganic and organic particles settling from the overlying water column in contrast to deep-sea sedimentation which simply referred to deposition of sediments in the deep sea which may include: (1) abyssal sedimentation by processes such as turbidity currents, and/or (2) pelagic depositional processes. Pelagic clays were classified as either alloigenic clays (derived from winds and rivers) or authigenic clays (derived from *in situ* alteration of preexisting material), however, sources and origins were unknown (Emiliani and Milliman 1966). These researchers defined red clay as a pelagic sediment as follows: "Red clays consist mainly of a mixture of clay minerals and other land-derived resistates (some 20 different mineral species), plus volcanic ash, cosmic spherules, and up to 30% of carbonate particles. The red clay of the South Pacific consists mainly of authigenic clay minerals apparently produced by the alteration *in situ* of volcanic products" (Emiliani and Milliman 1966). Berger (1978) suggested that the main constituents of pelagic sediments are of biogenic, terrigenous, volcanogenic, or cosmogenic origin, and from this definition a pelagic sediment is truly universal, especially in regard to its particulate content, geochemistry, and mineralogy.

Over the years, studies related to pelagic sediments have been associated mostly with the biogenous component. The terrigenous portion of pelagic sediments consisting of clay minerals, fine quartz, and feldspar are usually diluted by large amounts of biogenous material generated in shallower ocean depths (less than 3500 meters). Thus a difficulty in properly defining red clays and their relationship with pelagic sediments arises from a general misconception that pelagic processes are the causal antecedents of red clays. Further confusion in defining pelagic sediments results from

the misuse of red clays as a "type deposit" and the misunderstanding of the predominant processes and of the origin of the main constituents of red clays; e.g. quartz, illite, and smectite that make up approximately 80 percent of the particulates of the sediment (Bennett and others 1985a, Bryant and others 1985). Despite the long convoluted history of definitions of pelagic sediments and red clays and their interrelationship, a definitive link between terrigenous material, windblown particulates and dust, and the origin of red clays has not been clearly established until recently (Bennett and others 1985a, Bryant and others 1985).

Research Objectives

Sediment has been described as a particulate multiphase system; the particulate phase refers to the sediment (soil) particles or solids and multiphase refers to a system consisting of the solids and a fluid phase (Lambe and Whitman 1969). More precisely however, deep-sea sediment can be described as an organo-particulate multiphase system. When sediments are partially saturated with interstitial water such as with many shallow water marine sediments, they can be described as an organo-gas particulate multiphase system. The organic phase is the remains and by-products of biological activity, animal and plant debris. The surficial sediments often contain living organisms, animals and plants, ranging from micro- to megascopic in size. The organic phase can impart a significant influence on the physical and biochemical properties of marine sediment (Bennett and Nelsen 1983, Bennett and others 1985b).

This study focuses on the particulate phase of red clays and consists of three basic research objectives. The first objective was to examine in detail the fundamental nature of the solid particles in terms of their mineralogy, morphology, and microstructure (fabric and physico-chemistry). The microfabric refers to the orientation and spatial distribution and arrangements of the particles and the particle-to-particle relationships such as the types of particle contacts and associations (Bennett and others 1977). The physico-chemistry pertains to the combined influence and effects of the physical and electrochemical forces acting among the solid particles within a sedimentary mass or within a group of particles as in the case of flocculated particulates in suspension (Bennett and Hulbert 1986). In either case, sediments or suspensions, the particles are under the influence of both gravity and electrochemical forces and interactions. The fabric and physico-chemistry of fine-grained geological materials are the fundamental "building blocks" of sediments and rocks. Thus the microstructure is the

fundamental property that determines the ultimate, or basic, physical and mechanical properties of a sedimentary mass or suspension and its response to static and dynamic forces (Bennett and Hulbert 1986, Bennett and others 1979).

The second objective was to demonstrate clearly the genetic link between the major mineralogical components of red clay deposits and aeolian material transported from continental sources using the Pacific Basin as a model. Despite the numerous studies of atmospheric aerosols and in particular windblown particulates, the significance of the direct link of these materials with deep-sea deposits has not been adequately accomplished. The first and second objectives, (the microfabric, mineralogy, and particle morphology, and the genetic link of numerous red clays to aeolian transport processes were studied in detail) were accomplished using techniques of Transmission and Scanning Electron Microscopy (TEM and SEM).

The third objective was to evaluate the consolidation (compaction) properties and physical behavior of a red clay, the Pacific Ocean Basin deep-sea sediment as a model. The purpose was to characterize the physical and mechanical properties of a red clay deposit and to geotechnically evaluate the significance of burial diagenesis and consolidation in terms of long geological periods of slow and continuous deep-sea sedimentation processes. Clearly the microstructure plays an important role in determining the response of the deposit to quasistatic, but continuously increasing, overburden loads throughout geologic time. The microstructure largely controls important properties of fine-grained clays including sediment isotropy/anisotropy, permeability, porosity, and stress-strain behavior each of which is ultimately tied to the time-dependent consolidation processes.

Aeolian Transport to the Oceans: Background

The importance of aeolian transport to the oceans was recognized by Darwin (1846) while sailing off the Cape Verde Islands in 1833 when he observed dust coming from the coast of Africa. Darwin's observations on the aeolian transport process were explained in the statement, "Finally I may remark that the circumstances of such quantities of dust being periodically blown, year after year, over so immense an area in the Atlantic Ocean is interesting, as shown by how apparently inefficient a cause a widely expanded deposit may be in the process of formation."

A century later, Grim and others (1949) recognized the presence of quartz and the general clay mineral constituents in marine sediments off the California coast. Rex and Goldberg (1958) studied the quartz content of pelagic clays from the Pacific Ocean and

showed a marked latitudinal dependence with a maximum around 30°N. Their evidence indicated that the quartz was mainly transported to the oceans through the atmosphere. The distribution appeared to be related to latitude as determined from the values of atmospheric wind fluxes and exposed land areas.

Heath (1969) found that the northern equatorial Quaternary deposits in the Pacific Ocean are dominated by windblown continental debris rich in quartz and illite derived from northern hemisphere periglacial loess deposits. He attributed the nonbiogenic mineral phase of the modern equatorial Pacific deep-sea sediments to three principle sources: "continental," "oceanic," and "island arc." Each source contributed different minerals as follows: illite, quartz, and alkali feldspar (continental); smectite in early and middle Tertiary sediments (oceanic); and chlorite and pyroxene (island arc).

A study of atmospheric dust from the snowfields of Antarctica and Greenland showed that 25 to 75 percent of the detrital material of the South and North Pacific sediments were from atmospheric fallout with the predominant constituents quartz and illite (Windom 1969). During the late 1960s, data were accumulating from not only deep-sea sediment studies, but also atmospheric aerosol investigations that provided mounting evidence that ocean basin deposits distant from continental land masses were indeed composed of significant contributions of terrigenous particulates. This "picture" began to unfold as evidenced by sediment distribution maps of the world ocean basins (Rateev and others 1969). Noteworthy is the observation that the highest concentrations of illite in the less than 2 μm size fractions coincide with the occurrence of red clays in the North Pacific, North Atlantic, and South Indian Oceans (Fig. 1). Potassium-argon absolute age determinations of the illite minerals from the Antarctic regions proved to be considerably older (100 to 500 million years) than the age of the ocean basin sedimentary deposits.

Later studies supported the general conclusions that fallout from windblown dust was a significant factor in the depositional processes and accumulation of deep-sea sediments (Hein and others 1979, Janecek and Rea 1982, Leinen 1985, Windom 1976). The identification of specific detrital particles versus authigenic minerals, however, had not been accomplished. This was clearly borne out by the work of Windom (1976) in his conclusion that continentally-derived montmorillonite was analytically indistinguishable from its authigenic counterpart which originates from sub-marine weathering processes.

The lack of a conclusive, identifiable, link between deep-sea minerals, specifically the detrital components of red clay, and aeolian particulates was due to

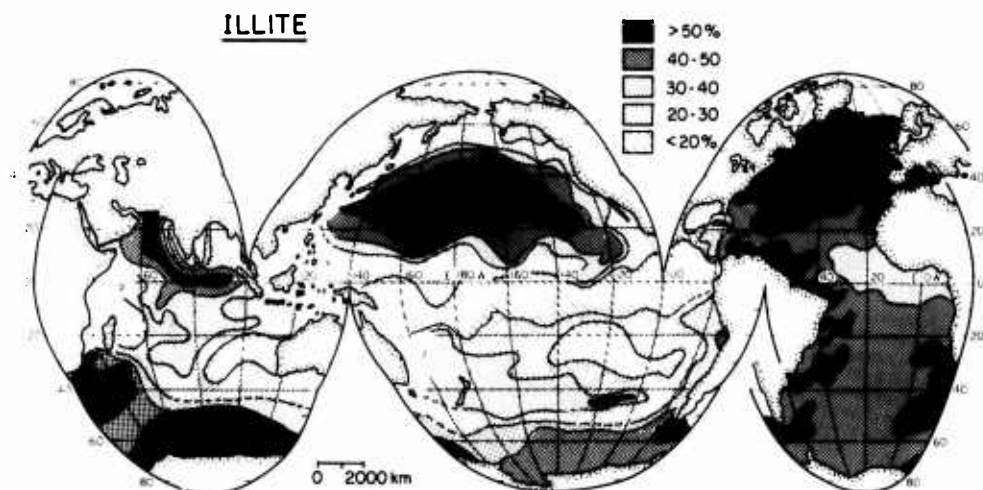


Figure 1. Illite concentration in the $<2 \mu\text{m}$ size fraction of sediments in the World Ocean. Modified from Windom (1976).

several factors. Prospero attributed a lack of interest in aeolian transport of sediments to the oceans to the fact that transport processes are not amenable to study; the winds are by their very nature ephemeral and elusive (Prospero 1981). Not only are the transport mechanisms ephemeral and elusive, but also the sediments likewise are. Volcanic material converts to the mineral smectite and other authigenic minerals *in situ* and could not be identified as to their origin on the basis of established analytical techniques. Essentially the only indicators of a terrigenous source was possible with quartz, but even quartz, once assumed to be only detrital in origin, has an authigenic counterpart (Aoyasi and Kazama 1980, Calvert 1977, Riech and Von Rad 1979, Von Rad and others 1978). Most diagenetic quartz is easily identified as beds or nodules of chert or porcellanite (Lener and McCave 1983).

The one fact that has been established from the various studies of ocean basin sediments, and more specifically, the Pacific Ocean Basin, is that quartz particles found in the red clay are of aeolian origin. The clay minerals illite and kaolinite also are considered to be fallout products of wind transport processes. This concept has been inferred by the association of the clay minerals with the quartz. The clay mineral smectite in the red clays, however, has been associated with authigenic processes and could not be differentiated from terrigenous smectite. Until recently, no other character or techniques except age could be used as "signatures" or "fingerprints" to identify the origin of the clay minerals associated with red clays (Bennett and others 1985, Bryant and others 1985).

Red Clays of the Northwest Pacific Basin: A Model

The physical nature (mineralogical, morphological, and microfabric) origin, and consolidation (compaction) characteristics of red clay recovered by high quality coring in the Northwest Pacific Ocean was studied in detail and used as a model for other submarine sediment deposits. Studies of sediments from other geographic locations and geological environments were incorporated in this investigation where appropriate. A dedicated core was recovered from Hole 576A (Initial Reports Deep Sea Drilling Project 86) for detailed geotechnical investigations and the data generated from a study of this core was used extensively in this article. The rationale for collecting cores at Hole 576A was to analyze a deep-sea deposit representative of a very slowly-deposited clay, far removed from continental land masses in water depths of approximately 6000 m, and free of calcium carbonate and associated biogenic components.

The red clay deposit was to be a standard for comparison with all other marine sediment geotechnical investigations. The North Pacific red clay was chosen as a standard under the assumption that the deposit would represent a normally consolidated clay section occurring in the world's oceans. Sedimentation progressed very slowly over geological time by particle-to-particle deposition in a stable, low energy environment where erosion and processes of mass movement and instability were absent. A total of 65.9 m of core was recovered at Hole 576A (Fig. 2). The sediments

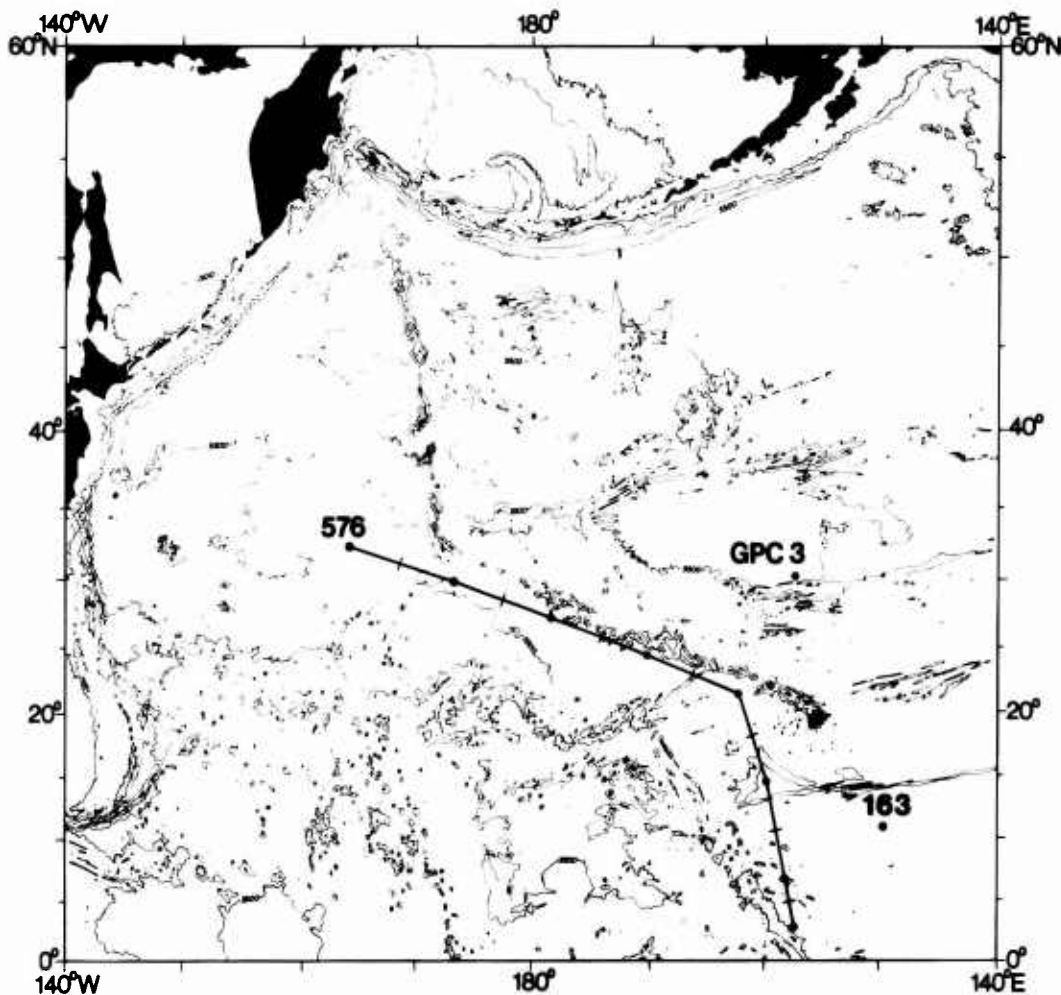


Figure 2. Location of Sites 576, 163 and GPC-3. The line emanating from Site 576 is the backtrack path along which the site traveled during seafloor spreading. The points along the path mark 5 m.y. intervals. This path was determined using methods developed by Jarrard and Clague (1977) and by examination of the path and age of the Hawaiian-Emperor seamounts (Clague and Jarrard 1973).

recovered represented a depositional history extending from the present to Cretaceous time, a period greater than 70 million years. Results from DSDP Hole 576A sediments represents the most complete geotechnical data set ever compiled for a continuous depositional sequence spanning this time period. Geotechnical analyses include index property and sediment characterization, consolidation, permeability, and triaxial testing. Excellent agreement exists between data generated in the multidisciplinary and multilaboratory effort (Initial Reports Deep Sea Drilling Project 86).

Three well-defined units that conform with major

lithological divisions were delineated on the basis of sediment characteristics and index properties. Data within the red clay subunit IA appear inconsistent with accepted geotechnical relationships such as water content, plasticity, and grain size increases over similar intervals; an atypical relationship. These unusual relationships were attributed to the presence of silt-size bonded clay aggregates (Initial Reports Deep Sea Drilling 86). In subunit IB the properties become more uniform and show a marked increase in x-ray amorphous material below 28 m subbottom. A dramatic change in the geotechnical behavior of the sediments from Hole 576A occurs in unit II which corresponds

to the presence of calcareous oozes. A large portion of the analyses in this article addresses issues relating to observed inconsistent geotechnical relationships. This investigation has placed emphasis on the issues concerning the consolidation history and physical characteristics, microfabric, and origin of red clays from the Northwest and Central Pacific Ocean Basin.

Sediment Sampling

Hole 576A sediment (Fig. 2) was recovered from a position of $32^{\circ} 21.38'N$, $164^{\circ} 16.52'E$ and a water depth of 6218 meters. Seven cores penetrated 65.7 m of sediments. The cores were recovered by use of a high quality hydraulic piston corer, stored vertically after recovery, and shipped to shore-based laboratories for geotechnical studies. Companion cores taken at Holes 576 and 576B were used to determine the lithology and age of the sediments at Hole 576A.

Lithologic Description

The sediments at Holes 576 and 576B (Fig. 3) consisted of three lithologic units. Subunit IA (0 to 28 m, contact is gradational over several meters) is a yellowish brown to brown pelagic clay of Pliocene and Quaternary age (based on paleomagnetics). The sedimentation rate decreases from 10 m/million years (m.y.) in the Brunhes Epoch to less than 3 m/m.y. at the base of the Matuyama Epoch. Based on earlier studies and the abundance of silt-sized quartz, the unit is largely of aeolian origin (Initial Report Deep Sea Drilling Project 86).

Subunit IB (28 to 55 m) is a dark brown "slick" pelagic clay, zeolithic in part. This material is extremely homogenous, very fine-grained, and manganese rich. Based on continuous deposition, the average sedimentation rate decreased from about 1 m/m.y. during the late Neogene to about 0.35 m/m.y. at about 40 m.y. ago, before increasing to 0.6 m/m.y. (uncorrected for compaction) during the late Cretaceous. By analogy with similar North and South Pacific pelagic clays, it is inferred that this subunit contains a large authigenic component.

Lithologic Unit II (55 to 65 m subbottom) is an interbedded dark brown pelagic clay similar to Subunit IB and it is interbedded with a pale brown nanofossil ooze of Campanian age. At the base of the unit, the clay layers also include pink bands and motles. Several of the carbonate layers are graded and have sharp erosional basal contacts; these are turbidites. Other layers may be pelagic. The absence of microfossils younger than Campanian age and the results of earlier DSDP drilling in this region suggest

that the components of the carbonate and clay layers are essentially contemporaneous. Whether the carbonate reflects enhanced biogenic deposition due to higher productivity (at the lower latitude of site 70 m.y. ago) or to fluctuations in the carbonate compensation depth (CCD) is unclear (Heath and Burckle 1985).

Additional samples were obtained from Site GPC-3 (Fig. 2) at $30^{\circ} 105'N$ and $158^{\circ}W$ in 6100 m of water. It is approximately 3500 km due east of Hole 576A. The sediments at Site GPC-3 consisted of 26 meters of material similar to that recovered at Hole 576 and covered the same time interval from the Holocene to the Upper Cretaceous. Samples at Site GPC-3 were recovered using the Giant Piston Corer and various box cores. At both sites the sediments cored rested upon oceanic crustal basalts.

Mineralogical Characteristics

Clays

Quantitative clay mineralogy results on sediments obtained with piston cores close to Holes 576 and 576A are consistent with known clay mineral distribution patterns in the North Pacific (Griffin and others 1968, Heath and Pisias 1979, Leinen and King 1985). Leinen and King reported data from samples located at the Brunhes/Matuyama boundary (ranging in subbottom depth from 3.84 to 5.02 m) within 10^4 km² area around Hole 576 and found virtually no variation in the <20 μ m opal-free mineral assemblage. Illite is the dominant clay mineral (\approx 39 percent) with lesser amounts of chlorite (\approx 19 percent) and minor amounts of kaolinite and smectite (\approx 10 percent). Detailed downcore clay mineral analysis on a piston core located approximately 10 km from Hole 576 shows a slight increase in smectite (\approx 5–6 percent to \approx 12–15 percent) and decrease in chlorite (\approx 38 percent to \approx 20–25 percent) with depth to 12 m subbottom. Leinen and King (1985) indicate these subtle changes suggest either a change in the weathering regime in the continental aeolian source areas or a change in the dominant wind patterns that transport the aerosol minerals to the Northwest Pacific.

Preliminary clay mineral analysis on Hole 576A sediments have emphasized sediments in subunit IB below 30 m (Table 1, M. Leinen, personal communication 1985). Results from one near-surface sample obtained within subunit IA are very similar to the piston core mineralogical results summarized above, except for a slightly higher illite component (50 percent as opposed to 39 percent) and a lower kaolinite component (trace amounts as opposed to 10 percent). Using a talc internal standard, clay mineral results from

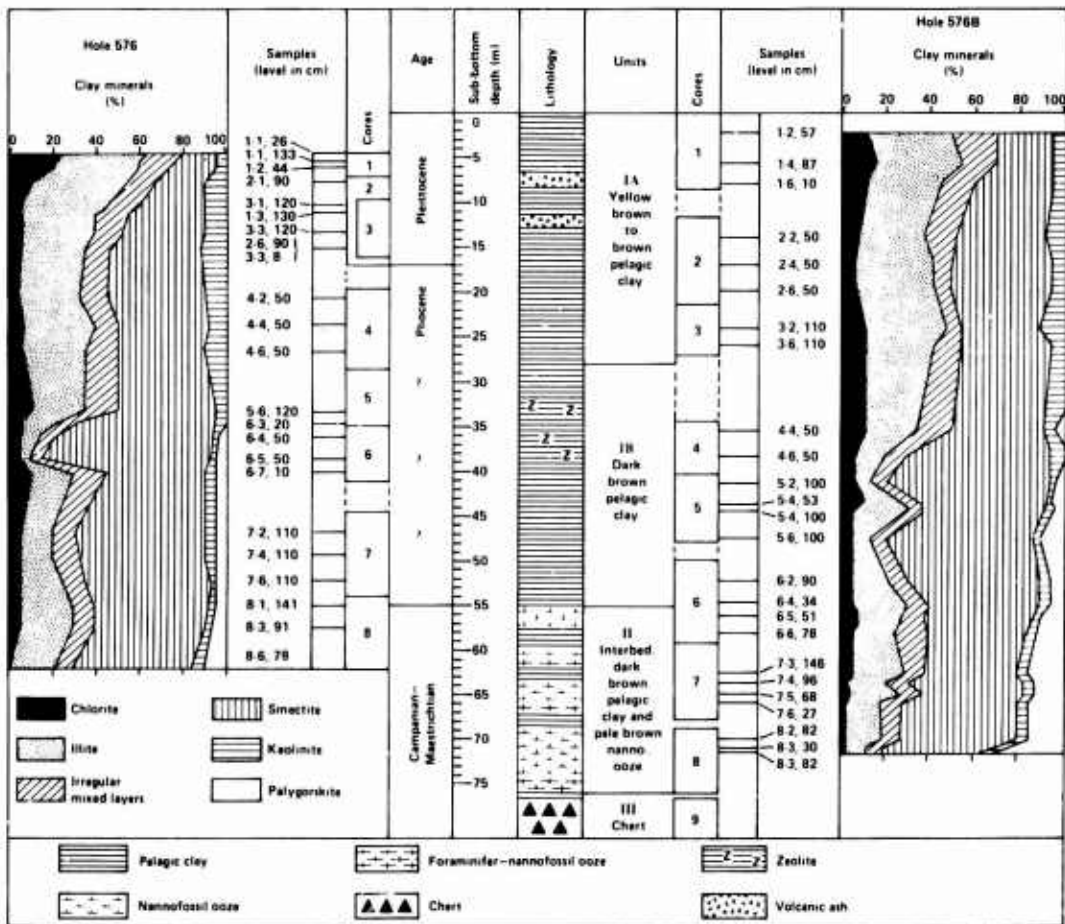


Figure 3. Lithology and clay mineralogy of Holes 576 and 576B plotted versus depth below the seafloor (Lenotre 1985).

subunit IB indicate that the single most important factor influencing the mineralogy is the pronounced downhole increase in the ratio of amorphous to crystalline material. This increase is particularly evident below 45 m subbottom (Table 1) and is attributed in part to a probable increase in the amount of iron oxides and manganese oxides present. The majority of x-ray amorphous material is a very fine-grained clay with insufficient crystal size to produce good diffractions. Another possible cause contributing to this marked increase in x-ray amorphous material is the effects of grain size on the standardization procedure (M. Leinen, personal communication 1985).

Mineralogical analyses of Hole 576A sediments used for consolidation testing at Texas A&M University reveal a downhole increase in the relative percentage of smectite compared to illite in the crystalline clay-size

fraction to a depth of 45 m subbottom. However, the much larger increase in the amount of x-ray amorphous material present in the clay-size fraction (up to 80 percent; Table 1) over the same intervals would be the controlling mineralogical factor affecting the geotechnical aspects and consolidation behavior of Hole 576A sediments.

Schoonmaker and others (1985), using material from Hole 576, determined that the average illite content in the upper 29 meters of the hole was 35.5 percent. The proportion of illite/smectite mixed layer present was 52 percent and the percent illite interlayers in the mixed layer averaged 37 percent. In general, the amount of total illite in the upper portions of Hole 576 was approximately 54 percent. Figure 3 shows the results of Lenotre and others (1985) clay analysis from Holes 576 and 576B. These clay percentages are based

Table 1. Mineralogical Composition of Hole 576A Sediments (M. Leinen, unpublished observations)

Core/ section	Depth (m)	Smectite (%)	Illite (%)	Kaolinite (%)	Chlorite (%)	Plagioclase (%)	Quartz (%)	Total (%)	Percent amorphous	Smectite:Illite ratio
1-1	0.23	8	50	1	22	3	17	100	0	0.16
4-2	30.25	9	23	5	6	3	9	55	45	0.39
4-5	33.91	13	31	6	6	1	4	61	39	0.42
4-6	35.81	6	46	3	4	1	5	65	35	0.13
5-5	44.59	14	30	10	10	1	3	68	32	0.47
6-1	47.61	3	8	3	2	1	4	26	74	0.38
6-3	50.65	7	11	2	4	1	5	30	70	0.64
6-4	53.99	2	7	1	2	2	5	20	80	0.29

on total clay content rather than percent of total solids. The most striking feature of this figure is the large increase in smectite relative to the other clays at the 18 and 33 to 41 meter levels in Hole 576 and 35 to 55 m level in Hole 576B.

Quartz

Leinen (1985) measured the quartz content and determined the mass accumulation rate for sediments of Hole 576A. The results are presented as a function of depth along with age in Figure 4. Leinen concluded that the dramatic change in quartz accumulation at 2.5 m.y. was clearly related to a *climatic* event. A gradual increase in quartz accumulation through the Miocene and early Pliocene probably reflected the combined effects of increasing northern hemisphere aridity and intensified atmospheric transport activity associated with global cooling during the interval.

Microstructure

The physical nature and consolidation behavior of the red clays can be best understood through a knowledge of the sediment microstructure. Two fundamental properties of a clayey sediment, the fabric and physico-chemistry, termed the microstructure, strongly influence and largely control the physical and mechanical properties of a sediment. These important properties include, but are not limited to, water content, porosity, shear strength, permeability, and compressibility. An insight into the nature and effects of the silt-size particles and clay-sized aggregates or domains (integral elements of the microstructure) that were considered to exist in the red clays can be studied using techniques of electron microscopy (EM). The clay minerals and larger sized particles in most sedimentary deposits are not of the same size, shape, and mineralogy; these characteristics which are intimately coupled to the microstructure play a significant role in establishing the ultimate fabric and sediment properties at the time of deposition and throughout the history of the deposit (Bennett and others 1977). An un-

derstanding of clay microstructure and the methods of analysis are important because the results and interpretations have far-reaching effects on the fundamental conclusions and ideas of the basic origin, nature, and sources of the red clays components. The understanding of clay microstructure is an important prerequisite to an understanding of the physical behavior of sedimentary deposits in response to static and dynamic loads and to variations in environmental conditions (Bennett and others 1977, Lambe 1958a).

Physico-chemistry of Clays

The physico-chemistry of clays is critical in determining the clay fabric of a marine deposit, especially in the early stage of formation (particles in suspension and at the depositional interface). Detailed studies of clay microstructure and its influence on the physical properties of sediment have been presented by Winterkorn (1948), Bolt (1956), Lambe (1958a), Fosenquist (1959, 1962), Warner (1964), Buchanan (1964), and Ingles (1968). Discussions and studies concerning the physico-chemistry of clays and colloids are found in Krut (1952) and van Olphen (1963).

The physico-chemical forces controlling clay mineral structure and the *initial* framework of clay fabric are essentially electrical in character. Suspended clay particles interact in response to the electrical nature of the particle surface and to the electro-chemical characteristics of the surrounding aqueous medium. The important electrical forces are classified as primary valence bonds, hydrogen bonds, van der Waals forces, and simple electrostatic interactions (Lambe 1958b). The phyllosilicate clay minerals, are composed of sheets (tetrahedral and octahedral coordination polyhedra) generally in 1-to-1 or 1-to-2 layers such as one tetrahedral sheet plus one octahedral sheet (kaolinite), or two tetrahedral plus one octahedral sheet (smectite, illite, and chlorite). This imparts a platy or sheet-like characteristic to many clay minerals and for practical purposes they can be considered as having approximately a two-dimensional shape. Most clay particles are considered colloids which range in size from about 1 μm to as small as 0.001 μm ; however,

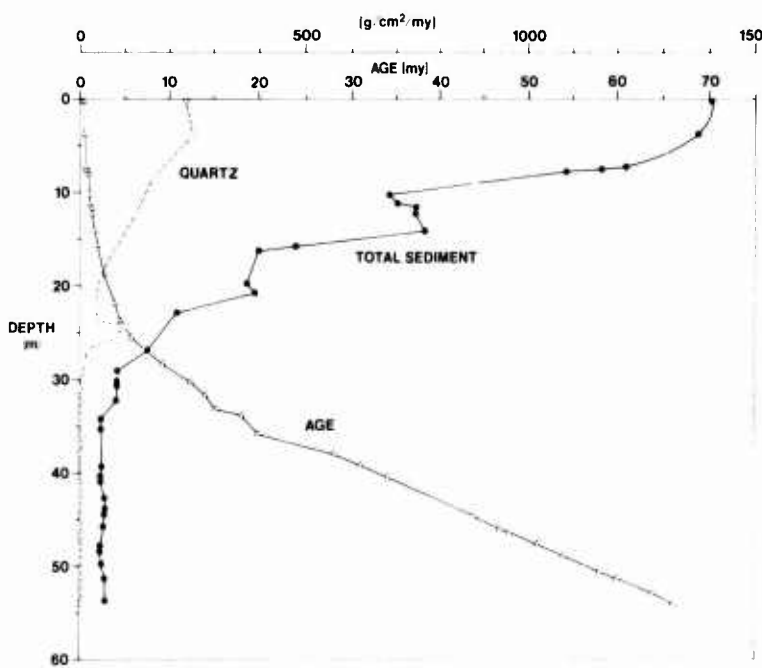


Figure 4. Quartz, total sediment accumulation rates and age versus depth downhole at Site 576.

some clay minerals are somewhat larger. In some cases, van der Waals forces and hydrogen bonds hold the two-dimensional like clay mineral layers together to form relatively thin particles. During flocculation of suspended clay particles, deposition, and also during low pressure diagenesis, clay crystals are not generally broken nor are the clay layers separated (Lambe 1958a). The breaking of interlayer bonds (absolute range of pressures may vary for different clay minerals) appears to be indicative of the onset of high pressure diagenesis as revealed through studies of consolidated kaolinite (Cabrera and Smalley 1971).

Electrostatic forces involve attraction between oppositely charged entities and repulsion between similarly charged ones. Electrostatic interactions are critical in determining clay microstructure, particularly clay fabric, because clay particles carry a net negative charge which is large compared to the particle mass and the net charge varies with the clay mineral type. The small positive charge carried by particle edges under certain conditions adds a complicating function to physico-chemical interaction (Bennett and Hulbert 1986, Bennett and others 1977, Thiessen 1942, Van Olphen 1963, Yariv and Cross 1979).

Clay Fabric

The early studies of clay fabric beginning with Terzaghi (1925) and Goldschmidt (1926), Casagrande (1932) and Lambe (1953, 1958b) provided the thrust

for clay fabric studies employing x-ray and high resolution electron microscopy techniques which depicted the actual arrangements and orientation of clay particles (fabric)—the “building blocks” of sediment structure. Clearly the previous section has shown that the physico-chemical factors involved in the formation of sedimentary deposits cannot be divorced from the physical and mechanical aspects for a complete assessment of sediment formation, diagenesis, physical properties, and fabric analysis (Bennett and others 1977).

The importance of fabric in determining the physical properties of sediments has been firmly established. The reader is referred to papers by Mitchell and Houston (1969), Houston and Mitchell (1969), and Torrance (1970) for further discussions concerning sediment structure interrelationships with the physical properties. A detailed study of bonding and effective stress and strength of soil (Mitchell and others 1969) followed by later studies (Andersland and Douglas 1970, Mitchell and others 1971, Singh 1970) revealed the importance of these factors on the microstructure of sediments. Olson and Mesri (1970) discussed the influences of both the mechanical and physico-chemical mechanisms important in the compressibility of clays.

A few typical fabric types have been classified as honeycomb, cardhouse, turbostratic, bookhouse, and staircase. Recently studies have revealed that the single plate concepts of fabric are not wholly tenable and

that the multiple unit, domain-type fabric is the rule for most sediments (Bennett and others 1977). The variation in particle size, shape, and composition coupled with the depositional environment, physico-chemistry, transport mechanisms and energies, and changing environmental conditions, all increase the complexity of the sediment fabric for a particular sedimentary deposit. Only a few studies of the fabric of natural sedimentary material have been made, however, numerous studies have dealt with the fabric and engineering behavior of laboratory prepared material. Qualitative and ultimately quantitative studies of sediment fabric and microstructure of naturally occurring sediments could lead to reliable predictive capabilities of the physical behavior of clay sediments, a clearer understanding of the geotechnical properties, and a much better understanding of complex sedimentological processes (Bennett and others 1977).

Microfabric Techniques

Critical Point Drying

Critical point drying has been recognized as a necessary dehydration method in order to maintain the particle-to-particle integrity and quality of a clay sample to be examined by electron microscopy. The critical point method was used extensively for biological applications in order to preserve delicate membrane tissues for electron microscopy studies (Hayat and Zirkin 1973). Gillott (1969) successfully applied the technique to clay sediment using both alcohol and CO₂ for critical point drying. Gillott claims that the appearance of the fabric was identical in both cases. Details of the critical point drying technique for high porosity, soft, submarine sediments have been thoroughly described by Bennett and others (1977).

The critical point technique is a significant improvement over other dehydration methods because surface tension forces are avoided. At a critical temperature and pressure of a liquid no boundary exists between the liquid and the gas phase, and when the temperature is held above the critical point, the gas may be released until atmospheric pressure is reached. Thus the sample can be dried without surface tension effects.

Techniques Employed for the Examination of Microstructure of Red Clays

The series of techniques developed by Bennett (1976) used for sample preparation of the clay specimens for the transmission electron microscope (TEM) fabric studies are as follows:

1. Subsampling of sediment from core segments.
2. Replacement of saline interstitial water by a series of miscible fluids (ethyl alcohol-amyl acetate). Complete removal of interstitial water checked by the silver nitrate test (precipitation of silver chloride).
3. Careful wrapping of small specimens in thin lens paper.
4. Further soaking of lens paper and specimen in amyl acetate.
5. Placement of wrapped specimens into the critical point chamber.
6. Purging of the specimen with liquid CO₂ replacing amyl acetate.
7. Critical point drying with CO₂.
8. Placement of dried, wrapped specimens into small individual desiccators.
9. Embedding of individual specimens under vacuum with a very low viscosity epoxy resin (SPURR).
10. Removal of specimens from the vacuum and subsequent curing of the epoxy resin at 60° to 70° C.
11. Trimming of the specimens with glass knives prior to ultrathin sectioning. Larger specimens were trimmed with a jeweler's saw prior to trimming with a glass knife.
12. Ultrathin sectioning with a diamond knife (sections cut approximately 5×10^{-8} to 1×10^{-7} m thick [500 to 1000 Å] on a microtome.
13. Placement of ultrathin sections on copper grids.
14. Very light carbon "sputtering" of ultrathin sections on grids in a vacuum evaporator.

After the above procedures have been accomplished the specimens are ready for examination of the clay fabric in the transmission electron microscope. Preparation of samples for SEM follow the same dehydration procedures (1-8) and samples are mounted on stubs and gold-palladium coated for observation.

SPURR epoxy resin was used because of its very low viscosity (60 cps). It has an impregnating advantage over ordinary epoxies (approximately 2000 cps). The usefulness and advantages of this epoxy have been determined by experiments on various Mississippi Delta and DSDP samples (Bennett and others 1977). Submarine sediment samples with a high water content (low cohesive strength) were found to remain intact if impregnated while under a vacuum, but similar samples were found to completely collapse if they were impregnated at ambient pressure (without vacuum). Samples having a very complex fabric were found to retain their particle-to-particle structural integrity (Bennett and others 1977).

The embedding techniques used during this study were similar to the methods described by Brewer (1964) for impregnating soil samples under a vacuum. Other embedding techniques for the study of soils by elec-

tron microscopy have been described by Pusch (1966, 1967, 1968), Smart (1967a,b), O'Brien (1971), and Foster and De (1971). A detailed investigation of impregnating techniques was carried out by Foster and De (1971), and their results showed that the observed strains in the original fabric were minimal in "soft" material. Their techniques, however, did not involve drying, but rather followed a series replacement of the interstitial water by diffusion processes to a final hardened resin. Photomicrographs of submarine sediment—prepared by freeze-drying, embedded with Maraglas Epoxy, and subjected to ultrathin sectioning—revealed detailed, complex fabrics that appear to be unaffected significantly by sample preparatory techniques (Bowles 1968a,b). The freeze-drying technique is time consuming and there is danger of ice crystallization during the process.

Microfabric Analysis

The clay fabric of an illite-smectite-rich marine sediment is depicted in Figure 5. The fabric shows that the clays form an open structure by the face-to-face and edge-to-edge arrangements and buildup of clay particles. The resulting fabric of randomly arranged

domains is typical of that found in marine areas such as the Gulf of Mexico (Bennett and others 1977, Bowles 1968a).

The typical fabric of red clays recovered from Hole 576A and GPC-3 is observed in Figures 6 and 7. The most striking feature of this fabric is the fractured appearance of many grains and the lack of obvious support for the large particles observed in the thin sections. The large grains are not in close proximity to each other; they appear as if suspended in a random mass of very fine particles. The large particles are silt- and clay-size particle aggregates (domains). Figure 8 shows the detailed nature of one of these particles; note the coneloidal fracture pattern and the stress fields within the fractured pieces. Observations of numerous TEM photomicrographs consistently reveal well rounded silt and clay size aggregates that are a significant contribution to the total sediment mass. SEM analysis (Fig. 9) clearly shows the well-rounded nature of the aggregates with the layered structure (face-to-face clay plates). The clay particles comprising the aggregates have been well compacted prior to erosion and removal from the parent rock. The high degree of induration of the aggregates and interlayer bonding enables them to become well-rounded and abraded



Figure 5. Clay fabric transmission electron microscope (T.E.M.) photomicrograph of a high water-content illite-rich marine clay from the Mississippi Fan, Gulf of Mexico. Note the edge-to-face and edge-to-edge particle arrangement of the dark clay particles. Scale Bar = 1 μ m.

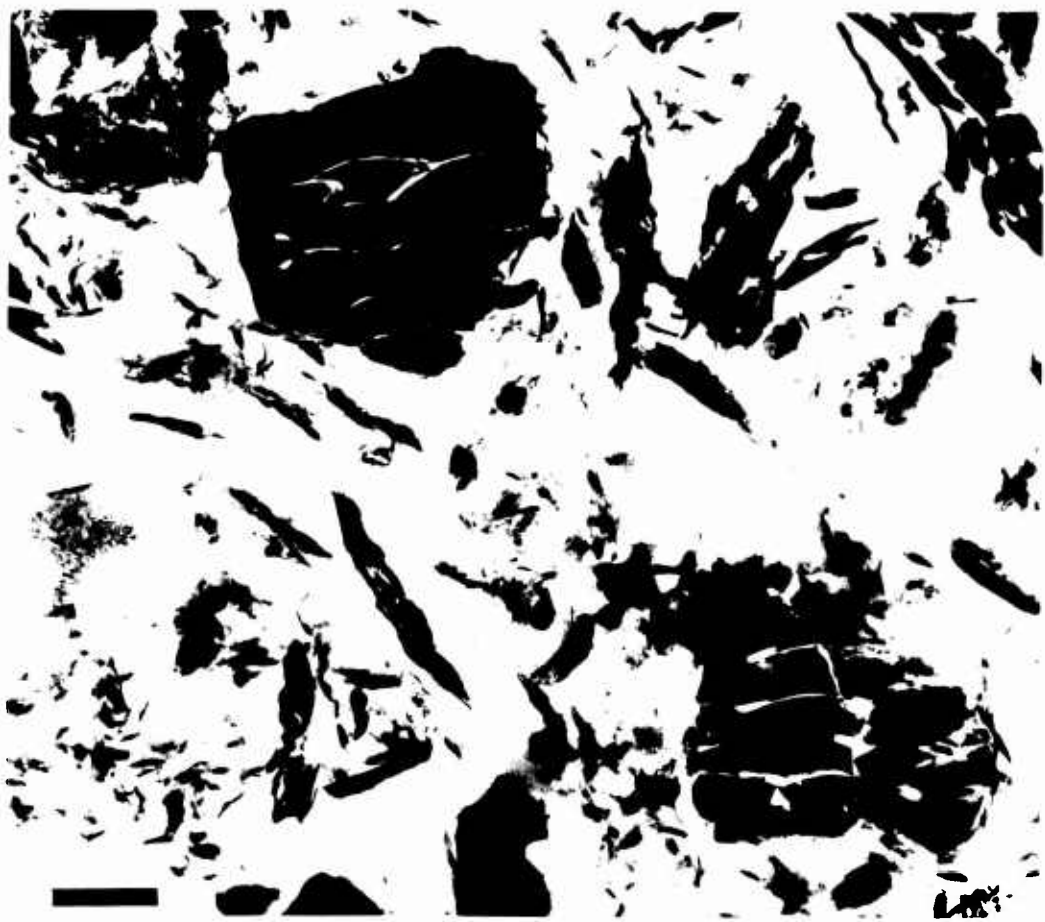


Figure 6. Clay fabric TEM photomicrograph of red clay taken at the 13 m level from Hole 576A. Note the fractured appearance of the large dark particles in the upper left and lower right portions of the figure. Scale Bar = 1 μ m.

during their transport history (Figs. 9 and 10). Mineralogical identification of these illitic, well-rounded, aggregates is discussed in a later section of this article. These particles are easily differentiated from quartz particles of similar size by virtue of their shape, microfabric, surface morphology, and layered nature in contrast to the conchoidal fracture patterns of the quartz, its surface features, and shape (Fig. 11, compare with Figs. 9 and 10). Selected area diffraction (SAD) techniques also are used to identify and differentiate the illitic aggregates from quartz particles which are important constituents of red clays. An interesting observation was made of a well developed smectite, another type of clay aggregate, and compared with the illitic aggregates (Fig. 12, compare with Figs. 9 and 10). Note the significant difference in the large intravoids of the smectite aggregate compared

with the illite; the two types are thus easily differentiated. The morphological nature of the smectite observed in this study compares very favorably with the observations of smectite made by Welton (1984).

A mosaic consisting of 20 individual photomicrographs was constructed (Fig. 13) in order to gain insight into the particle-to-particle relationships of the Plio-Pleistocene red clays to a high degree of resolution over a "large" field of view. Examination of the mosaic shows that the larger individual particles fracture in the same direction. The fractured particles align in the same direction regardless of the particle orientation. It was determined from the direction of the knife scours on the thin section that the fracture pattern of the particles is oriented normal to the direction of the cut of the diamond knife.

All particles displaying these fractured features have

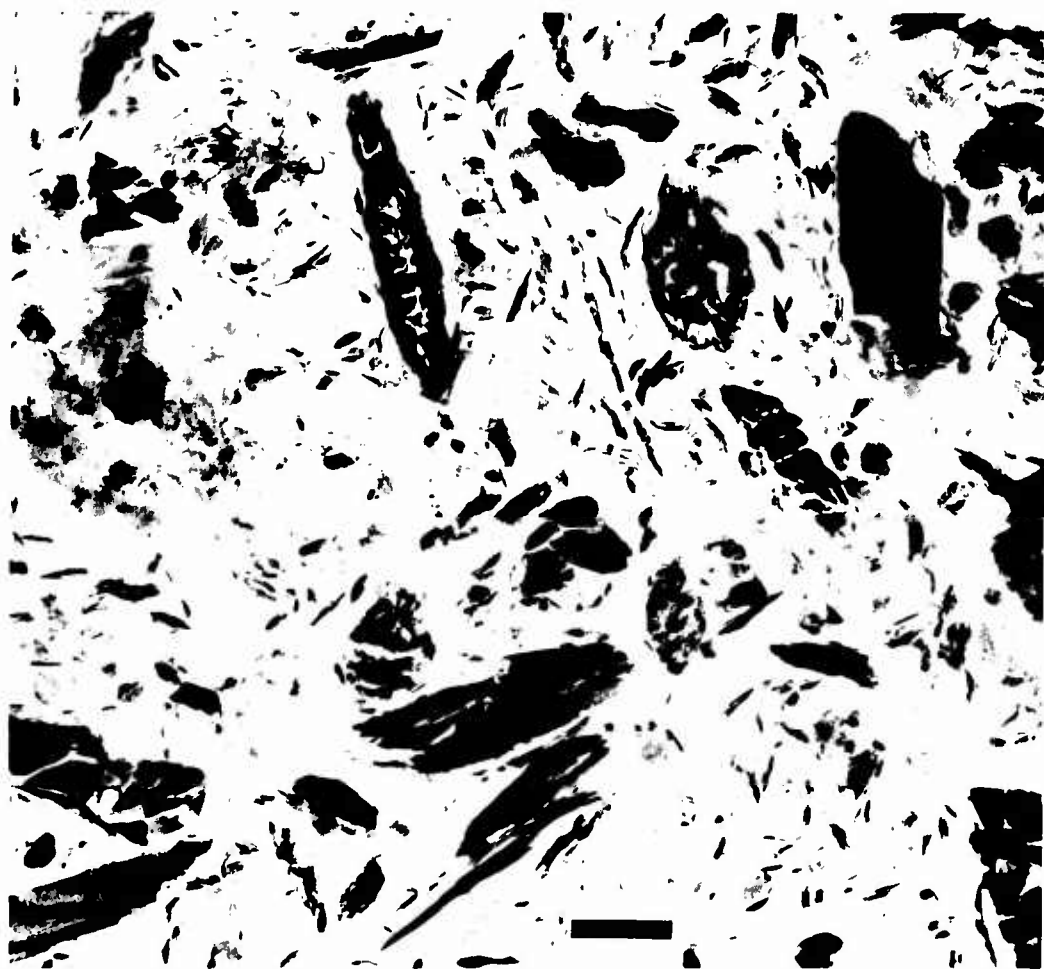


Figure 7. TEM photomicrograph of red clay taken at 1 m subbottom at Site GPC-3. Scale Bar = 1 μ m.

been highlighted and the background subdued in Figure 14. Some of the features appear as voids having only the remains of several of the fractured parts. As can be seen from the figure, the fractured particles comprise the majority (up to 70 percent) of the sediment. Another interesting feature of the particles is that they are all well rounded and evenly dispersed; the observations of hundreds of thin-sectioned fields reveals the fact that these larger particles in general are not in contact which is in part a function of the thin sectioning process.

The fact that the particles fracture in a direction normal to the path of the diamond knife indicates that the knife fractured the particles during the thin-sectioning process. Examination of the microtoming process, however, reveals that the fracturing of the par-

ticles is the result of the bending of the section during the cutting process. Figure 15 displays the particulars of the microtoming process in a greatly magnified "view." A diamond knife which forms a 44° wedge is offset 4° from the plane of the moving block containing the sediment sample. As the sample block moves past the knife, a thin-section approximately 700 Å thick is cut by the knife. The knife is retained in a container called a "boat" which is filled with an appropriate fluid (usually water) upon which the section can float free of the knife thus avoiding folding and other forms of disturbance due to friction along the knife face. The section experiences a minimum bend of 48° as it is separated from the block by the cutting action of the knife. This bending action shatters the brittle large particles in a conchoidal pattern typical



Figure 8. T.E.M. photomicrograph of a fractured particle in the red clays (see Fig. 7). Note the characteristics of the fracturing and the stress fields within the fractured pieces. Scale Bar = 1 μ m.

of a microcrystalline material. Elongated thin particles, which may be large flat particles sectioned on end, tend to fracture into blocky segments. This bending and fracturing of the particles explains the uniform orientation of the fractured pieces, normal to the direction of the cutting knife.

It was determined by selected area electron diffraction analysis that the fractured particles observed in Figure 8 are composed of illite clay. Selected Area Diffraction Analysis (SAD) was performed with a 100 kV Transmission Electron Microscope (TEM) on individual mineral grains. Utilizing the TEM/SAD techniques, diffraction patterns were obtained on photographic plates as depicted in Figure 16(A). Using calibration factors of the TEM obtained with a mineral standard, precision measurements were obtained from the diffraction pattern (column 1 and 2) and Miller Indices are assigned and obtained for the various rings which were constructed from the original diffraction pattern (Column 5, Fig. 16(B)). By comparing the precision measured parameters (column 2) with known ASTM Files (column 3), individual minerals can be identified.

Illite was identified as a major component of the red clays. The term "fractillite" denoting a fractured illite-rich shale or argillaceous clast was coined to de-

scribe the unique features or "fingerprint." The term illite refers to a nonexpanding, diotahedral, aluminum, potassium mica-like mineral (a two-to-one layer hydrous aluminum silicate) that is a major component of shale.

An additional mosaic of the clay fabric of red clays was constructed and depicted in Figures 17 and 18. In almost all cases the fractured particles (fractillites) are well rounded and are not in close contact with each other. In the lower righthand corner of Figure 17 a series of particles is shown that is different from the fractillites. They consist of parallel laminated sections of clay that have been disrupted by the microtoming process. These laminated sections are particles where the clay layers are directly perpendicular to the plane of the thin-section.

Fractillites found in the thin-sections make up 50 to 70 percent of the total Pleistocene red clay sediment distribution at Sites 576 and GPC-3 and are:

1. Brittle (fracture upon bending during the thin-sectioning process);
2. Composed mostly of illite, possess 2:1 layer illite (selected area diffraction patterns (SAD) on ultra-thin section);
3. Well-rounded;



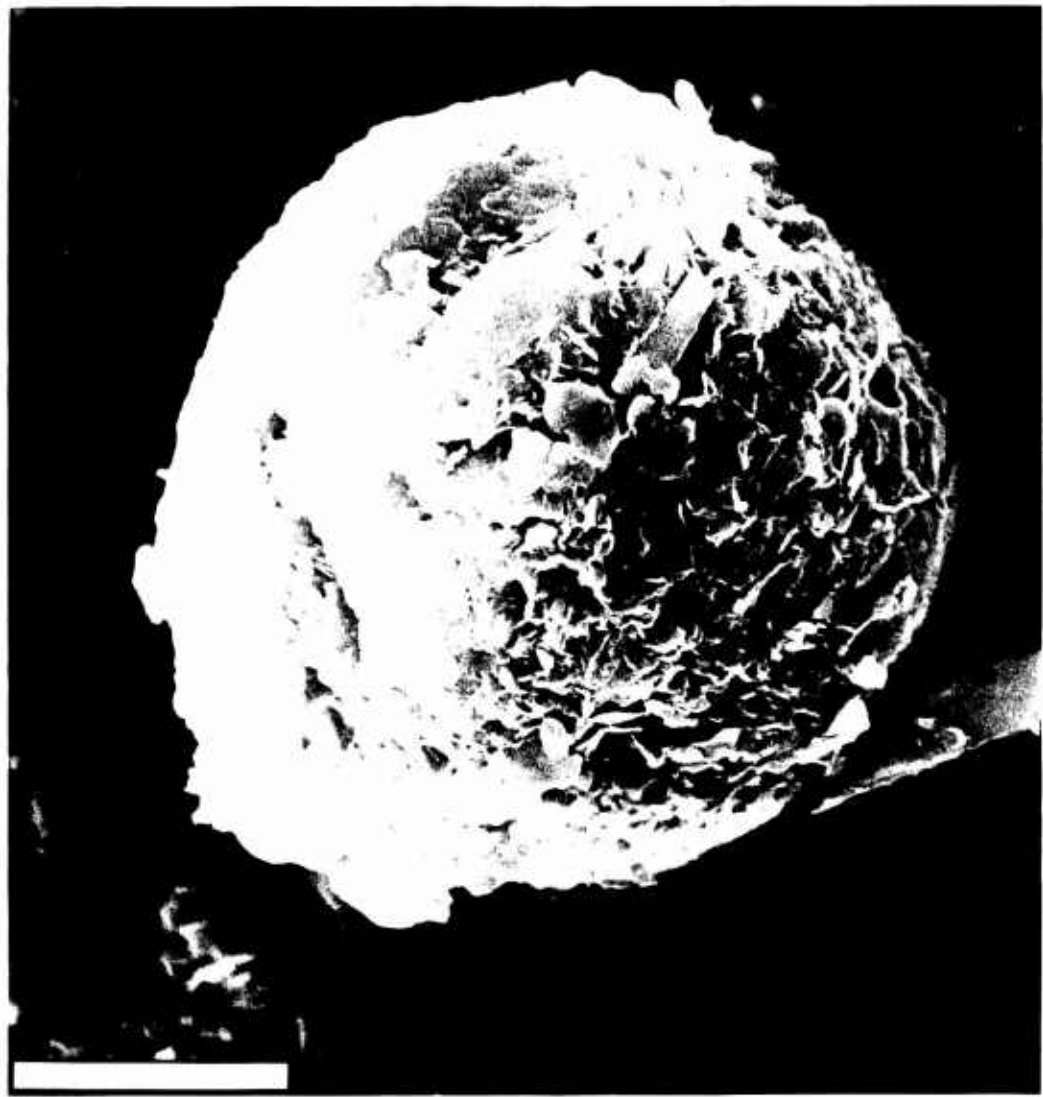


Figure 10. SEM photomicrograph of a well rounded highly spherical illitic shale clast from Core 2, Section 2 (21 m subbottom) of Hole 876A. Scale Bar = 10 μ m.

shale fracture during ultrathin sectioning, pieces of Minerva Shale (an illite type formation) were pulverized, embedded, and thin sectioned using similar techniques as used on the red clays. The results are shown in Figure 19. The nature of the fracturing is virtually identical to the fractillites found in the sediments at Sites 576 and GPC-3.

Examination of sediments from the Central Pacific Basin, the Japan Trench, the Mid America Trench,

the Gulf of Mexico and the Bootlegger Cove Clay also reveal the presence of illite-shale clasts in the form of fractillites in thin-sections, examples will be illustrated later.

In addition to the illite clasts present at Sites 576 and GPC-3, smectite forms an increasingly important constituent; its amount increases with depth below the seafloor. In the sediments of these sites one form of smectite appears as extremely small, feathery sheets



Figure 11. S.E.M. photomicrograph of an aeolian quartz particle from Core 2, Section 2 (21 m subbottom) of Hole 576A. Scale Bar = 10 μ m.

(Figs. 20, 21, and 22) which are x-ray amorphous, and often form well defined agglomerations. Considerably lower percents of well developed smectite occur in the form depicted in Figure 12.

Consolidation Characteristics

Consolidation is the primary form of diagenesis in clayey marine sediments. It is the physical process that converts high water content muds into mudstones

and shales. The consolidation process begins at the time of sedimentation on the sea floor and continues throughout the history of the deposit.

Skempton (1970) defined consolidation as the result of all processes causing the progressive transformation of an argillaceous sediment from a soft mud to a clay and finally to a mudstone or shale. He suggested that the process of consolidation include interparticle bonding, desiccation, cementation, and the squeezing out of pore water under increasing weight

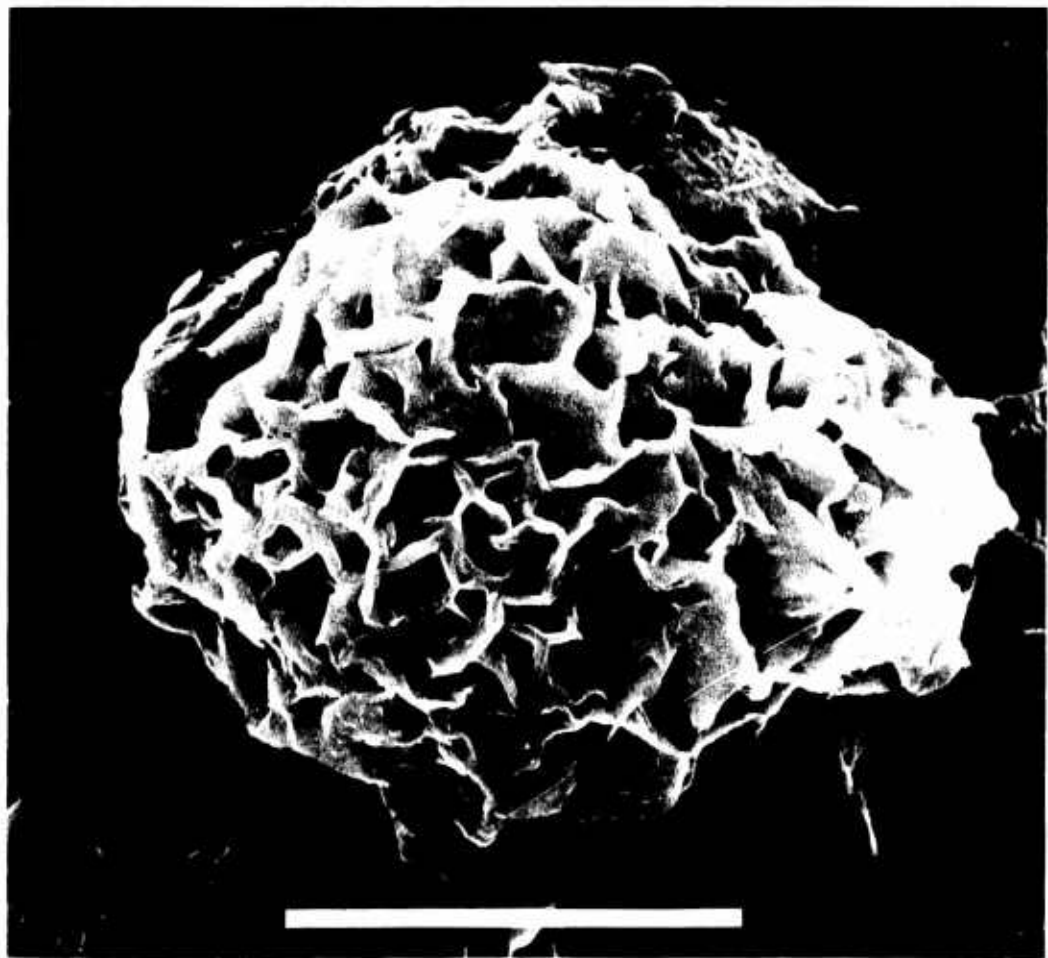


Figure 12. SEM photomicrograph of a well developed smectite aggregate from Core 2, Section 2 (21 m subbottom) of Hole 526A. Scale Bar = 5 μ m.

of overburden. The latter process, essentially the reduction of porosity with increasing imposed load, is the same process that is simulated in the laboratory using an oedometer. The time factor in the laboratory study of the consolidation characteristics of a sediment sample necessarily precludes changes in interparticle bonding and cementation that may take place with time in the natural environment. Thus the reduction of the porosity of a sediment under a rapidly applied load in the laboratory most certainly does not have the exact same effect as extremely slow, continuous loading occurring over long periods of geological time.

An ultrathin section of an unconsolidated smectite illite-rich marine sediment (Fig. 23) reveals that its microstructure is a loose, open, random arrangement

of particles. Figure 24 shows the microstructure of similar material consolidated by an imposed load of 800 kPa. The loading resulted in a much denser packing of particles and a tendency for the particles to be oriented in packets, some without a high degree of preferred orientation. Studies have shown that similar orientation is obtained in nature at equivalent *in situ* pressures (Bennett and others 1977, Bryant and others 1981). Even with the severe limitation of oedometer testing and the impossibility of obtaining truly undisturbed samples in most cases in the areas covered by the world's oceans, an examination of the results of such testing is helpful in gaining insight into the process of consolidation and the permeability and porosity depth relationship of marine clays (Bryant and others 1981).

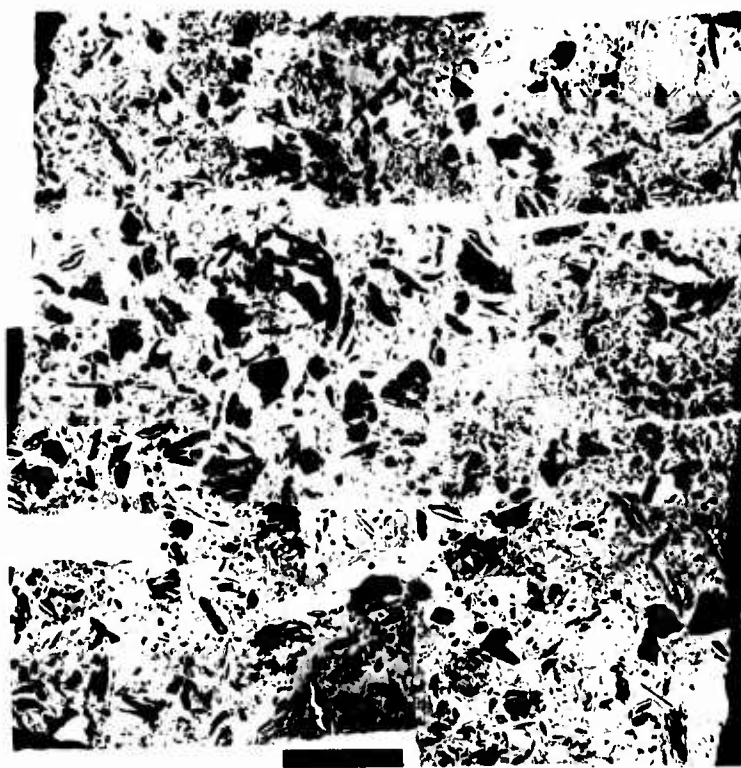


Figure 13. Mosaic of T.E.M. photomicrographs of red clay from Site GPC-3 (1 m subbottom). Scale Bar = 5 μ m.



Figure 14. Mosaic of T.E.M. photomicrographs (same field as Fig. 13) with fractured particles highlighted and the supporting matrix background subdued. Arrow points to fractured particle. Scale Bar = 5 μ m.

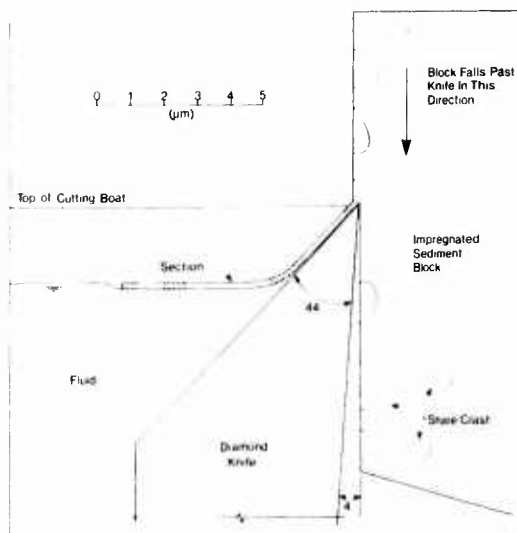


Figure 15. Diagram illustrating the mechanics of the thin-sectioning process used for this study. Note the bend in the thin-section as it is cut by the diamond knife.

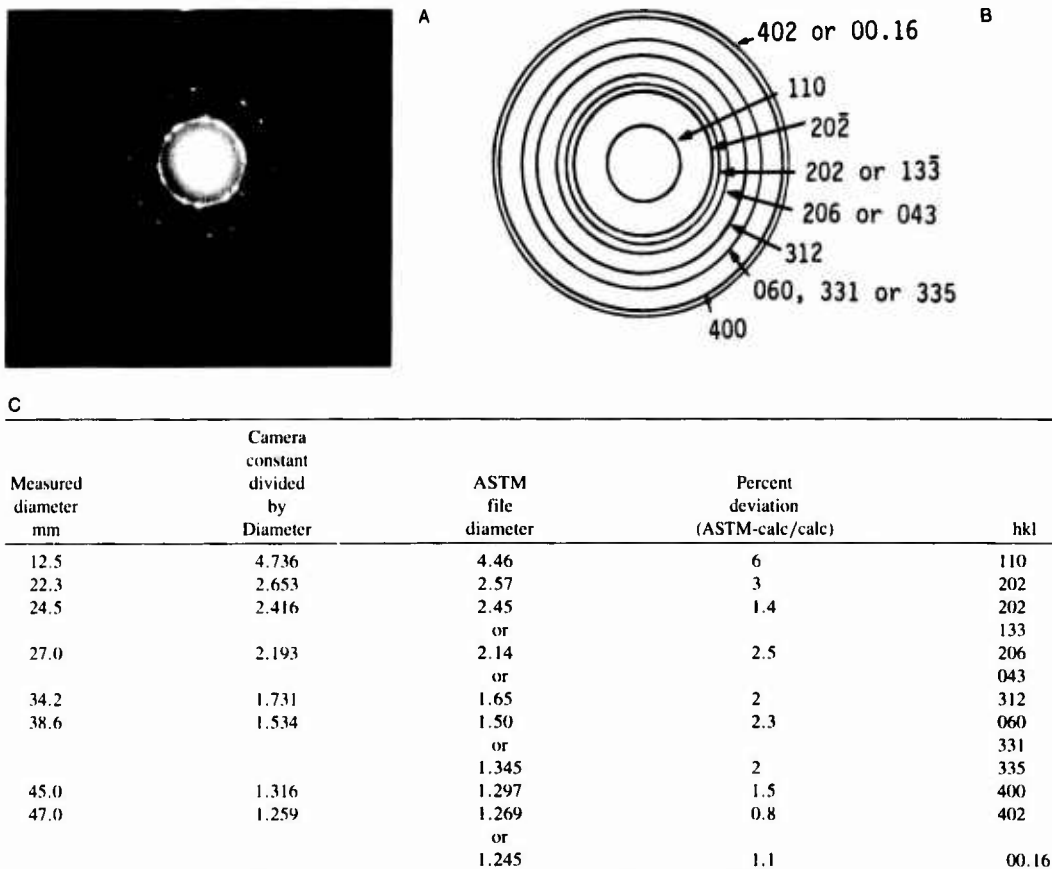


Figure 16. Illite identification using Selected Area Diffraction (SAD): (A) A T.E.M. micrograph of polycrystalline illite; (B) Drawing of the ring pattern with their indexed Miller indices (hkl); (C) Table showing the less than 6% deviation from the measured diameters of the unknown sample and the ASTM file values.

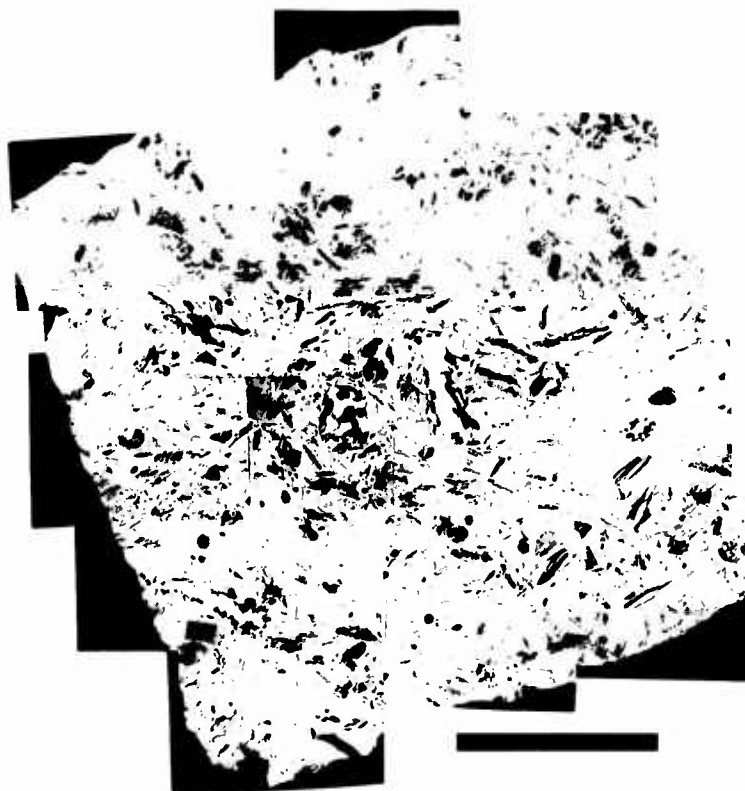


Figure 17. Mosaic of T.E.M. photomicrographs of red clay from Core 2, Section 2 (21 m subbottom) of Hole 576A. Scale Bar = 5 μm .

Previous Studies on Consolidation of Marine Sediments

Early marine sediment consolidation studies of a red clay environment were performed by Hamilton (1964) on samples obtained during the MOHOLE Project. His results represent the first attempt to evaluate the reduction of void ratio or porosity as sediments become increasingly buried. Later, Richards and Hamilton (1967) reported on the findings of the MOHOLE in a comprehensive volume on marine geotechnology. These two studies, based on somewhat disturbed samples, point to a sediment having an open, porous structure resistant to collapse under loads in excess of the overburden stress. The state of consolidation was concluded to be one of apparent overconsolidation in the upper sedimentary column and progressing down-hole into a normal to underconsolidated unit. The reason given for the phenomenon of overconsolidation is that of probable interparticle bonding through chemical cementation, although this effort was not at all visible or confirmed.

Analysis of laboratory and field consolidation curves

by Richards and Hamilton (1967) resulted in ambiguity regarding compression indices. The compression index (C_c) is a measure of the change in void ratio with respect to change in effective stress along the natural, or virgin, consolidation curve. Laboratory values for this measure, C_c , resulted in 0.77 to 0.90, whereas a field estimate of C_c , corrected for rebound, was computed at 2.1. The reason this difference exists was not explained.

Bryant and others (1967) published the results of an extensive examination of consolidation characteristics of Gulf of Mexico sediments. The surficial sediments were found to be normally consolidated but the sediments 3 meters below the seafloor were under-consolidated. Delflache and Bryant (1970) and Delflache and others (1971) analyzed a series of marine sediments and concluded that the physical behavior of marine clays differed from those ordinarily observed in clay soils on land.

Trabant and others (1975), Shephard and Bryant (1980), Shephard and others (1982), Shephard and Bryant (1983), and Taylor and Bryant (1985) examined the physical properties, primarily the consoli-

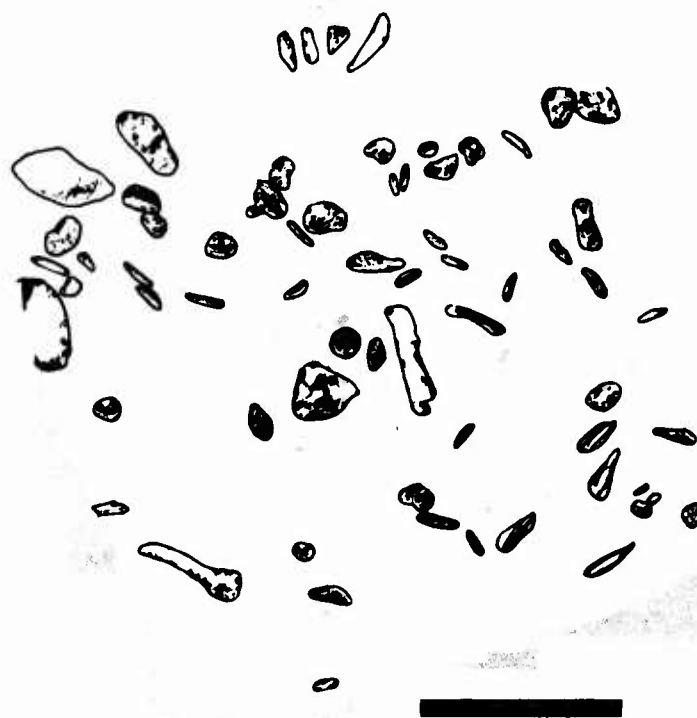


Figure 18. Mosaic of T.E.M. photomicrographs shown in Figure 17 with the fractured particles highlighted and the background subdued. Scale Bar = 5 μ m.

dation characteristics, of Pacific Marine sediments. Sediments in the Middle America and Japan Trench were underconsolidated while sediments of the Washington continental margin, Aleutian Trench, and Nankai Trough were overconsolidated. The consolidation characteristics were associated with the type of subduction of oceanic sediments.

Keller and Bennett (1973) analyzed red clays from the Northeastern Equatorial Pacific recovered during DSDP Leg 16. The red clays were zeolithic and limited to the upper 10 to 30 meters. Two consolidation tests were performed within the red clay material and yielded results similar to the MOHOLE results mentioned above in that the clay displayed apparent overconsolidation in the upper section but normally consolidated with depth. Again, incipient cementation is called upon as the responsible agent for this state. Once again, though, the disturbance caused by drilling techniques casts a question on the accuracy of these findings.

Bryant and others (1975) and Bryant and others (1981) examined the available data on the shear strength, consolidation, porosity, and permeability of oceanic sediments. Their main contribution was the

association of permeability and porosity of marine sediments. The underconsolidated conditions found in a large portion of oceanic sediments were correlated with very low permeabilities that ranged from $k = 10^{-6}$ to 10^{-10} cm/sec.

Recent studies in red clays conducted for nuclear waste disposal programs in the Northwestern Pacific have been published by Walker (1981) and Dadey (1983). These two theses present the results from piston core sampling and the latter includes DSDP Site 576 data. The outcome of these studies reiterates the overconsolidated nature of the upper section of the red clay column and the present study now addresses the possible reasons for this observation.

Theory of Consolidation

Complete discussions of the theory of consolidation are presented by Taylor (1948), Terzaghi (1956), Means and Parcher (1963), and Znidarcic and Schiffman (1983), and only a brief summary will be presented here.

The consolidation of marine sediment involves



Figure 19. T.E.M. photomicrographs of thin-sectioned Minerva Shale from Illinois. Scale Bar = 5 μm .

drainage, compression, and stress transfer under static loading. When a load is first applied to a saturated sediment, the pore water carries the load. As water leaves the void spaces, the load is transferred to the sediment structure. This application of load to the mineral grains will cause loss of free water and adjustment of the grains to a more compact structure.

The relationship between the amount of solid material and the void spaces is expressed by either the void ratio (e) or the porosity (n). Porosity is the ratio of the volume of void space (V_v) to the total volume (V_T) of a sample, $n = V_v/V_T$. The void ratio is defined as the ratio between the volume of void space and the volume of solid material (V_s), $e = V_v/V_s$. Since the total volume is equal to the volume of voids plus the volume of solids, porosity may be written as $n = e/(1 + e)$. The consolidation of a sediment will result in a loss of void space. In a test situation, the diameter of the core sample is fixed, and the change in

void ratio can be measured by a decrease in sample height.

The change in sample height resulting from an applied load in an oedometer is plotted against the log of elapsed time to form a compression curve (Fig. 25). These curves have two straight-line segments which reflect different stages of consolidation as determined by the rate of compression.

1. Primary consolidation, rapid compression during which free water is forced out of the sediment and measurable pore pressure exist.

2. Secondary consolidation ensues when pore water pressure is virtually absent and the microstructure carries the imposed load. At very high loads and low void ratios, secondary consolidation may result in the removal of chemically bound viscous water from the structure and realignment of the mineral grains.



Figure 20. T.E.M. photomicrograph of x-ray amorphous smectite found in Core 2, Section 2 (21 m subbottom) from Hole 576A. Scale Bar = 1 μ m.

The intersection of the two straight, slope lines determines the theoretical point of 100% primary consolidation. The change in void ratio resulting from any given load increment can be calculated from the total change in sample height at the point of 100% primary consolidation. A plot of the calculated void ratio for 100% primary consolidation for each load is plotted to form a void ratio-log of effective stress (e -log σ') curve. Each sample tested will have a unique curve similar to that in Figure 26. This type of curve is used in interpreting the consolidation history of the sample and is the basis for geological interpretations of the consolidation test results.

Since the sample has been under load in nature, the initial part of the e -log σ' curve (B to B') represents reloading and is essentially horizontal for a small segment (Fig. 26). The sediment supports this reloading stress without significant change in void ratio since it has already been consolidated under a similar natural load. The curved portion (B' to C) is the transition

from reloading to new loads and the straight-line portion (A to E) is the virgin compression curve resulting from the application of loads greater than those experienced in the natural environment. Release of applied stress allows the sample to rebound (C to D) as water is drawn back into the void spaces and an elastic readjustment is made. Each time the sample is compressed, there is an adjustment of the grains, producing a small, inelastic deformation. The curve between recompression and virgin compression (B to C), therefore, does not pass through the *in situ* void ratio and stress point (A).

Two points marked on an e -log σ' curve are used in interpreting the geological history of the sample tested. These are the preconsolidation stress (σ'_p) and the effective overburden stress (σ'_o). Taylor (1948) defined the preconsolidation stress as the "maximum past pressure." This is the degree of consolidation that has occurred in nature. Casagrande (1936) introduced a graphic method by which an approximate preconso-



Figure 21. Enlarged section taken from the same field (lower central portion) as in Figure 20, of x-ray amorphous smectite. Needle-like appearance results from dehydration and curling of smectite sheets. Scale Bar = 0.25 μm .

lidation stress can be determined from the $e\text{-log } \sigma'$ curve. This technique has become a standard method in all geotechnical investigations and has been used to determine values of preconsolidation stress for the red clays. The Casagrande method for the determination of the preconsolidation stress is described as follows. On the reload portion of the $e\text{-log } \sigma'$ curve (Fig. 27) a line is drawn tangent to the curve at the point of maximum curvature. A horizontal line also is drawn through the point of maximum curvature. A line that bisects the angle formed by the horizontal and tangent lines is extended to intersect the extension of the virgin curve. This point of intersection (σ'_v) is considered the amount of the preconsolidation stress.

In the marine environment the effective overburden stress (σ'_v) which acts on the sediment to cause consolidation is the weight of the overlying sediment minus the weight of the water; that is, the buoyant weight of the sediment grains in sea water.

The removal of water and the rearrangement of sed-

iment particles under stress are complex functions of particle size, clay mineralogy, carbonate content, interstitial electrolyte, initial particle arrangement microfabric and permeability. The theory of consolidation and the determination of preconsolidation stress involve only the concept of mechanical loading of the sediment. However, Hamilton (1964) suggested that any factor or combination of factors which cause unusual sediment structural strength will give the same effect as mechanically driven overconsolidation, defined as the state where overburden stress (σ'_v) is less than preconsolidation stress (σ'_v). The factors include unusually strong interparticle bonding, low rates of deposition over long time periods, and cementation due to chemical and biological processes. The theory of consolidation, therefore, does not include the effect of cementation or other factors such as effect of microstructure, which play a major role in the consolidation process of marine sediments. The determination of preconsolidation stress (σ'_v) by the Casagrande



Figure 22. Enlarged section of x-ray amorphous smectite taken from same field as in Figure 21. Scale Bar = 500 Å.

method is based solely on the concept of mechanical deformation resulting from overburden stress.

Test Procedure

The general technique of laboratory consolidation testing is discussed in Lambe (1951). Back pressure consolidometers were used for the consolidation tests described in this article. The technique differs somewhat from Lambe's methods. The release of hydrostatic pressure resulting from removing the sediments from the marine environment permits formation of gas bubbles which may be entrapped in the pore water. The application of back pressure redissolves any gas and results in a test performed under the hydrostatic conditions of the environment except for extremely deep depths. Details of the technique can be found elsewhere (Bryant and others 1981, Lowe 1974).

The loading sequence was started after the samples adjusted to the back pressure. The initial loading of

the sample began with a very small load (10 kPa). The loading sequence consisted of doubling the previous load until a stress of 3200 or 6400 kPa was reached. The loading sequence was thus 10, 20, 50, 100, 200, 400, 800, 1600, 3200, and 6400 kPa. The time required to run one consolidation test was normally 3 to 4 weeks.

Consolidation Characteristics And Analysis

The results of 52 consolidation tests on material recovered at Site 576 are presented in Table 2. The consolidation testing of the Site 576 cores represents the most intensely tested marine sediment section. The statistical average values for the important parameters are:

Overconsolidation Ratio (σ'_{c1}): 1.99

Compression Index (C_c): 1.74

Expansion Index (C_e): 0.17

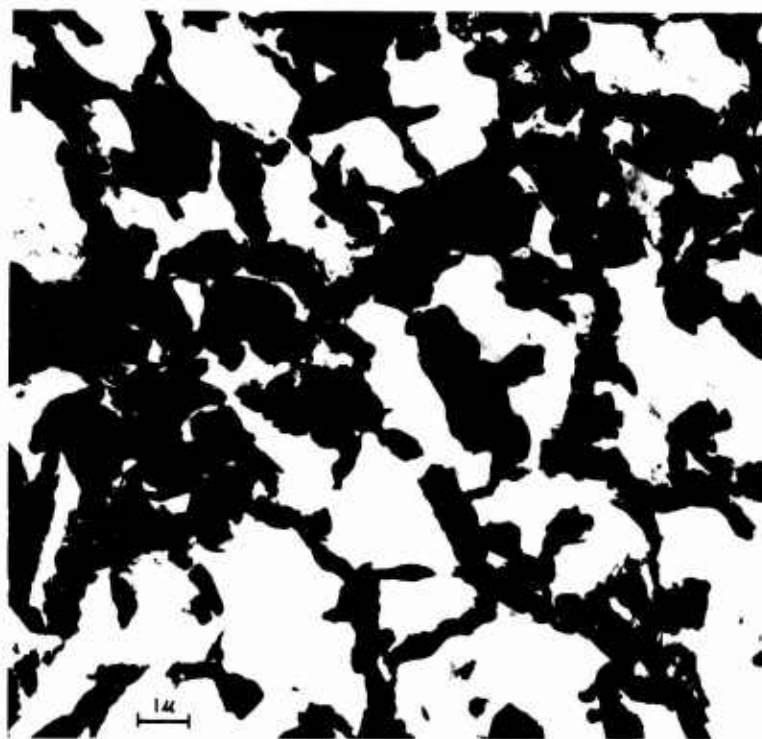


Figure 23. Typical clay fabric T.E.M. photomicrograph of a high water-content, clayey marine sediment from the Mississippi Fan, Gulf of Mexico, at a subbottom depth of 2 m. Scale Bar = 1 μ m.

Permeability at preconsolidation stress (σ'_{c1})

Consolidation Theory: $k = 2.3 \times 10^{-6}$ cm/sec

Direct Measurement: $k = 2.6 \times 10^{-6}$ cm/sec

Typical e -log σ' curves are shown in Figures 28 and 29. The curves in Figure 31 are from sediments in the subunit I-A (depth: 0–31 m), Pliocene to Quaternary quartz-rich illite muds. The curves in Figure 29 are from sediments of subunit I-B (depth: 28–55 m), Tertiary illite/smectite-rich pelagic clays. Figure 30 is a compilation of the results of the consolidation testing. Void ratios at various imposed loads, 50, 100, 300, and 1000 kPa, are plotted against depth. This compilation of test results illustrates the compressional nature of red clays. High void ratio material such as found between 10 to 15 meters was highly compressible. The change in void ratio under an imposed load ranging from 50 to 1000 kPa resulted in a decrease in void ratio, e , from 5.2 to 1.6 ($n = 84$ –62 percent).

The state of consolidation of a sediment sample can be determined by comparing the computed *in situ* effective overburden stress (σ'_s) to the maximum past effective stress (σ'_c) with which the sample is in equi-

librium. The ratio of these two stresses (σ'_s/σ'_c) is called the overconsolidation ratio (OCR).

A normally consolidated sample (OCR = 1) is one in which the current vertical effective stress is the greatest effective stress which has ever been applied to the sample. An overconsolidated sample (OCR > 1) is one in which there is a history of vertical effective stress greater than the current effective overburden stress. An underconsolidated sample (OCR < 1) is one in which the current vertical effective stress is less than the calculated effective overburden stress. In general, underconsolidated sediments exhibit excess pore water pressure (pressure in excess of hydrostatic) and are not yet completely consolidated.

The OCR is the traditional means of gauging the state of consolidation. However, in stratigraphic representations it can be misleading. As the sediment-water interface is approached, the effective overburden stress σ'_c becomes nearly zero, thus the OCR must approach infinity, which gives a highly distorted consolidation state relationship. Figure 31 displays the plot of the overconsolidation ratio (OCR) as determined by the use of the Casagrande method for the determination of the preconsolidation stress (σ'_{c1}) (Table 2).

Originally, the consolidation testing of deep sea

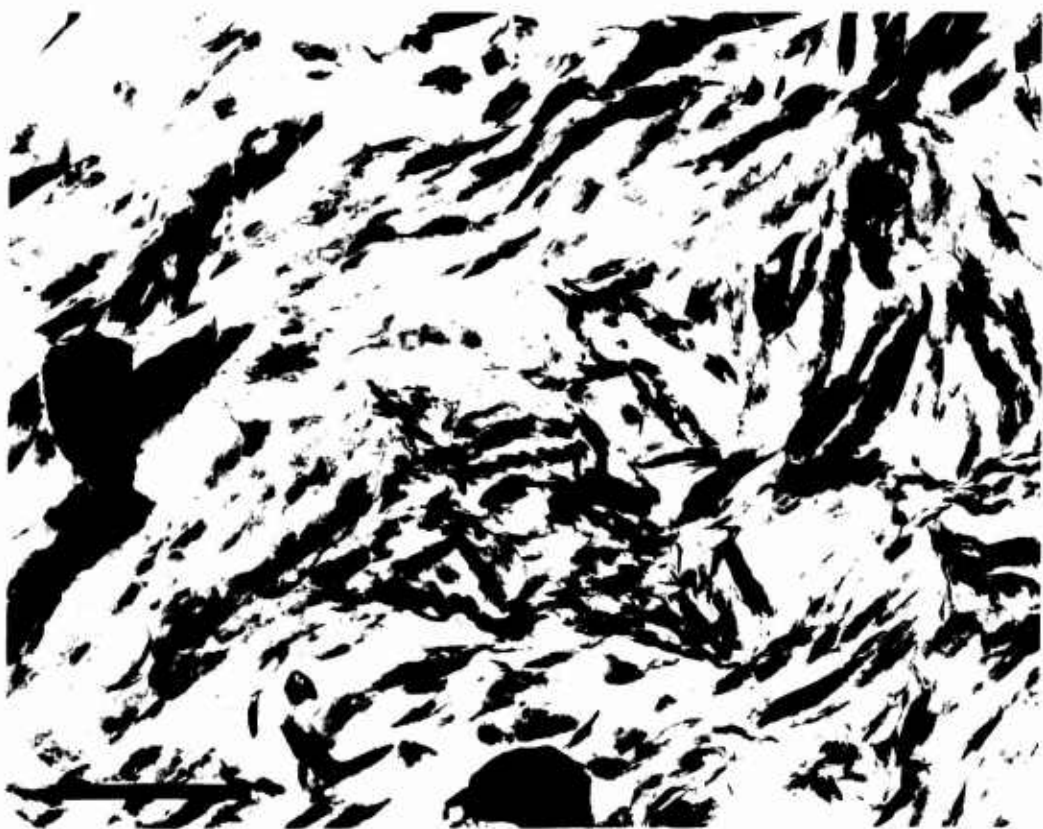


Figure 24. Clay fabric T.E.M. photomicrograph of an illite/smectite-rich marine clay from the Mississippi Delta, Gulf of Mexico, at a subbottom depth of 50 m and consolidated by an imposed load of 800 kPa. Scale Bar = 1 μ m

sediments was undertaken to determine the consolidation characteristics of a fine-grained marine clay section that had a known stress history. Such a study might result in defining the model of the consolidation process of the "normally consolidated marine clay section"; an example model to be the red clays of the Pacific. What was expected to appear is a section of sediment that is normally consolidated ($OCR = 1$), that is, one that has had sufficient time to consolidate with no indications of erosion, no unknown stresses, only stresses created by the overburden having been applied. Thus, the sediments tested should be in a state of equilibrium where the fabric of the sediments is supporting the overlying material and the pore water pressures are equal to the hydrostatic pressure. An examination of Table 2 and Figure 31 shows the OCR for values of σ'_1 and indicates that the sediments at Site 576 are overconsolidated in the upper 30 meters, normally consolidated in the interval between 30 and

39 meters, and underconsolidated in the 39 and 52 m interval. The interval from 56 to 62 meters contained nannofossil ooze, which will not be considered in this discussion.

The overconsolidation characteristic of the surficial sediment at Site 576 was not totally unexpected. Numerous researchers have observed that in most marine deposits the uppermost sediments are in a state of "apparent overconsolidation," that is, the surficial sediments have strengths that are attributed to cohesion which exceed the preconsolidation stress. The strength of these surficial sediments is larger relative to the small overburden stresses imposed upon them in the field as well as in the laboratory during testing in an oedometer. The result is that the value of preconsolidation stresses is much larger than the effective overburden stresses, resulting in the "apparent overconsolidation effect." The overconsolidated sediments at Site 576, however, extend to a depth much

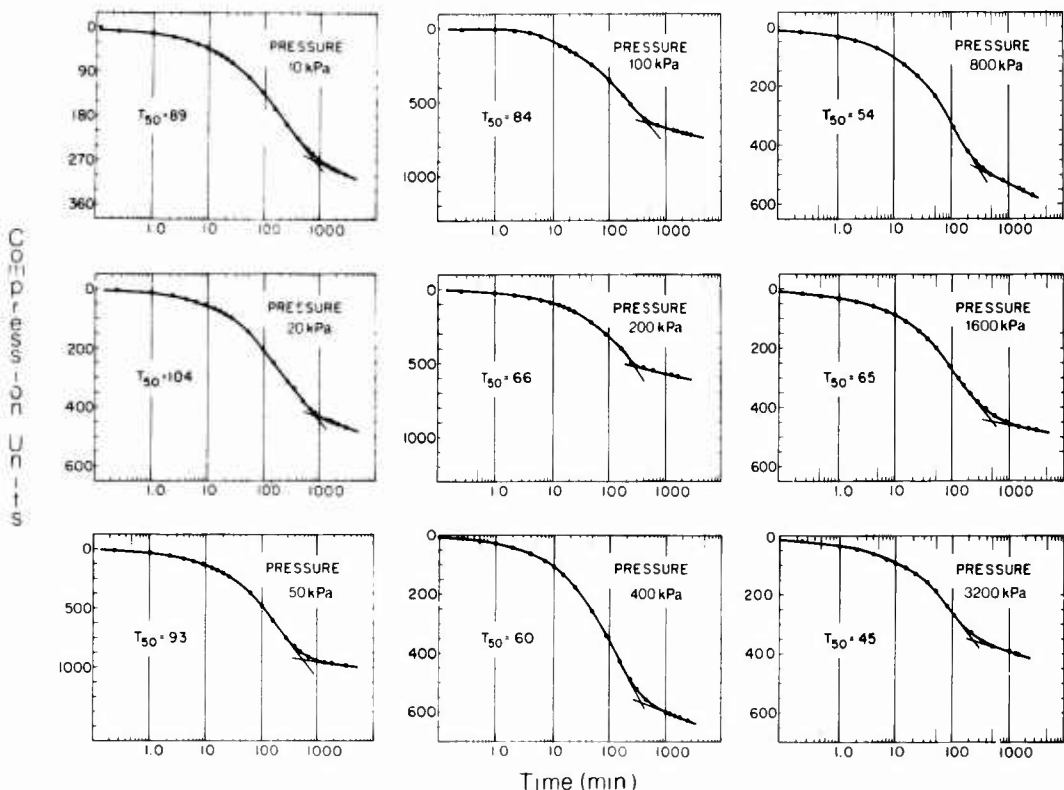


Figure 25. An example of time-compression curves of a high water-content marine clay. T_{50} indicates time required to reach 50% consolidation.

deeper (28 m) than has been previously observed in most other marine environments.

The appearance of underconsolidated sediments as determined by the Casagrande method (Casagrande 1932) in the 39 to 53 meter interval is much more difficult to explain than the overconsolidated shallow sediments. The sediments at Site 576 have been deposited over a long time period, sufficiently long for the sediments to have reached a state of equilibrium related to the consolidation process in both primary and secondary consolidation.

In addition to the use of the overconsolidation ratio (OCR) to express the consolidation state in terms of the preconsolidation stress (σ'_c) an additional quantity $\sigma'_c - \sigma'_o$ is used and referred to as the overconsolidation difference (OCD). The consolidation state defined by the OCD is as follows:

$$\text{OCD} = \sigma'_c - \sigma'_o = 0 \text{ normally consolidated}$$

$$\text{OCD} = \sigma'_c - \sigma'_o > 0 \text{ overconsolidated}$$

$$\text{OCD} = \sigma'_c - \sigma'_o < 0 \text{ underconsolidated}$$

The relationship of the overconsolidation difference (OCD) to the overconsolidation ratio (OCR) is illustrated in Figure 32. The parameters used for the illustration are from a normally consolidated marine sediment that has had portions of its overburden removed.

Figure 32(A) shows the overburden stress (σ'_o) and the preconsolidation stress (σ'_c) in the sediment. The overburden stress is zero at the seafloor while the preconsolidation stress has a value larger than zero because of its cohesion and the effects of loading from that portion of the overburden that has been removed. Figure 32(B) shows the OCR varies with depth and increases dramatically near the seafloor, whereas Figure 32(C) shows the OCD is constant with depth whose magnitude equals the buoyant weight of the overburden removed and the effects of cohesion. The use of the OCD avoids the mathematical variation, which is pronounced near the seafloor. The OCR with depth is unrelated to the geological history of the sediment (Olsen and others 1986).

Figure 33(A) displays the overconsolidation differ-

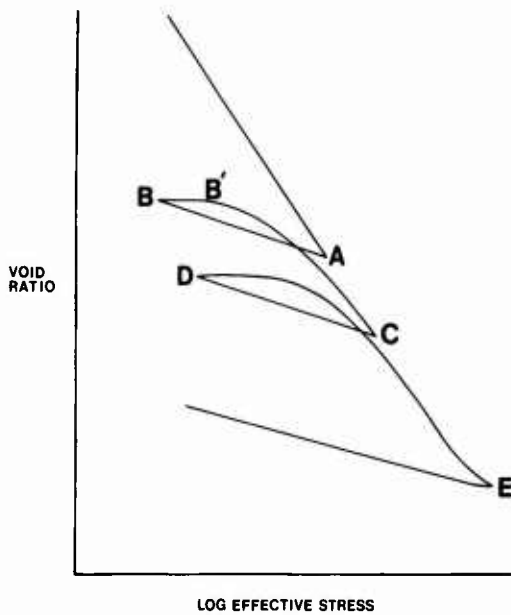


Figure 26. Void ratio (e) versus log of effective stress (σ') curve of a typical marine clayey sediment.

ence of the preconsolidation stress (σ'_{c1}) determined by Casagrande's method and the overburden stress (σ_o'). The results are similar to those shown in Figure 31 for the overconsolidation ratio (OCR) except the overconsolidation difference is almost constant (≈ 50) for the sediment in the upper 25 meters. It is obvious from their comparisons that the interpretation of the state of consolidation using standard consolidation test techniques depends upon the validity of the determination of the preconsolidation stress.

Preconsolidation Stress

Various investigators, including Cooling and Skempton (1942), Schmertmann (1955) Bernhard (1963), Bishop and others, (1965), concluded that the Casagrande method was inadequate under certain circumstances for determining the preconsolidation stress when applied to curves from oedometer tests. Other procedures for the determination of preconsolidation stress have been proposed by Burmister (1951) and Schmertmann (1955) but both methods require a rebound and reloading cycle. Schmertmann's technique applied to the red clays did not supply realistic values for the sediments between the 29 to 55 meter interval of Site 576 sediments. A multitude of possibilities may produce an apparent preconsolidation stress. Table 3

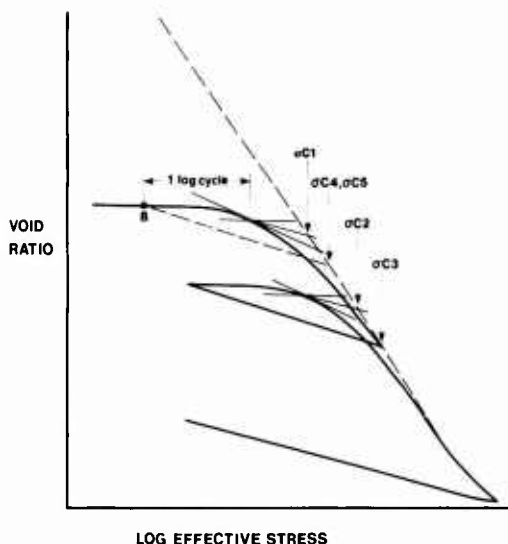


Figure 27. Hypothetical void ratio-log effective stress (e -log σ') curve showing how the calculated preconsolidation stress varies depending on the technique used (see explanation in text). σ'_{c1} is the preconsolidation stress calculated using the Casagrande (1936) technique. σ'_{c2} is the preconsolidated stress calculated using the Casagrande technique on the hysteresis loop on the e -log σ' curve. σ'_{c3} is the actual preconsolidation stress for the hysteresis loop. σ'_{c4} is the preconsolidation stress determined using the rebound characteristics and the hysteresis loop or the following relationship: $\sigma'_{c4}/\sigma'_{c2} \times \sigma'_{c1}$. The σ'_{c5} is the preconsolidation stress determined using point B and the slope of the rebound curve.

summarizes the main mechanisms and processes than can cause a preconsolidation stress (modified from Brumund and others 1976). The effects of coring (remoulding or disturbance of the clay fabric by overcoring, side friction, etc.) and high hydrostatic pressures have been added to Brumund's list.

The most probable causes of the apparent overconsolidation of the upper 28 meters of sediment at Site 576 are changes in the soil structure due to chemical alterations in the form of cementing agents, aging effects, the development of authigenic smectite and high electrical interparticle bonds. The effects of high hydrostatic pressures may cause induced effective stresses but the magnitude is unknown and presumably is insignificant. Brumund and Callender (1975) suggested that the apparent preconsolidation stress present in deep marine sediment is related to high hydrostatic pressures. Lee (1984), however, suggested that clays exposed to hydrostatic pressure of 75 to 100 MPa would have an induced effective stress of 2 to 5 kPa. These values, however, are insignificant in relationship to the values of preconsolidation stress determined by

Table 2. Summary of Preconsolidation Stress Values Calculated Using Casagrande's Techniques Incorporating the Sediment Expansion Characteristics Described in the Text

Depth (m)	Initial void ratio e_0	Preconsolidation stress (kPa) σ'_0		Overconsolidation ratio		Preconsolidation stress (kPa) σ'_1		Overconsolidation ratio		Preconsolidation stress (kPa) σ'_2		Overconsolidation ratio		Investigator	
		Overburden stress (kPa)	solidation stress (kPa) σ'_{01}	solidation difference (kPa)	Overconsolidation ratio	Overburden stress (kPa)	solidation stress (kPa) σ'_{12}	Overconsolidation ratio	Overburden stress (kPa)	solidation stress (kPa) σ'_{23}	Overconsolidation ratio	Overburden stress (kPa)	solidation difference (kPa)		
1.40	6.12	4.48	25	5.58	20.52	25	5.58	20.52	70	15.60	65.52	1	—		
2.45	3.77	7.52	76	10.11	68.48	76	10.11	68.48	—	—	—	—	—	2	
2.55	3.78	7.86	52	6.62	44.14	52	6.62	44.14	—	—	—	—	—	3	
3.00	4.70	9.44	34	3.60	24.56	—	—	—	—	—	—	—	—	4	
4.52	4.34	14.67	49	3.34	34.33	49	3.34	34.33	45	3.06	30.33	2	—		
5.00	4.19	16.40	57	3.38	40.60	—	—	—	54	—	37.60	5	—		
5.60	4.46	18.10	88	4.86	69.90	—	—	—	—	—	—	4	—		
7.40	4.56	23.90	67	2.79	43.10	67	—	43.10	—	—	—	1	—		
7.54	4.62	24.27	69	2.84	64.73	96	3.95	91.73	64	2.84	59.73	2	—		
9.72	4.77	30.81	89	2.89	58.19	89	2.89	58.19	—	—	—	2	—		
10.23	5.64	32.39	106	3.27	73.61	106	3.27	73.61	85	2.62	52.61	5	—		
11.11	5.16	34.74	121	3.48	86.26	136	3.91	101.26	110	3.16	72.26	2	—		
11.60	5.27	36.22	84	2.32	47.78	—	—	—	68	1.87	71.78	5	—		
11.66	4.91	36.39	74	2.03	37.61	74	2.03	—	—	—	—	5	—		
12.21	5.74	38.12	106	2.78	67.88	—	—	—	—	—	—	5	—		
13.15	5.04	40.96	152	3.71	111.04	170	4.15	129.04	—	—	—	1	—		
13.52	4.77	42.12	140	3.23	97.88	140	3.23	97.88	85	2.01	42.88	2	—		
15.50	4.58	48.80	94	1.93	45.20	121	2.48	72.20	75	1.53	26.20	5	—		
16.15	4.61	50.65	135	2.67	84.35	171	3.37	120.35	110	2.17	59.35	1	—		
16.22	4.48	50.86	135	2.65	84.15	207	4.07	156.15	97	1.90	46.15	2	—		
19.54	4.22	63.00	96	1.52	30.00	114	1.80	51.00	83	1.31	20.00	5	—		
20.76	2.97	67.87	195	2.87	127.13	208	3.06	140.13	190	2.79	122.13	2	—		
22.43	3.81	74.64	61	0.82	-13.64	151	2.02	76.36	115	1.54	40.36	5	—		
22.65	3.65	75.53	73	0.97	-2.53	82	1.08	6.47	—	—	—	1	—		
22.86	2.75	76.40	113	1.48	-36.60	—	—	—	—	—	—	5	—		
24.34	3.66	82.70	120	1.45	37.30	120	1.45	37.30	74	0.89	-8.70	2	—		
25.65	3.10	88.04	218	2.48	-29.60	—	—	—	—	—	—	1	—		
26.02	3.24	89.63	96	1.07	105	1.17	15.37	85	0.95	-4.63	2	—			
Average Values		—	3.09	42.24	—	3.48	71.88	—	2.94	45.85	—				
30.09	3.24	106.13	90	0.85	-16.13	90	0.85	-16.13	80	0.75	-26.13	2	—		
30.40	4.33	107.67	88	0.82	-19.67	—	—	—	—	—	—	4	—		
30.60	4.13	108.02	88	0.81	-20.02	160	1.48	51.98	61	0.56	47.02	5	—		
32.15	4.11	113.51	145	1.28	31.48	190	1.67	76.49	125	1.10	11.49	1	—		
32.47	4.32	114.62	140	1.22	26.49	230	2.00	116.49	—	—	—	2	—		
34.40	3.66	121.58	140	1.15	18.42	281	2.31	159.42	180	1.48	58.42	5	—		
35.29	3.56	125.09	155	1.24	29.90	254	2.03	128.90	210	1.67	84.70	2	—		
39.37	4.00	141.52	113	0.80	-28.52	—	—	—	110	0.77	-31.52	2	—		
40.36	3.84	145.35	70	0.48	-65.45	169	1.16	33.55	78	0.54	-57.45	2	—		
41.04	3.32	147.86	120	0.81	-27.86	237	1.60	89.14	180	—	32.14	2	—		
41.65	3.22	150.46	130	—	—	—	—	—	—	—	—	1	—		
42.02	3.18	152.05	120	0.78	-32.05	237	1.56	84.95	180	1.18	27.95	2	—		
43.30	2.80	157.78	90	0.57	-67.78	126	0.79	-31.78	140	0.88	-17.78	5	—		
44.61	2.67	163.66	109	0.66	-48.78	145	0.88	-12.78	180	1.10	22.22	2	—		
44.65	2.88	163.83	155	0.95	-8.83	299	1.82	135.17	340	2.07	176.17	1	—		
44.97	3.26	165.23	92	0.56	-72.23	236	1.43	70.77	200	1.21	34.77	2	—		
45.60	3.31	168.50	140	0.83	-28.50	275	1.63	106.50	200	1.18	31.50	2	—		
47.20	3.74	174.47	75	0.43	-99.47	273	1.56	98.53	185	1.06	10.53	2	—		
48.15	3.62	177.93	183	1.03	5.07	—	—	—	—	—	—	1	—		
48.21	3.14	178.15	130	0.73	-48.15	319	1.79	140.85	250	1.40	71.85	2	—		
49.60	3.76	183.95	130	0.71	-53.95	—	—	—	250	1.36	66.05	5	—		
49.65	3.40	184.00	67	0.36	-117.00	—	—	—	—	—	—	5	—		
51.36	3.20	191.45	110	0.57	-81.45	299	1.56	107.55	170	0.88	-21.45	2	—		
53.65	3.09	201.40	180	1.39	78.60	—	—	—	330	1.64	128.60	5	—		

(1) P. Schultheiss, Institute of Oceanographic Sciences; (2) W. Bryant, Texas A&M University; (3) R. Schiffman, University of Colorado; (4) M. Noorany, San Diego State University; (5) A. Silva, University of Rhode Island.

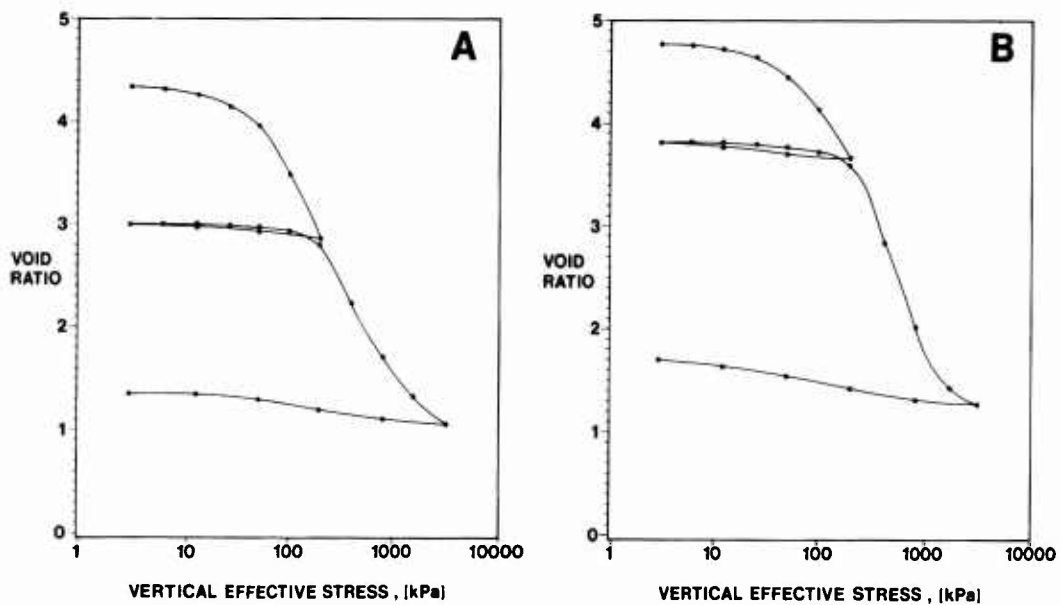


Figure 28. Void ratio versus log of effective stress (e -log σ') curves of Hole 576A sediments located in subunit 1A. (A, sample from 4.2 m and B, from 13.5 m subbottom).

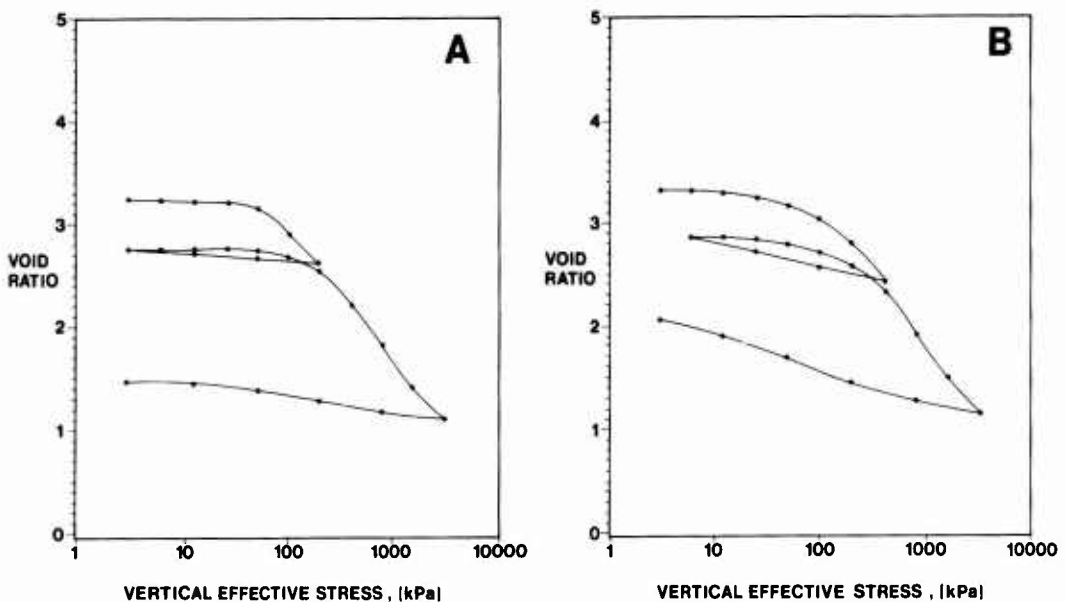


Figure 29. Void ratio versus log of effective stress (e -log σ') curves of Hole 576A sediments located in subunit 1B. (A, sample from 32.5 m and B, from 45.6 m subbottom).

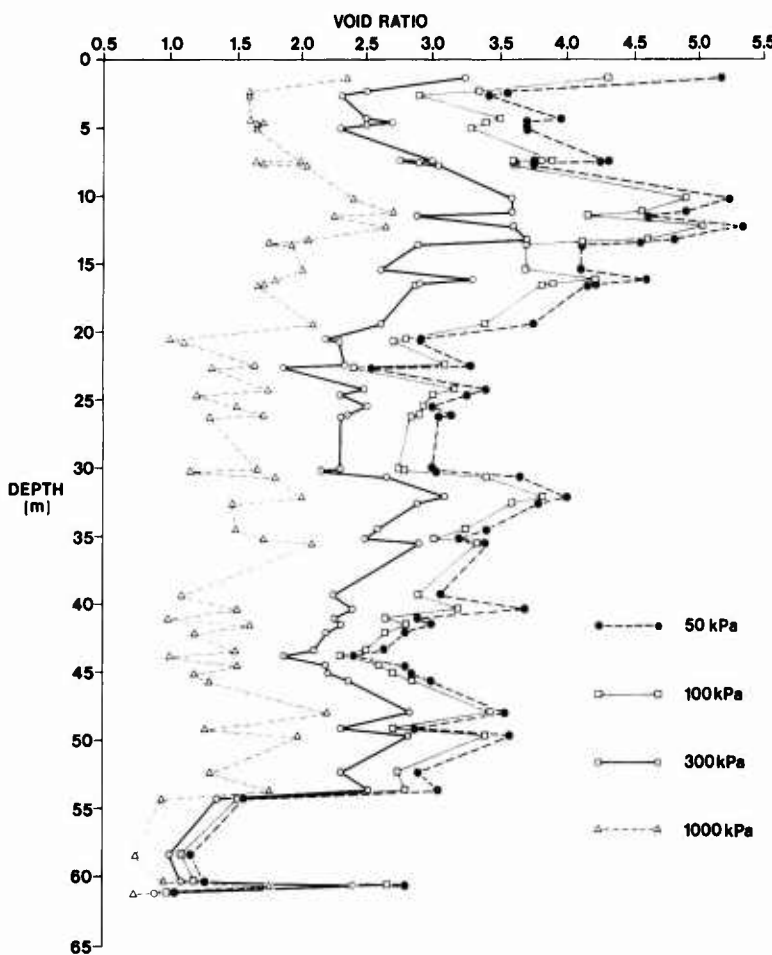


Figure 30. Summary of consolidation test results for Hole 576A sediments. Sediment response to increasing applied stress for each sample tested is displayed as changing void ratio at the same depth. A pronounced change in compressibility with depth at four applied stress levels occurs between subunit 1A and 1B (28 m subbottom).

the Casagrande method for Site 576 sediments. The effects of coring, cementation, secondary compression (aging), and electrical bonds appear only to apply in the upper 28 meters of sediments. The sediments below that level are in normal to underconsolidated states as determined by the Casagrande method for determining σ'_{c1} . The sediments between the 38 to 53 meter depths are underconsolidated to the same order of magnitude as the upper sediments are overconsolidated (Fig. 33(A)).

The mechanisms attributed to low preconsolidation stress relative to the overburden stress (underconsolidation) are rapid rates of deposition, coring disturbance, chemical alterations, and the presence of excess pore pressures (Bennett and others 1981). The only acceptable explanation for the observed degree of underconsolidation of Site 576 sediments is that the method of determining the preconsolidation stress

(σ'_{c1}) is inadequate and underestimates σ'_c . Core disturbance may be a factor but we do not think it is the governing factor for these sediments.

Examination of the e -log σ' curves (Figures 28 and 29) shows that the rebound of the unloading portions of the curves increases with depth below the seafloor. A plot of the expansion index (a measure of the rebound) versus depth is shown in Figure 34. From examination of the e -log σ' plots it appears that as the magnitude of the expansion index increases, an error arises in the determination of the preconsolidation stress as determined by the Casagrande method. This can be demonstrated by examining the unloading and reloading portions of the hysteresis loop of the e -log σ' curve in Figure 29(B). The unloading portion of the hysteresis loop started at a stress level of 400 kPa. Thus the preconsolidation stress at the time of unloading was 400 kPa. However, a value of 260 kPa

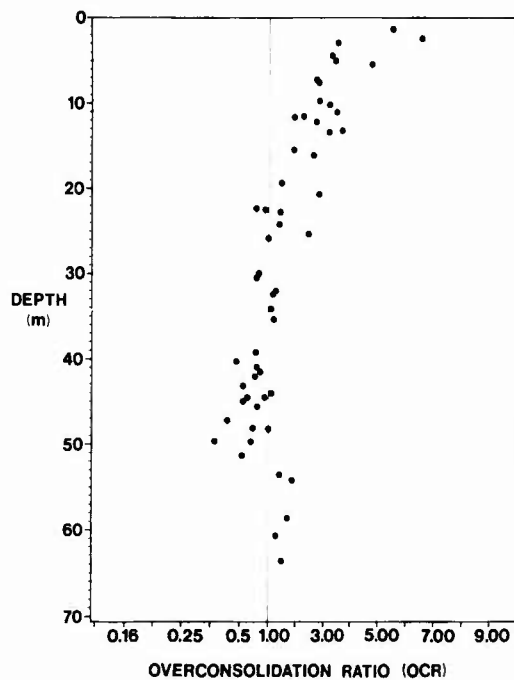


Figure 31. Overconsolidation ratio-depth profile using preconsolidation stress value σ'_c , determined from static-load consolidation test results from Hole 576A sediments. Overconsolidation scale reciprocal below 1.00 and linear above 1.00.

was determined for the preconsolidation stress by the Casagrande method. From the known value of the preconsolidation stress, and that determined graphically, a relationship between the difference in preconsolidation stress as determined by the Casagrande technique and the expansion index of the material was determined (Fig. 35). This relationship was used to adjust the values of preconsolidation stress of the initial reload portion of the e -log σ' curve as determined by the Casagrande method. These adjusted values are listed in Table 2 as σ'_{c4} .

Another method devised herein to determine the preconsolidation stress is shown in Figure 27. This method is based on the characteristics of the rebound curve and the assumption that those characteristics are constant for a given sediment sample. Examination of all the Hole 576A e -log σ' curves with rebound portions substantiates this assumption. Schmertmann (1955) addressed a similar problem and demonstrated that variations were predictable. The rebound method to determine the preconsolidation stress is as follows: a point on the recompression curve where the void ratio is constant or at a maximum is chosen. This point

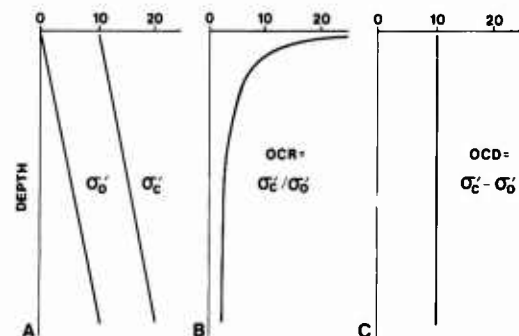


Figure 32. Preconsolidation and overburden stress plots: (A) Overburden stress (σ'_0) and preconsolidation stress (σ'_c) versus subbottom depth; (B) Overconsolidation ratio as a function of depth downhole; (C) Overconsolidation difference as a function of depth downhole.

is the largest vertical effective stress along the line of constant e , (point B in Fig. 27). If that point is ambiguous, a point one log-cycle before the point of maximum curvature of the reload curve is used. From that point a line parallel to the rebound portion of the e -log σ' curve is extended to intersect the virgin curve. That intersection is determined to be the preconsolidation stress. Values derived by this method are listed in Table 2 as σ'_{c5} . Thus, Table 2 lists the values of preconsolidation stresses as determined by three different techniques:

1. Casagrande (σ'_{c1}),
2. the intersection of an assumed rebound curve and the virgin curve (σ'_{c5}),
3. adjustment of Casagrande values (σ'_{c4}) using the difference between Casagrande values (σ'_{c1}) and known values of σ'_{c3} of the unload and reload curve (σ'_{c2}) (Fig. 27).

A plot of the overconsolidation difference (OCD) using the preconsolidation stress values (σ'_{c5}) (Fig. 33(B)), shows that the sediments are in a similar state of consolidation as those of Figure 33(A) except that the sediments below the 33 meter level are more overconsolidated. Figure 36(A) is the OCD conditions for values of σ'_{c4} . It shows that all the sediments except for a short segment between the 27 and 30 meters interval are overconsolidated. Figure 36(B) shows the compression index for the red clays. The compression index is a constant C_c in the relationship

$$e = e_o - C_c \log \frac{\sigma'}{\sigma'_o} \quad (1)$$

where e_o is the void ratio at pressure σ'_o and e is the void ratio at pressure of σ' ($e < e_o$, $\sigma' > \sigma_o$). This is the equation of the straight portion of the virgin curve

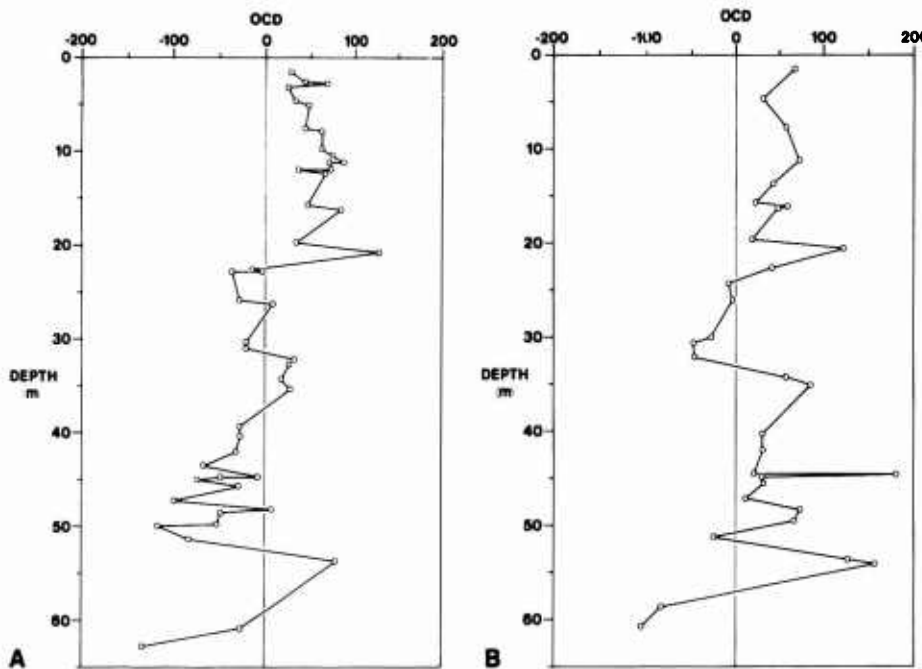


Figure 33. Overconsolidation differences: (A) Calculated using the preconsolidation stress values σ'_4 , versus subbottom depth at Hole 576A; (B) Calculated using the preconsolidation stress values σ'_c , versus subbottom depth at Hole 576A.

plotted with the logarithm of pressure as the abscissa and the void ratio as the ordinate. Comparisons of Figures 36(A) and (B) show that there is a direct correlation between the OCD of σ'_4 and compression index (C_c).

The horizontal lines on Figure 36(B) indicate the top and bottom of the seven cores taken at Hole 576A. Trends in the values of the compression index, such as the decrease in C_c across the boundary at the 18 m level and an increasing trend at the 8.5 m core boundary, indicates the cores were relatively undisturbed. The compression index is highly affected by the disturbance of the sediment. Trends that continue across the bottom of a core and into the top of the next core indicate minimal disturbance.

Factors Affecting the Consolidation Process

Examining the factors that affect the consolidation process provides insight into the various methods of determining the preconsolidation stress presented above. The major factors that affect all physical properties at Site 576 are:

1. Core disturbance—this offsets the test results.
2. Mineralogy

3. Grain size
4. Time dependent processes
5. Depth of burial
6. Microstructure.

The term "disturbance" is used in two contexts. First, sampling (coring process) will, by its very nature, induce a stress relief and rebound of the sample. If no major fabric changes have been induced by the sampling process and subsequent handling, the virgin compression curve can be reconstructed in the laboratory. The Casagrande (1936) construction is predicated on this concept of no disturbance, or "perfect sampling." The second form of disturbance is one in which the fabric of the sediment is altered in the coring process, handling, and initial testing phases. This remoulding type of disturbance can be caused by double coring, friction of the core barrel, laboratory handling, etc. The remoulding effect is generally indicated by flattening of the e -log σ' curve (lower values for the compression index C_c). The discontinuity between the overconsolidated and the normally consolidated portion of the e -log σ' curve becomes less distinct.

Oedometer tests on soft sediments often show a modified preconsolidation stress (Scully and others

Table 3. Mechanisms that Cause a Preconsolidation Stress

Item	Remarks and References
Change in total stress due to:	
(1) Removal of overburden	
(2) Past structures	
(3) Glaciation	
(4) Coring	
(5) High hydrostatic pressures	Brumund and Gallender (1975)
Changes in pore water pressure due to:	
(1) Changes in water-table elevation	Kenney (1964) gives sea level changes
(2) Artesian pressures	Common in glaciated areas
(3) Deep pumping	Common in many cities
(4) Desiccation due to drying	May have occurred during deposition
(5) Desiccation due to plant life	May have occurred during deposition
Changes in soil structure due to:	
(1) Secondary compression (aging)	Leonards and Ramiah (1959) Leonards and Altschaeffl (1964) Bjerrum (1967, 1972, 1973)
(2) Environmental changes, such as pH, temperature, salt concentration	Lambe (1958)
(3) Chemical alterations due to: 'weathering', precipitation of cementing agents, ion exchange	Bjerrum (1967)
(4) Coring	
Change of strain rate on loading	Lowe (1974)

1984). This effect can be attributed to the initial seating of the porous stones and loading platens in the test, and possibly side friction during the test. This effect certainly contributes to the characteristics of Site 576 samples, but its magnitude is undoubtedly small.

In most deep marine environments, and especially the one at Site 576, the depositional mineralogy and grain size of illite, quartz, and kaolinite are relatively constant. These properties do not change significantly with time or depth of burial as long as the depth of burial is fairly shallow (~ 1000 meters). Illite, kaolinite, and quartz, the main minerals present in the upper sections at Site 576, do not undergo major diagenetic alteration except in the presence of high temperatures, high pressures and ion exchange. Time alone, or shallow depth of burial, does not have a diagenetic effect, except for consolidation. The smectite present, however, is a diagenetic product.

The sediments at Site 576 have been deposited over such a long period of time and at such a low rate of

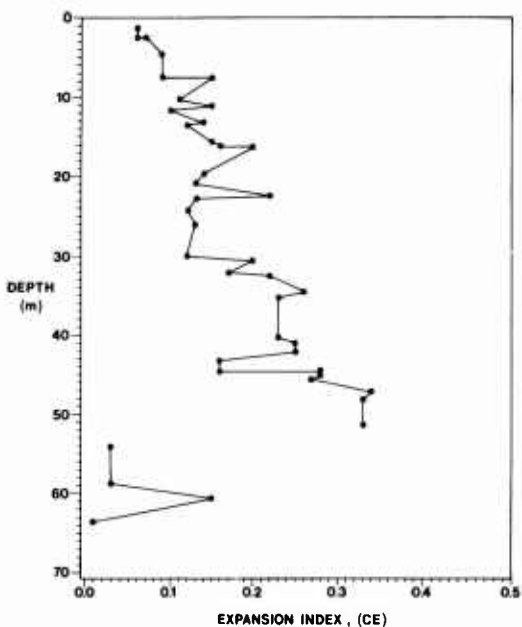


Figure 34. Expansion index-depth profile determined using the rebound portion of the e -log σ' curve generated from consolidation test results completed on Hole 576A sediments.

accumulation that time related to consolidation is essentially infinite. All physical processes related to time, i.e., primary and secondary consolidation, have taken place and the sediment system should be in a state of total physical equilibrium. Thus, if disturbance is minimal, the major factors affecting the consolidation process at Site 576 are mineralogy, microstructure and depth of burial (overburden stress).

Mineralogical changes due to chemical alterations in the form of cementing agents, such as organics, calcium carbonate, or silica, have been suggested as the factors responsible for the overconsolidation of the upper sediment at Site 576 (Dadey 1983). There is no conclusive evidence that such conditions existed. It would be fortuitous indeed if the cementing process only takes place in the shallow deposits of the oceans and is not observed in the deeper buried sediments. Of course, the effects of cementation may have the greatest influence on the consolidation process in the near-surface sediments than those buried deeper. It would be difficult to accept the effects of cementation if the preconsolidation stresses presented by σ'_{c1} in Table 2 are correct. If, however, the preconsolidation stresses represented by σ'_{c4} and σ'_{c5} are valid, then cementation effects are made more plausible. If cementation of the clay particles has taken place and has had a marked effect on the consolidation process, the ce-

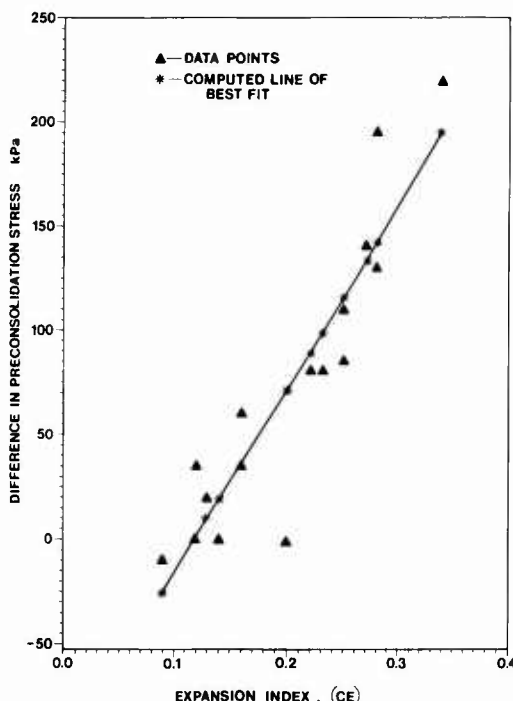


Figure 35. Relationship between the expansion index and the difference between known preconsolidation stress determined using a hysteresis loop and the preconsolidation stress determined graphically using the Casagrande technique (see text for explanation). As the expansion index increases the difference between the known and calculated preconsolidation stress values also increases. Asterisks (*) represent regression analysis results ($\gamma = 0.83$).

mentation also should be reflected in the strength of the sediments. No such effect has been observed (Initial Reports of DSDP, 86).

Illite comprises approximately 50–70 percent of the clay minerals present in the red clays and quartz appears in amounts ranging from 1.76 to 18.1 percent. Thus, one of the largest variations in mineralogical content is the amount of quartz present. Figure 37 shows the relationship between depth, void ratio (at 50 kPa), percent quartz, and percent sand and silt. The largest variations in percent sand and silt present occur where the quartz content is the largest, in the upper 20 meters and at a position between 38 and 47 meters where the quartz content is consistently low. An unusual relationship is found between the void ratio and the percent sand and silt in the upper 23 meters; the higher the sand-silt percentage the higher the void ratio. This is not the normal relationship between void ratio and grain size for marine sediments. In the interval between 42 to 45 meters in the core the void

ratio decreases from 3.9 to 2.5 over a 3 meter section and then increases to 3.8 over a 5 meter interval. Over these two intervals grain size (percent sand and silt) increases in almost equal proportions to the decrease in void ratio. This inverse relationship between grain size and void ratio is the normal one found in most marine sediments.

Figure 37 shows that in the upper 20 meters of sediment the quartz content ranged from 8.87 to 18.11 percent. Over that 20 meter interval the void ratio increased from 3.0 (75 percent porosity) to 5.2 (84 percent porosity). This means that the amount of quartz present accounts for approximately 1.44 to 4.5 percent of the total volume of the sediment. In this low concentration none of the quartz particles could be touching each other; then when they are suspended in a clay matrix the quartz would have little effect on the strength or the consolidation process of the sediments at Site 576. In addition, not all of the sand- and silt-sized material is quartz. Figure 37 shows that at the 13 meter level quartz accounts for only 17 percent of the 52 percent of the sand and silt fraction. No material in the silt range was detected other than quartz and shale clasts (domains; face-to-face clay particles). The only conclusions one can draw is that the major part of the silt fraction in the upper 20 meters consists of domains (aggregates).

Bennett and others (1981) performed a clay fabric analysis on a Pacific red clay sample taken during DSDP Leg 16 and described the fabric as a highly complex structure of linked chains of clay flocs with large intravoid spaces (Figs. 38 and 39). The presence of clay flocs in red clays is consistent with the concept of clay aggregates being the main source of the silt-sized sediments. The zeolitic aggregates were sufficiently bonded to resist the deflocculation process that takes place during size analysis and remoulding (Fig. 40). The red clay is a good example of a fabric creating a high void ratio which is maintained at depths of 143 m; reasonably strong structural integrity with high overburden.

If the illite, chlorite, and kaolinite clays at Site 576 have not undergone extensive alterations with time, which has been suggested, then the unusual consolidation behavior of these clays must be from high bonding strength of smectite and fine-grained nature x-ray amorphous material. This would account for the observed overconsolidation results obtained from the oedometer tests.

There are several conclusions that can be drawn from the above data. First, the Pacific red clays are clearly not the standard marine sediment in a soil mechanics sense that was originally presumed. In fact, these clays behave in ways which diverge from conventional wisdom.

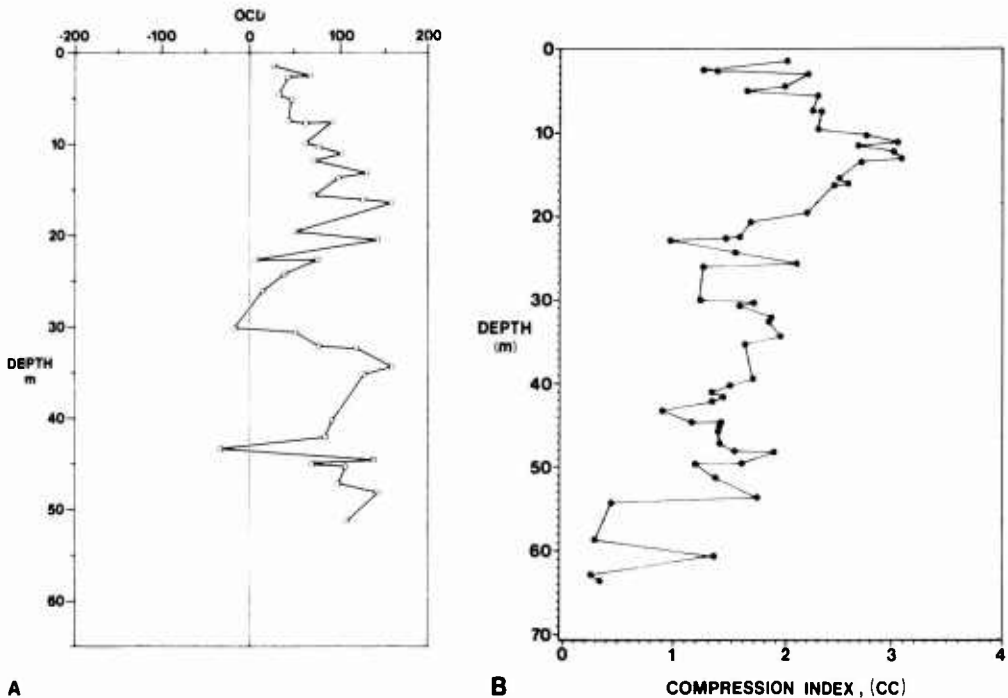


Figure 36. Relationship between the consolidation difference and compression index; (A) Overconsolidation subbottom depth plot. Overconsolidation difference determined using preconsolidation stress value σ'_c ; (B) Compression index plotted against subbottom depth. Horizontal lines indicate top and bottom positions of the seven cores taken at Hole 576A.

Regardless of how we determine the preconsolidation stress (σ'_c) by graphical means, the data indicate that the material is overconsolidated by classical definition. Several reasons have been hypothesized. These are:

1. Microstructure, microfabric electrical bonding between clay particles, mainly smectite.
2. Cementation-chemical bonding.
3. Inaccuracies in the calculation procedure for the preconsolidation stress.
4. Mechanical effects including core disturbance, remoulding, and testing procedures.
5. High hydrostatic pressure.

Discussion

Fabric of Red Clays

The fabric of the red clays consists of illitic-shale clasts, quartz, and authigenic smectite accompanied by small amounts of chlorite and kaolinite. Authigenic smectite appears as diagenetic by-products of volcanogenic material. The nature of the smectite is shown in the

TEM and SEM photomicrographs (Figs. 41–45). The smectite revealed in the TEM consists of very fine, thin sheets with their edges curled (Figures 41 and 42). The curling of the smectite gives it a needle-like appearance and is attributed to the dehydration process that the material undergoes during the critical point drying procedures. The effects of dehydration on smectite sheets was demonstrated by Fukushima and others (1980) and their examples are identical to those shown in Figure 18.

Extensive microfabric analysis during this study has shown that the authigenic smectite occurs in three forms and is ubiquitous throughout the red clay section. One form is extremely fine-grained and x-ray amorphous (Fig. 20). An intermediate form is x-ray detectable and slightly better developed in size and shape (Fig. 41). A third form is well developed in size and shape (Figs. 43, 44, and 45). Smectite is the common material that supports and binds the shale clasts and provides the necessary strength (cohesion) that resists deformation to the point of rendering the sediment "overconsolidated." Similar "binding" material was observed to surround the large particles which formed the primary elements of the fabric in Mississippi Delta

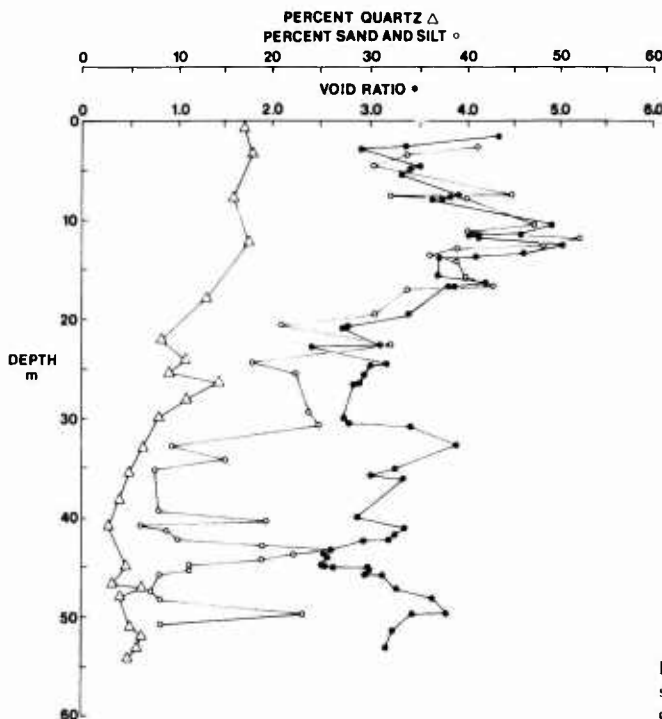


Figure 37. Variations in void ratio (●) sand- and silt-size fraction (○) and percent quartz (Δ) with depth in core for Hole 576A sediment.

clays (Bennett and others 1977, p. 66). This binding material was observed in TEM stereographs.

The pre-Miocene red clays consist of up to 70 percent authigenic smectite and 30 percent aeolian quartz and shale clasts. Lyle (1979) alluded to the presence of smectite in the Pacific Basin. He theorized that amorphous Fe-Mn oxyhydroxides recrystallize into iron-rich smectite and manganese micronodules. The majority of the amorphous material present in the red

clays examined by Leinen (1985) may be the microcrystalline smectite shown in Figure 20. Repeated attempts to identify this material by selected area diffraction (SAD) proved to be fruitless because of the small crystal size. The identification of authigenic smectite is based solely on transmission electron microscope and scanning electron microscope observations of the morphology which is supported by observations of smectite by Welton (1984). The binding strength of smectite lies in its large surface area (actively e.g., large CEC) relative to its total volume. The smectite sheets may be only 2 to 5 layers thick, but the total exposed surface area relative to its mass is very large.

Examination of the major constituents of the sediment and their contribution to the fabric and the strength of the clay system provides considerable information regarding the nature of these clay deposits. The most significant component of the clays are the shale clasts. They form the main body of the clay fabric. However, unlike fluvial detrital or sheet-like illitic clays, the well rounded shale clasts do not interact with each other to form a randomly arranged domain fabric as is depicted in Figures 5 and 23, which is typical of many marine deposits (Bennett and others 1977). Instead the shale clasts appear to be suspended in the



Figure 38. T.E.M. photomicrograph of DSDP Leg 16 red clay, 143 m subbottom. The clay is Cretaceous age and consists of smectite, illite, clinoptilolite, quartz, and other minerals. Scale Bar = 1 μ m.



Figure 39. Enlarged TEM photomicrograph of central portion of Figure 38 showing smectite floes with high intra voids and long linking chains. Scale Bar = 1 μ m

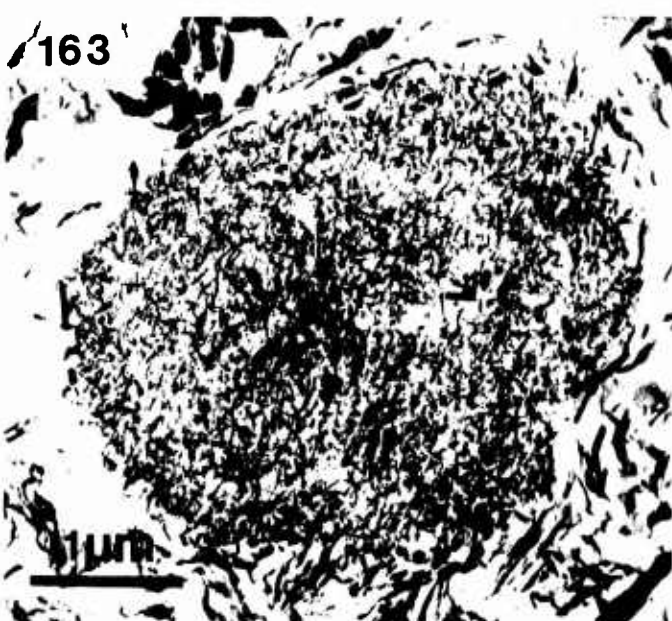


Figure 40. TEM photomicrograph of sediment from same area and depth as Figure 38 showing a large clinoptilolite aggregate with high intra voids that maintains structural integrity during remolding. Scale Bar = 1 μ m



Figure 41. T.E.M. photomicrograph of smectite fabric from Core 2, Section 2 (21 m subbottom), Hole 576A. Contrast development of smectite in this figure with that in Figure 20. Scale Bar = 0.5 μ m.

smectite and other materials and this microfabric may be explained by the shape of the clasts. In all photomicrographs taken the clasts display a high degree of roundness. Rounding may be due to abrasion or chemical degradation during transport processes and/or the aeolian history of the clasts. The presence of round clasts may be attributed to a sorting process during aeolian transport. In any case, the rounding produces an unusual effect; it essentially exposes predominately the edges of the individual clay sheets. The broken ends of an illite particle often carry a *small positive charge*. Figure 46 shows that regardless of the shape of the particle, the edges of the clay layers are predominately exposed in a particle that has a high roundness factor. This in essence inhibits the mutual attraction or interparticle bonding of the clasts but would promote their interaction with the face (flat portion) of the smectites and sheet-like illite particles as observed in the micrographs. The results are that the shale clasts are dispersed within the fabric and are supported by the authigenic smectite. The small end

charge of the illite particles may actually induce repulsion between the clasts. There also may be a symbiotic relationship between the shale clasts and the smectite in that the clasts may act as catalysts for the precipitation of the smectite on the surface of the illite.

A series of models depicting the fabric of North Pacific Basin Pleistocene red clays is presented in Figures 47 through 49. In each case the proceeding figure represents a section which is one order of magnitude smaller than the following figure. Figure 47(A) depicts the fabric of a section 10^{-2} m square. The quartz is represented by small spheres. In all cases the amount of material shown as quartz is in proportion to the amount present in a real sample. Figure 47(b) represents the fabric of a section 10^{-3} m square. This figure shows that the quartz is necessarily dispersed throughout the fabric due to its low concentrations. The supporting agent is authigenic smectite. Figure 48(A) represents an area 10^{-4} m square. This figure shows the relationship between the shale clasts



Figure 42. T.E.M. photomicrograph of smectite, same section as in Figure 41. Scale Bar = 0.1 μ m.

as has been depicted in the electron photomicrographs. Part of a quartz particle is shown in the upper right-hand corner of the figure. The shale clasts displayed represent their true concentration in thin-section. The shale clasts are held together by authigenic smectite. Figure 48(B) covers an area 10^{-5} m square. The relationship of the smectite and shale clasts are illustrated as well as the sparse nature of the clasts in a 80 percent porosity sediment. Figure 49(A) and (B) represent areas 10^{-6} m square and 10^{-7} m square. Figure 49(B) shows a portion of shale clast with authigenic smectite appearing in close contact. Similar models of the pre-Plio-Pleistocene red clays would consist of mostly smectite. Both quartz and illitic-shale clasts would appear in minor amounts relative to the smectite.

It appears that the three forms of smectite are the major factors that control the physical properties of red clays. The shale clasts, quartz, and other particulate material act as fillers which shorten the smectite links thus strengthening them and in the process es-

tablish a strong fabric that imparts an overconsolidation characteristic with a very low permeability. The strong bonds thus established explain the anomalous condition where the highest void ratios encountered in Site 576 sediments occur where the largest amount of silt-sized clay clasts are present. Examination of the data presented by the Geotechnical Consortium (1985) substantiates this interpretation. They showed that the liquid limit, plastic limit, water content, and shear strength of red clays increased with an enrichment in smectite and silt-sized aggregates.

Origin of North Pacific Red Clays

There is unanimity on the continental origin of the quartz present in the North Pacific red clays. The numerous references cited in the introduction all expressed the opinion that the quartz was transported by aeolian processes from an Asian source, mainly the loess deposits of Central and Eastern Asia.



Figure 43. S.E.M. photomicrograph of well developed smectite particles surrounding several large aggregates. Sediment from 21 m subbottom at Hole 576A. Scale Bar = 5 μ m.

In the past the origin of the clay minerals in the red clays has not been as controversial as the origin of the quartz. The reason is that detrital quartz is easily identified as aeolian by mineralogy and origin while the clays only could be identified by mineralogy. All the clay minerals, except smectite and palygorskite, in the Pacific red clays are probably detrital minerals inherited from the Asian continent. The process by which they are transported to the deep Pacific basin has not been well established. Illite has always been associated with the quartz, thus an aeolian origin of the illite is an accepted hypothesis.

The average mineralogical composition of the pre-Plio-Pleistocene red clays at Sites 576 and GPC-3 is as follows:

Illite 49 percent

Smectite 18 percent

Kaolinite and Chlorite 8 percent

Quartz 17 percent

Feldspar 6 percent

Other Material 2 percent

The average mineral composition of pre-Miocene red clays is:

Illite 25 percent

Smectite (including x-ray amorphous smectite) 55 percent

Kaolinite and Chlorite 9 percent

Quartz 5 percent

Feldspar 1.5 percent

Palygorskite 0.5 percent



Figure 44. S.E.M. photomicrograph of well developed smectite particles. From same area as sediment in Figure 43. Scale Bar = 5 μ m.

Amorphous Material (excluding amorphous smectite) 4 percent

It was recognized early that marine clays, in particular illite, were derived from continental sources (Correns 1939). Dietz (1941) did suggest, however, that illite found in samples from the Challenger Expedition were derived from montmorillonite by fixation of potassium ions in seawater. This reaction, however, is mainly dependent on high temperatures, large pressures, and time (Perry and Hower 1970, 1972). The authigenic origin of illite in surficial marine sediments, particularly deep water marine sediments such as the red clays, is now viewed as improbable. The conversion of smectite to illite is, however, an important reaction in the thick sediment that constitutes the major shale bodies on land as well as on the continental margin. Additional evidence that illite is detrital was given by Hurley and others (1959,

1963). They demonstrated that illite in recent sediments from rivers to pelagic deposits show clay fractions with potassium-argon ages greater than 100 m.y. In Prospero's (1981) extensive review of aeolian transport of sediment to the world ocean, illite was found to be the most prominent mineral in atmospheric aerosols. In the western North Pacific it constituted 52 percent of the total mineral aerosol. Quartz was 20 percent and plagioclase was 10 percent of the distribution.

The identification of illitic shale and argillaceous clasts by microfabric analysis (morphology and mineralogy) in this study essentially establishes that illite in the red clays is an inherited detrital mineral.

Most of the smectite in the North Pacific Basin is considered authigenic (Hoffert 1980, Leinen and Heath 1981). Schoonmaker and others (1985) suggested that the diagenetic imprint of authigenic smectite on the sediment composition of Site 576 is significant. They



Figure 45. S.E.M. photomicrograph of two large particles suspended in a matrix of well developed smectite. Sediment from Core 4, Section 4 (34 m subbottom) of Hole 576A. Scale Bar = 5 μ m.

base their conclusion on their observations of the correlation of abundance and composition of illite/smectite mixed-layer clay: the abundance of Fe, Mn, and associated trace metals and the presence of palygorskite. Contrasting views on the origin of smectite at Site 576 are presented by Lenotre and others (1985). They suggest the absence of large smectite laths or tufts typically developed from the alteration of volcanic lava, ash, or glass indicates a detrital origin of the smectite. Other indications are that palygorskite and smectite were not developed in nodules, concretions, or at specific levels but were dispersed completely among the detrital minerals. They found no relationship between the abundance of smectite or palygorskite and the presence or abundance of morphologically distinct volcanic particles and zeolites such

as phillipsite, or palagonite. In addition, the abundance and morphology of smectite was not correlated with the presence or abundance of opaque minerals, micronodules, iron oxide, or siliceous debris.

The mineralogical analysis of Hole 576A sediments by Leinen (unpublished observations 1985) (Table 1) shows that the total amount of x-ray detectable pre-Miocene clays was quite small while the amount of amorphous material present ranges from 45 to 80 percent of total mineralogical content.

Examination of the microfabrics of the Pacific red clays (Figs. 20 and 22) reveals the presence of a fleecy substance which is identified as x-ray amorphous smectite. This material is ubiquitous throughout the sediment column at Site 576 and is the major component of the pre-Plio-Pleistocene sediments. The

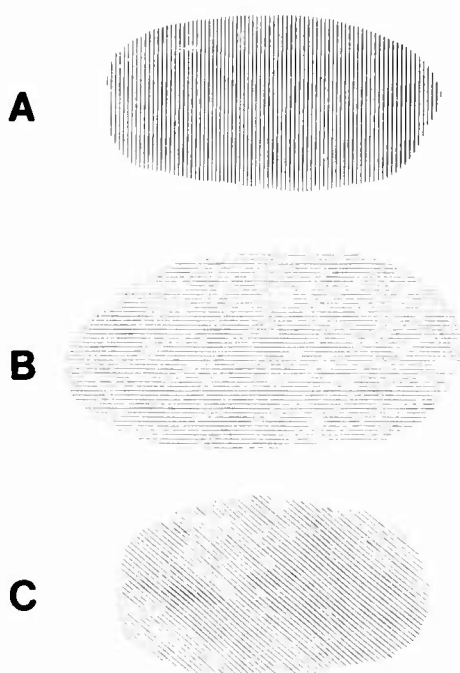


Figure 46. Illustration of cross-sectioned, well-rounded layered particles. Regardless of shape and layer orientation the majority of the surface consists of exposed ends of the layered material.

smectite of the x-ray amorphous material consisted of extremely small sheets, while another form of the smectite is well developed and consists of fairly large, individual sheets. Contrary to suggestions of Lenotre and others (1985) that the absence of large smectite laths or tufts indicates a detrital source for the smectite, the presence of the extremely small, delicate sheets of x-ray amorphous as well as a fairly crystalline smectite are indicative of authigenic processes.

The kaolinite, chlorite, and feldspar in the red clays are of the same origin as the illite, mainly windblown from the Asian continent. The amorphous material other than smectite present in the pre-Plio-Pleistocene sediments is amorphous metal oxides. Iron oxides were found to be the primary source of the other metal oxides (M. Leinen, personal communication 1985). The iron oxides are very fine (clay size), noncrystalline and are of an authigenic origin. The probable origins of the metal oxides in the pre-Miocene sediments as outlined by Leinen are:

1. During the early-mid Cenozoic, seawater in the oceans was not in equilibrium with elements such as iron and manganese. Consequently, these elements were precipitated and deposited at the sediment-water interface. The very fine-grained clay particles previously deposited at the interface then provided nuclei for the formation of fine-grained metal oxides.

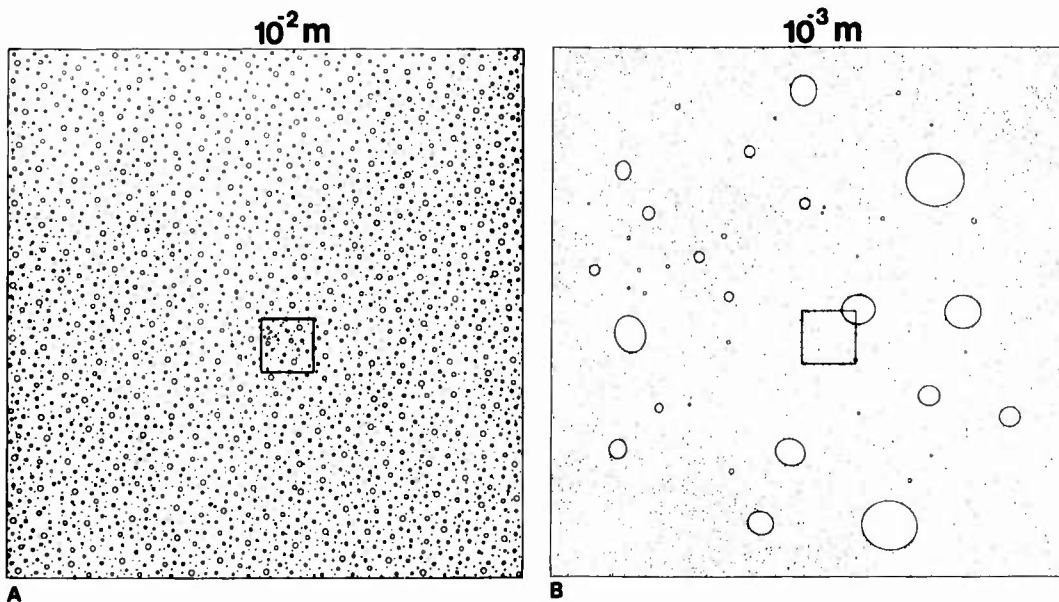


Figure 47. Graphic presentation of generalized model of red clay microfabric; (A) Dimension of field is 10^{-2} m. Small circles represent quartz particles. Small square in center of figure is field covered by Figure 48; (B) Dimension of field is 10^{-3} m. Large circles are quartz particles.

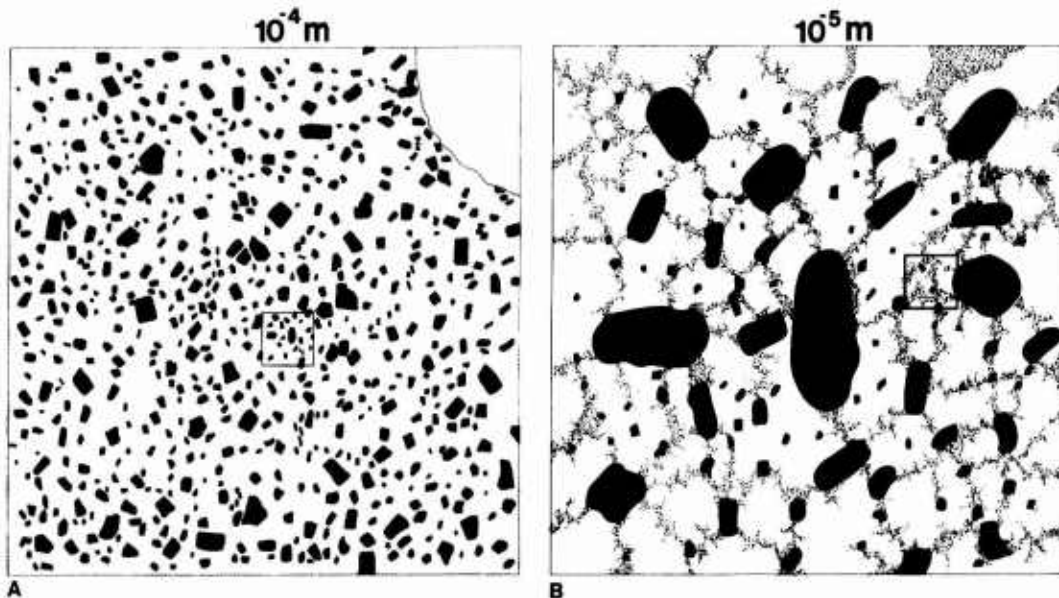


Figure 48. Graphic presentation of generalized model of red clay microfabric. (A) Dimension of field 10^{-4} m. Large particle in upper right represents quartz particle. Small irregular black particles represent shale or argillaceous clasts; (B) Dimension of field 10^{-5} m. Large black particles are shale or argillaceous clasts and are connected by smectite (supporting matrix).

2. Iron and manganese sulphide have been reported to precipitate at hydrothermal vents and then to be transported for thousands of kilometers in the North Pacific. Such sulphides are unstable and with time are transformed to metal oxides.

In summary, the red clays of the North Pacific Basin consist of detrital illite, kaolinite, and chlorite, in the form of shale clasts, detrital quartz, feldspar, and authigenic smectite. Portions of the smectite may be detrital but the majority (including authigenic x-ray amorphous smectite) is formed by *in situ* authigenic processes. Metal oxides are also present as authigenic materials.

Sources of the Red Clays

The paleopositions of Site 576 through time were determined in order to establish the specific source of the various minerals that make up the red clay. Figure 2 shows the backtrack path along which the site traveled during seafloor spreading. The points along the path make 5 m.y. intervals. This path was determined using methods developed by Jarrard and Clague (1977) and by examination of the path and age of the Hawaiian-Emperor seamounts (Clague and Jarrard 1973).

The backtrack path of Site 576 indicates that the site

traveled northward from its original position near the equator and arrived in close proximity to the Hawaiian hot spot approximately 45 m.y. ago. Table 4 lists the quartz accumulation rates of Hole 576A sediments. The accumulation rate at 46 meters, age dated at 47 m.y., is $1.4 \text{ g/cm}^2/\text{m.y.}$ In the interval from 46.01 m to 39.11 m the average rate is $1.4 \text{ g/cm}^2/\text{m.y.}$ This interval has the lowest quartz accumulation rate at Hole 576A. Quartz rates above this interval average $2.5 \text{ g/cm}^2/\text{m.y.}$ to a depth of 31.69 m where the rates start to increase exponentially.

In the interval of low quartz accumulation, smectite is present in the largest amounts (Table 1). Figure 3 shows a large increase in smectite at the 31 to 43 m interval. This increase is attributed to volcanic material derived from the Hawaiian hot spot. Low level winds blowing from the northeast were the transporting mechanism of the volcanic material. Today's winds at 500 mb during the summer in the region of the Hawaiian Islands are from the northeast while the winds at 300 mb are from the west. Similar conditions during deposition of the intervals discussed above must have taken place. The quartz and other minerals deposited during the interval from 31 to 47 m.y. ago were deposited from high altitude westerly flow.

Table 4 and Figure 4 show that quartz accumulation rates were almost constant up to 11 m.y. ago. At a

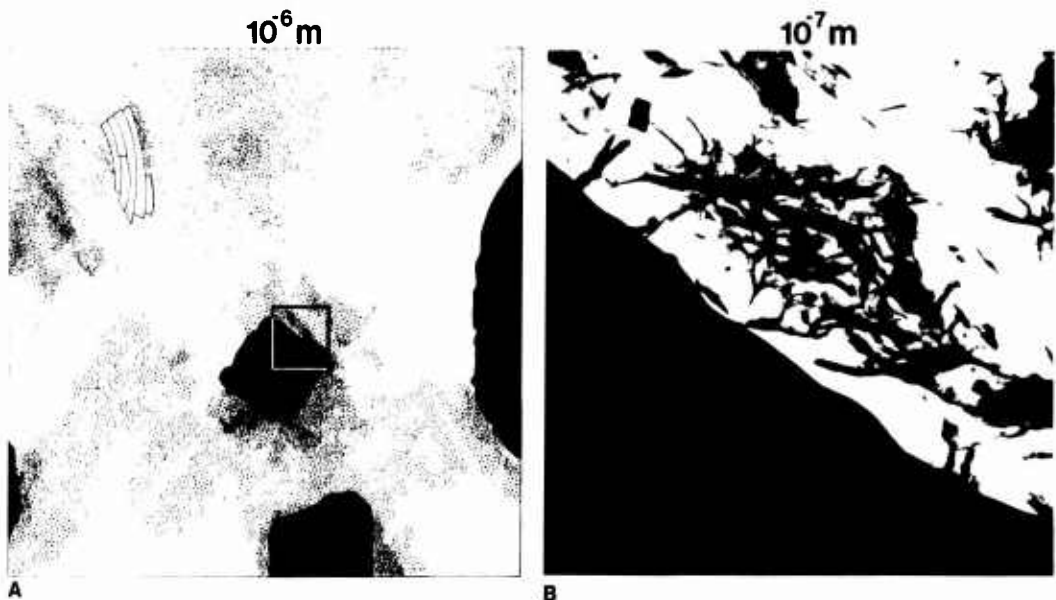


Figure 49. Graphic representation of generalized model of red clay microfabric: (A) Dimension of field is 10^{-6} m; (B) Dimension of field is 10^{-7} m. Shale or argillaceous clasts (black field) covered with smectite.

point 11 m.y. ago the quartz started to increase and the other aeolian-derived sediment such as illites, kaolinites, and chlorites found at Site 576 experienced the start of an exponential increase in accumulation rates. The position of Site 576 at that time was 28° N which suggests that the site moved into the full influence of westerlies approximately 11 m.y. ago. In addition it was suggested by Leinen (1985) that the increase in quartz accumulation through the Miocene and early Pliocene reflect the combined effects of increasing northern hemisphere aridity and intensified atmospheric activity associated with global cooling and an increase in the equator-pole temperature gradient. The large increase in quartz accumulation started 2.5 m.y. ago and corresponds to a depth of 18.7 m at Hole 576A is associated with the onset of glaciation in the north. At that stage Site 576 was positioned above 30° latitude, not far from the maximum intensity of the westerlies.

There is little doubt that the detrital sediments, quartz, illite, kaolinite, and chlorite, of the Pacific red clays have their source to the west, but where they came from specifically is still an open question.

During nonglacial times the influence of the westerlies extended from 25° N to 65° N. The tricellular theory of atmospheric circulation predicts an easterly wind at upper levels in middle latitudes. Modern wind observations, however, reveal that in the middle lati-

tudes, westerly winds extend through the entire depth of the troposphere and into the lower stratosphere. During a glacial stage, the influence of the westerlies is extended to the south as far as 20° N latitude. In addition the mean dune belt also migrates southward from its nonglacial position (30° N latitude) to as far south as 5° N latitude. Thus, the combined effects of the increase in the magnitude of the westerly flow and the migration of the dune belt south as well as the large increase in arid lands in the middle latitudes during periods of glaciation set the stage for a period of intense aeolian activity in the Afro-Asian areas.

Few investigators have expressed ideas on the precise sources of the quartz and clays of the North Pacific Basin. The Gobi Desert and various loess deposits within China have been inferred as major sources. The loess deposits of China are, however, an inadequate source for the vast amount of sediments deposited in the approximately 25,000,000 sq km area of the North Pacific occupied by the red clays. Most investigators of red clays endeavor to explain the source of the quartz because it is the most obvious inherited detrital mineral. However, the clay, and in particular the illite, constitutes three times the amount of sediment as does the quartz. The source of the illite is then the key to the major source of the red clays.

Based on the evidence of this study, the main source of inherited detrital clays is from various shales lo-

Table 4. Quartz Accumulation Rates of Hole 576A Samples (Leinen and King 1985)

Core-section (interval in cm)	Sample depth (cm)	Quartz (%)	Age ^a (m.y.)	Quartz accumulation rate ^b (g/cm ² /m.y.)
1-1, 21-25	23	16.63	0.26	237.0
1-3, 81-85	383	18.11	0.53	254.0
1-6, 80-83	831	15.52	0.87	166.0
2-3, 47-50	1219	17.35	1.32	129.0
3-1, 47-50	1869	13.06	2.56	47.0
3-3 70-73	2191	8.87	3.59	33.0
3-4, 117-120	2389	11.66	4.39	37.0
3-5, 127-130	2549	9.02	5.86	8.3
3-6, 110-113	2681	14.64	7.60	14.0
4-1, 50-53	2821	10.92	9.44	10.0
4-2, 103-106	3025	8.57	12.13	7.2
4-3, 98-101	3169	5.81	14.03	4.8
4-4, 104-107	3325	5.86	16.35	2.7
4-5, 20-23	3391	4.25	17.94	2.0
4-6, 60-63	3581	5.31	25.00	2.6
5-1, 87-90	3809	5.16	28.00	2.5
5-2, 40-43	3911	1.76	31.00	0.8
5-3, 30-33	4051	2.64	34.00	1.3
5-5, 137-140	4459	4.67	44.00	2.4
5-6, 130-133	4601	2.88	47.00	1.4
5-7, 25-28	4646	6.18	48.00	3.0
6-1, 90-93	4761	3.96	51.00	1.9
6-2, 47-50	4869	4.21	54.00	2.0
6-3, 93-96	5065	4.81	58.00	2.4
6-4, 11-14	5132	6.12	60.00	3.2
6-5, 12-15	5283	5.41	64.00	2.8
6-5, 127-13	5399	4.54	66.00	2.4
6-6, 17-20	5439	5.29	Carbonate turbidites	
6-7, 22-25	5593	3.91	Carbonate turbidites	
7-1, 137-140	5759	4.16	Carbonate turbidites	
7-2, 22-25	5793	5.50	Carbonate turbidites	
7-3, 17-20	5939	6.46	Carbonate turbidites	
7-3, 35-38	5946	3.51	Carbonate turbidites	

^aDetermined by interpolation between paleomagnetic datums for 0-24.76 m and by interpolation between ichthyolith datums for 24.76-54.0 m.

^bMass accumulation rates for sample depths were interpolated from data in Table 2.

cated in the arid zones of North Africa and Central Asia and subsequently transported by erosion and the westerlies.

Based on the above hypothesis, the red clays would have a mineral composition similar to that of shale. The average mineralogical composition of 34,516 shale samples from the Russian Platform compiled by Yaa-lon (1962) was determined to be:

Clay minerals 61.3 percent

Quartz 19.3 percent

Feldspar 8.0 percent

Carbonates 7.3 percent

Fe-oxides 2.3 percent

Other 2.2 percent

The average mineral composition of the detrital portion of the Plio-Pleistocene sediments of the red clays at Sites 576 and GPC-3 is:

Illite 49 percent

Kaolinite and Chlorite 8 percent

Quartz 17 percent

Feldspar 6 percent

Others 2 percent

(Smectite) authigenic 18 percent

The average mineralogical composition of the detrital sediments of the red clays and the average shales of Asia are almost identical except for the carbonates in the Asian shale. If the carbonate fraction of the shale

was deposited in the North Pacific Basin along with the other minerals it would have dissolved as it sank below the carbonate compensation depth. A good comparison is rendered in the ratios of quartz to clay minerals (Asian Platform 31 versus red clays 30) or similarly within one percent.

Figure 50 displays the average mineralogical composition of the Plio-Pleistocene red clays at Hole 576A and GPC-3, Asian shale and Barbados dust from Africa. The sediments from these three areas have similar mineralogy.

Prospero (1981) alluded to the connection between mineral aerosols which have an elemental composition similar to that of a winnowed average crustal material that is similar to shale in composition. But he stated that he did not want to imply that the dust is derived from shale, but that both had gone through a winnowing process. In the case of shale the winnowing agent is water, while for mineral dust (aerosol) it is wind. Prospero (1981) states that the effect of winnowing is evident in the concentrations of Si and Al in the end product. The average Si/Al ratio for the continental crust is 3.43, for shales, 2.97, deep-sea clay 2.98, and Saharan dust 2.95. He recognized the rather striking similarity in the Si/Al ratio of the three end products, shales, deep-sea clay and Saharan dust. The Si/Al ratio of red clays at Site 576 was found to fluctuate between 3.20 to 3.46—a range that covers the ratio of continental crust (3.43).

In an attempt not to minimize the differences in comparing the characteristics of mineral aerosols, shales and deep-sea clays, Prospero compared the boron

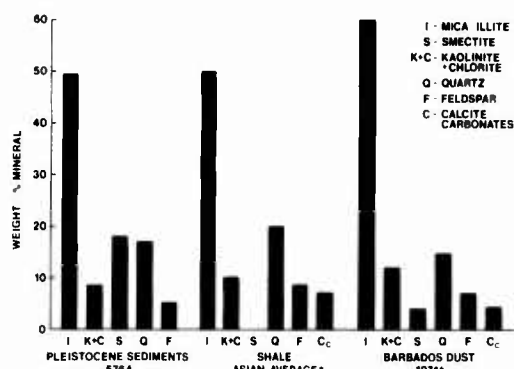


Figure 50. Bar graphs of the average composition of Hole 576A, Asian shales and Barbados dust. (*) Asian shale average from Yaalon (1962). Barbados dust data from Prospero (1981).

concentration in mineral aerosol (53 ppm) with that of the shales and deep-sea clay (230 ppm). He concluded that the mineral aerosol is not a remobilized sediment from a marine depositional environment, although such a source could not be precluded in some areas. However, shales and deep-sea clays have a similar boron concentration, supporting the idea that one may be derived from the other.

Broecker and Peng (1982) published data (Table 5) concerning the chemical composition of average basalt, granite, igneous rock, shale, and red clay. They state that when they compared the composition of deep-

Table 5. Comparison of the Chemical Composition of Average Igneous Rock (Equal Parts Granite and Basalt) with the Chemical Compositions of Shale and Red Clay. (Concentrations are in Parts per Million by Weight.) Note the Large Excesses of Mn, Ni, Co, Cu, and Fe in red clays. After Broecker and Peng (1982)

Element	Basalt	Granite	Average igneous rock	Shale		Red clay	576A Red clay
				Shale	Red clay		
Na	26,000	18,000	22,000	10,000	15,000	4,000	
K	8,000	42,000	25,000	27,000	25,000	26,000	
Rb	30	170	100	140	110	110	
Cs	1	4	3	5	6	6	
Mg	46,000	1,600	24,000	15,000	21,000	20,000	
Ca	76,000	5,000	40,000	22,000	29,000	4,500	
Sr	470	100	290	300	180	133	
Ba	330	840	590	580	2,300	100	
Fe	86,000	14,000	50,000	47,000	65,000	46,000	
Mn	1,500	400	950	850	6,700	450	
Ni	130	5	70	70	225	119	
Co	50	1	25	19	74	83	
Cu	90	10	50	45	250	218	
Cr	170	4	90	90	90	60	
Th	4	18	11	12	12	29	

sea red clays with that of shale, the agreement was good except for barium and the elements enriched in manganese nodules. It was emphasized that this enrichment in deep-sea clays relative to shale does not apply to all trace metals. Chromium and thorium are examples of metals that do not show an anomaly. The Ba concentration listed for red clays in Table 5 must be a mistake; it is an order of magnitude too high. Included in Table 5 is the chemical composition of red clay at Site 576 as determined from data published by Heath and others (1985) and Schoonmaker and others (1985). The values in the table are average values for Plio-Pleistocene red clays. These values match the values for shale better than they match the red clays in column 5.

Lerman (1979) measured the $^{18}\text{O}/^{16}\text{O}$ ratio of quartz found in Hawaiian soils and Pacific Ocean sediments. He found that the $^{18}\text{O}/^{16}\text{O}$ ratio for the quartz measured consistently between $\delta^{18}\text{O} = +16$ and $+19\text{\textperthousand}$ (relative to standard ocean water). These $^{18}\text{O}/^{16}\text{O}$ ratio values overlap those of quartz found in shales of different geologic ages ($\delta^{18}\text{O}$ between $+17$ and $+24\text{\textperthousand}$). From these associations Lerman concluded that the quartz occurring in Hawaiian soils and the pelagic sediments of the Pacific Ocean is likely to have been derived by erosion from older shales and transported by wind.

The evidence presented strongly suggests that the source of the detrital minerals of the red clays is the shales of the Afro-Asian area. Because shales are the most common sedimentary rock it would be impossible to identify the precise source areas of the red clays in Africa and Asia. To state categorically that all detrital minerals found in the red clays were transported by wind would be misleading. There is no doubt that portions of the detrital component of the red clays are transported by fluvial and ocean current systems. However, the amount is obviously very small. During the Pleistocene the areas in eastern Asia that fell under the influence of the westerlies were extremely dry suggesting that the amount of runoff from precipitation to the ocean was much less than it is today. Runoff of glacial meltwaters was not present to any degree in China. Unlike areas such as the Gulf of Mexico where glacial runoff increased the amount of sediments delivered to the sea by a factor of 100 compared to today's accumulation rates, areas in eastern Asia such as the area drained by the Huang Ho were less active than today.

Recent observations by G. Keller (personal communication 1985) indicated that 95 percent of the present sediments coming from the Huang Ho in China are deposited within about 10 miles of the mouth of the river. Those not deposited must survive the journey across a back-arc basin and over the Japan Trench

before they can be picked up and transported by the Kuroshio and North Pacific current to areas of the North Pacific Basin.

In general the amount of continental sediment that finds its way to the deeper parts of the world's oceans transported by ocean currents is extremely small. Most terrigenous sediments are deposited on the continental margins or on the abyssal plains adjacent to the margins. An example of this is the Gulf of Mexico, a semienclosed basin, where sediments accumulate at the rate of 30 cm/yr on the Mississippi Delta while the accumulation rate in the deeper portions of the basin are less than 10 cm/1000 yr and consists of 70 percent foraminiferal ooze.

The amount of noncarbonate and nonaeolian transported detrital material in the Plio-Pleistocene red clays is considered insignificant and probably not measurable. The classic idea that the majority of the red clay sediments deposited in the deeper portions of the world's oceans consist of degraded material from pelagic processes and/or individual clay particles or flocs that are transported by fluvial and ocean current systems is incorrect. The direct evidence indicates that the red clays of all the world's oceans consist predominantly of aeolian transported shale or argillaceous-clasts and lesser amounts of quartz or *in situ* authigenic smectite, volcanogenic materials, and amorphous metal oxides.

Red Clays Redefined: The Pacific Basin as a Model

A major objective of this study has been to gain an in-depth understanding of the fundamental physical and mineralogical nature and origin of deep sea red clays with emphasis on the Pacific Ocean Basin. Extensive deep sea sediment coring and sampling was carried out in the Pacific Basin by numerous academic institutions, industrial research groups, and the Deep Sea Drilling Project during the past two decades and has provided a wealth of material and technical data for research and synthesis. Numerous earlier studies of aeolian material and aerosol particulates has added immensely to the databases and to our understanding of the significance of windblown material from continental land masses to the world's ocean basins. This study has drawn extensively upon results of the earlier investigations which through synthesis of the various studies has clearly shown repeated confusion and contradiction of not only the definition of red clays but also of their origin, physical, and major mineralogical nature. With the advent of the Transmission Electron Microscope (TEM) and Scanning Electron Microscope (SEM), a new perspective and insight of red clays has been made possible.

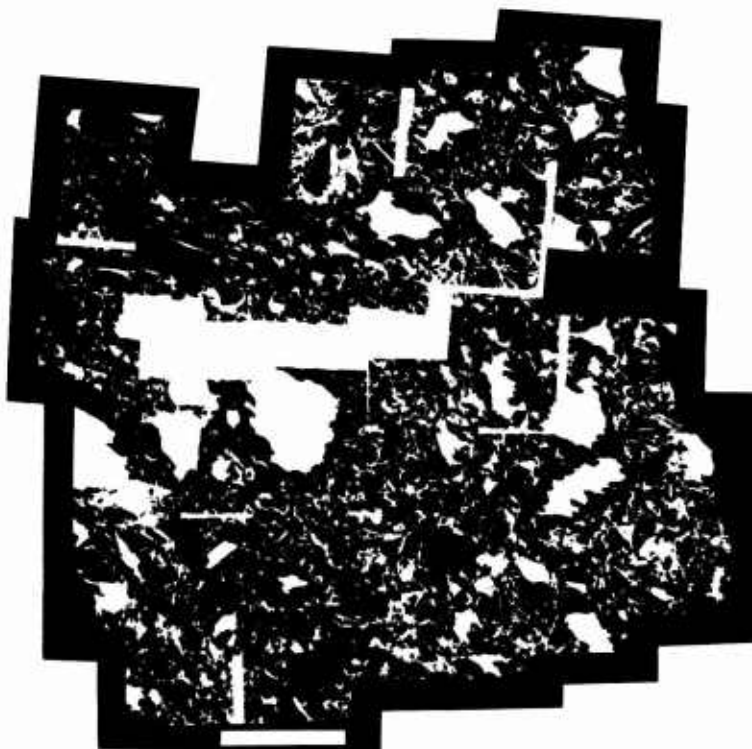


Figure 51. Mosaic of T.E.M. photomicrographs illustrating the nature of the fabric of clay from Bootlegger Cove, Alaska. Scale Bar = 10 μ m.

This study has clearly shown the important contribution of windblown terrigenous rock fragments and minerals to the ocean basins in the depositional history of red clays. The red clays of the Pacific Basin are characterized by varying amounts (percentage by weight) of authigenic and detrital smectites, aeolian shale clasts and quartz, small percentages of other clay minerals, and occasionally zeolites. Cretaceous red clays commonly have an abundance of smectite either detrital and/or authigenic as determined by x-ray diffraction analysis and TEM observations, in contrast to Pleistocene red clays that are characterized by an abundance of aeolian shale clasts with considerably lesser amounts of smectite. The smectite of the Cretaceous deposits from Site 163 southwest of Hawaii appear to consist of considerable amounts of detrital smectite in the form of floccules and linking chains. In contrast, the Cretaceous deposits of Site 576 have an apparent abundance of authigenic smectite. The amount of authigenic smectite is largely determined by the availability of silica, aluminum, and associated elements which were readily available during the depositional history of Site 576 Cretaceous red clays. Volcanic processes associated with the Hawaiian hot

spot could have provided the essential mineralogical ingredients necessary for the formation of authigenic smectite at Site 576 (see section on Sources of Red Clays). Sources of Site 163 red clays were probably dominated by aeolian processes with only minor influences of volcanic activity. The relative abundance of smectite versus silt size shale clasts and quartz and the microfabric largely controls the physical and mechanical properties of the red clays. The high bonding strength of smectite in concert with its "ultra-fine grained" particle size, results in a deposit that greatly resists compaction and severely reduces permeability thus inhibiting the consolidation process. Porosities are commonly equal to or greater than 75 percent, indicative of an open microfabric characterized by large voids as observed in the numerous TEM and SEM micrographs.

Revised Description of Red Clays

Red clays occur in deep sea environments distant from continental land masses and at ocean depths well below carbonate dissolution. The typical "clean" red clays are virtually free of calcium carbonate but become di-

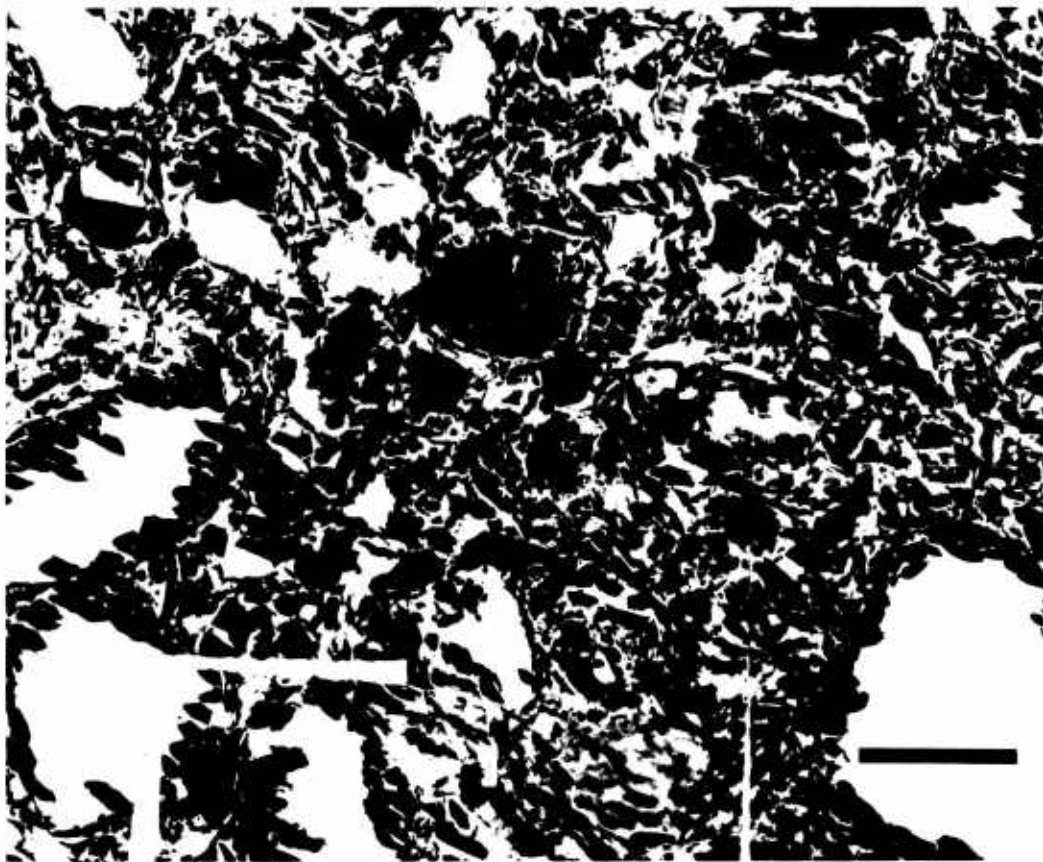


Figure 52. Enlarged portion of mosaic of Bootlegger Cove clay, Figure 51. Scale Bar = 5 μ m.

luted and "dirty" with increasing amounts of calcium carbonate debris. The most abundant mineralogical components are authigenic and detrital smectite, aeolian shale clasts of illite, chlorite, and kaolinite in variable proportions, quartz, and minor contributions of zeolites. Porosities are generally greater than 75 percent and permeabilities are very low ($k = 10^{-6}$ to 10^{-10} cm/sec). Typically the red clays resist consolidation by virtue of the high bonding strength of the smectite and the low permeabilities. Windblown illite shale clasts and quartz are ubiquitous, but vary from deposit to deposit in absolute percentages.

Shale Clasts Observations in the Marine Environment

During the course of this study, TEM and SEM micrographs of clay fabric, representative of several marine environments, were examined for possible pres-

ence of shale clasts. The objectives were to assess the relative importance of shale clasts and indurated clay aggregates in (1) a variety of depositional environments, (2) detrital versus aeolian deposits, and (3) to determine if "fractillite" like particles were observable in TEM micrographs representative of deposits that are totally distinct from red clays. From a broad perspective a "first order" assessment was made to determine if "fractillites" could be used as a "fingerprint" for the presence of shale and argillite source material in marine deposits. Thus an assessment of the volumetric importance of terrigenous mud rocks as source materials of marine sediments could be initiated.

Sediment samples from the "Bootlegger Cove Clay" were examined by TEM and compared with SEM micrographs (sediment samples and micrographs provided by H. R. Schmoll and H. Olsen, U.S.G.S.). The "Bootlegger Cove Clay" is described as a quar-



Figure 53. S.E.M. photomicrograph of Bootlegger Cove clay illustrating the large amounts of aggregates present and the nature of the supporting clay matrix. Scale Bar = 10 μ m.

ternary glacio-marine deposit that occurs in the Turnagain Arm-Anchorage, Alaska area. The material has a high silt content and is relatively coarse in respect to typical marine clay deposits. TEM micrographs revealed numerous "fractillites" in a generally dense microfabric clay-matrix (Figure 51). The "fractillites" shale clasts made up the greatest proportion of the coarse clay to fine silt. Numerous pieces of the largest "fractillites" were removed by the microtome process (Figure 52). SEM micrographs reveal the coarse nature of the "Bootlegger Cove Clay" and the presence of dense well rounded aggregates (Figure 53). Quartz fragments are also visible. The general microfabric of this deposit (Figure 54) was described earlier by Updike and others (1986).

A Pleistocene marine deposit from the Mississippi Delta (145 m subbottom) reveals several "fractillites" in highly consolidated illitic-smectite clay (Figure 55 and 56). The degree of consolidation is depicted by the highly oriented clay particles and low porosity. An enlargement of a single "fractillite" sampled 121

m subbottom reveals a typical conchoidal-type fracture pattern.

A clayey sediment recovered from Site 440 Japanese Trench Inner Slope 13 m below subbottom reveals several "fractillites" (Figure 57), suspended in the fine-grained matrix containing abundant organic debris. These micrographs reveal the ubiquitous nature of "fractillites" in the various terrigenous deposits.

Consolidation

The consolidation characteristics of the Plio-Pleistocene sediments from Sites 576 and CPC-3 indicated that, no matter how it was determined, the preconsolidation stress was always higher by a factor of from 2 to 5 than the effective overburden stress. The overconsolidation state of Plio-Pleistocene sediments at these sites has been attributed by other writers to age, slow rates of sediment accumulation, extremely strong interparticle bonds, and cementation by iron oxides

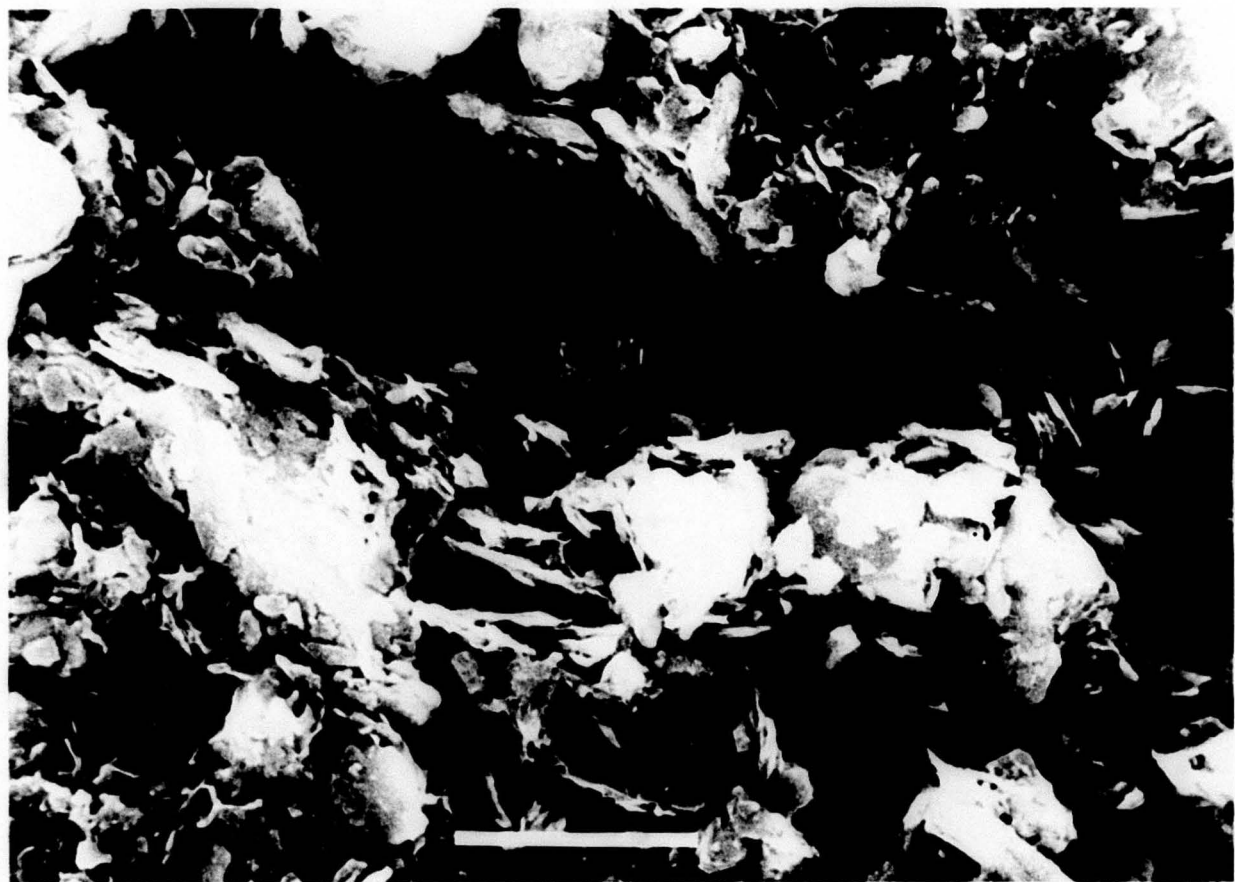


Figure 54. S.E.M. photomicrograph of Bootlegger Cove clay. Note the face-to-face domains that surround the larger aggregates. Scale Bar = 10 μ m.

or silica (Dadey 1983, Geotechnical Consortium 1985).

The state of consolidation of pre-Plio-Pleistocene sediments (30–55 m) subbottom depth ranged from overconsolidated/normally consolidated to underconsolidated, depending upon the method used to determine the preconsolidation stress. It is suggested here that a state of overconsolidation exists for all North Pacific red clay sediments. This is based on the assumption that the trend of the overconsolidation difference (OCD) results from the use of preconsolidation stress as measured by C'_{c4} correlates with other physical properties, such as void ratio and, in particular, compression index.

Dadey (1983) examined samples from similar areas and stated that the value of the preconsolidation stress estimated from consolidation test results was in excess of the calculated overburden stress and the sediments examined were reported as overconsolidated, but the sediments were not overconsolidated in the traditional sense, i.e., they have never sustained a stress greater than that which they are presently experiencing. This assumes that preexisting overburden had not

been removed by erosion. Thus there is a certain amount of confusion about what constitutes overconsolidation. As Dadey suggests, any phenomenon or material property which gives rise to greater structural integrity or tenacity than originally hypothesized for terrestrial sediments by early researchers in soil mechanics will result in anomalously high overconsolidation rates and differences, because traditional theories and analyses do not account for any type of extraordinary strength. It becomes apparent that attempts to utilize the red clays of the Pacific as a standard accreting clay section to which all other sections and geotechnical properties could be compared has to be abandoned in the light of the unusual nature of these deposits.

Conclusions

Evidence provided by the geotechnical, mineralogical, and microstructural analysis of red clays from the North Pacific Basin result in the following conclusions:



Figure 55. T.E.M. photomicrograph of Mississippi Delta sediments recovered at a depth of 120 m subbottom. The fabric of this material is dense and orientated. The sediment is composed of smectite and illite and contains "fractillites" in the upper portion of the photograph. Scale Bar = 1 μ m.



Figure 56. T.E.M. photomicrograph of a large "fractillite." This material is from the Mississippi Delta and recovered from a depth of 120 m subbottom. Scale Bar = 1 μ m.

1. The main constituents of the red clays of the North Pacific Basin are illite-rich argillaceous or shale clasts, quartz, and authigenic smectite. The main source of the shale clasts and quartz are aeolian in nature and are derived mainly from African and Asian shales.

2. Illite-rich argillaceous or shale clasts are identifiable by their morphology (high degree of roundness) and their unique fracture characteristics created by an ultrathin-sectioning process. The fractured illite-rich argillaceous or shale clasts have been given the name "fractillites" (fractured illites). Unlike other clay particles, argillaceous or shale clasts are brittle and they fracture upon bending while being cut from a thin section by a diamond knife. This unique event and morphology allows for the identification and differentiation of illite-rich shale clasts from other clays, including detrital illite, kaolinite, and smectite.

3. The Plio-Pleistocene red clays of the North Pacific Basin have a mineralogy, exclusive of smectite,

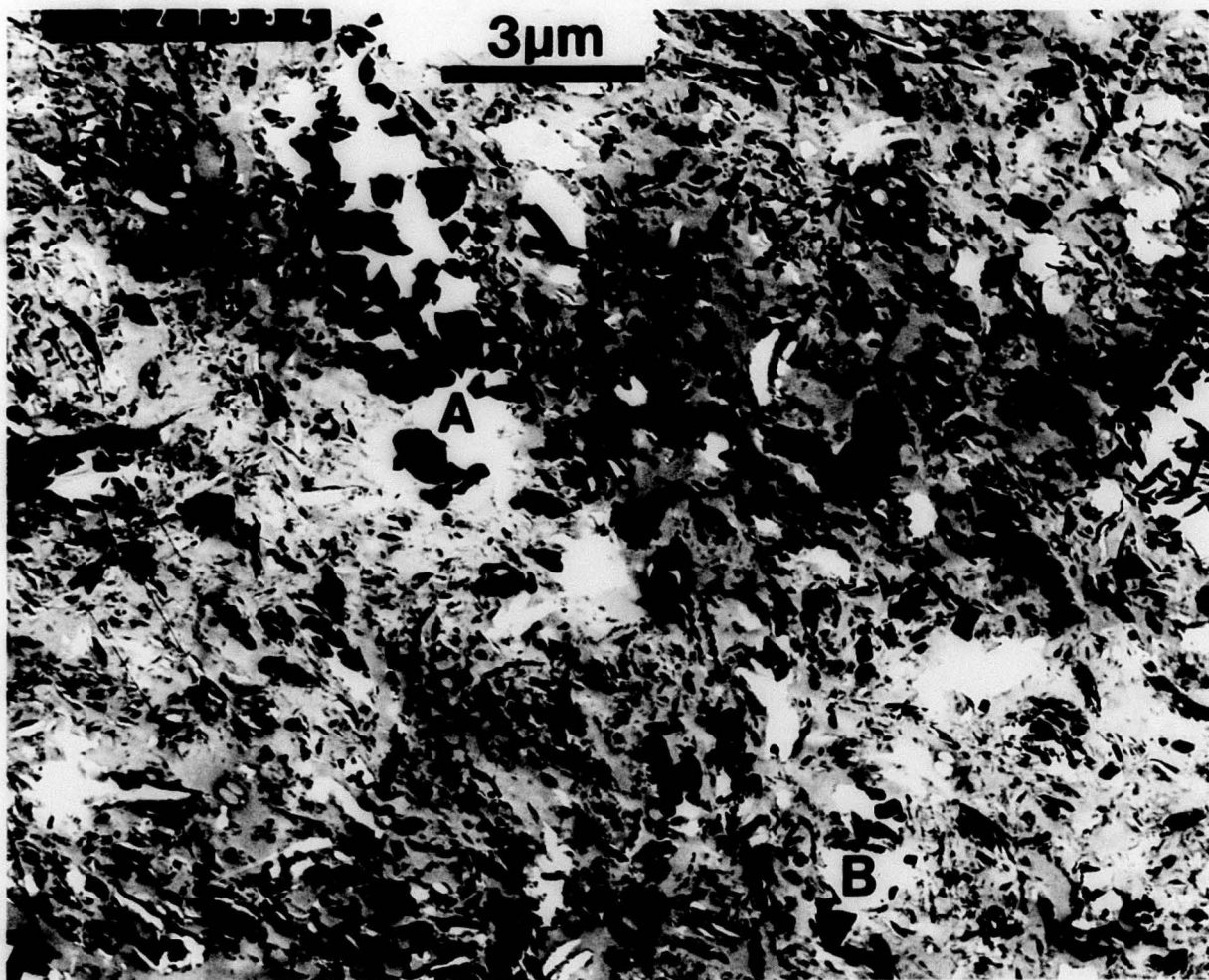


Figure 57. T.E.M. photomicrograph of sediment recovered from the Japan Trench, DSDP Site 440, 3.5 m subbottom. Note the occurrence of fractured particles at positions A and B. Scale Bar = 3 μ m.

similar to that of an average Asian shale. The fact that illite-rich argillaceous or shale clasts make up the bulk of the sediments of the red clays (exclusive of smectite) and the similarity between their mineralogy and that of Asian shales would indicate the red clays of the North Pacific Basin are derived from shales in North Africa and Asia and transported to the Pacific Basin by aeolian processes.

4. The study of clay microstructure can provide insight and solve problems in a number of scientific and technical problems in the areas of geology, geochemistry, paleoclimatology, and soil science.

5. The geotechnical character, consolidation, void ratio variation, sediment strength, and grain-size of the red clays are dissimilar from conventional marine and continental fine-grained sediments.

6. Standard geotechnical techniques, such as the use of Casagrande's graphic method to determine pre-

consolidation stress, are not valid for red clays that have a large expansion index.

7. The red clays are overconsolidated: their pre-consolidation stress is in all cases larger than the vertical effective (overburden) stress. The overconsolidation is attributed to the strong bonding of argillaceous or shale clasts, quartz, and other particulate matter by x-ray amorphous and well developed crystalline sheets of authigenic smectite.

8. Observations of numerous marine sediments indicated the ubiquitous nature and presence of "faecalites" (illitic shale clasts) in various depositional environments.

Acknowledgments

The authors wish to extend their appreciation to the colleagues who contributed various geotechnical studies and data to the orig-

inal DSDP investigations of Pacific red clays recovered from Sites 576. We gratefully acknowledge the efforts of Drs. R. Schiffman, I. Noorany, A. Silva, P. Schultheiss, L. Shephard, and E. Taylor. Ms. P. J. Burkett, provided the TEM mosaics of the Pacific red clay and the Bootlegger Cove Clay and assisted in processing various micrographs for this study. J. Bryant drafted numerous figures that contributed substantially to this study. F. L. Nastav assisted in reviewing and editing the manuscript. We appreciate the effort of H. R. Schmoll and H. Olsen who provided core samples for TEM study of the Bootlegger Cove Clay. H. R. Schmoll and R. Updike provided the SEM micrographs of the "Bootlegger" sample. Various versions of the manuscript were typed by Ms. S. Drews, E. Schields, and S. Vreeland. Support for the second author, provided by the Naval Ocean Research and Development Activity (NORDA) under Program Element Number 61153N, is very much appreciated. The program is administered by Dr. H. Eppert. Support was also provided by NORDA for P. J. Burkett under a student cooperative program with Texas A&M University. We appreciate the efforts of A. Delgado for arranging this program.

References

Andersland OB, Douglas AG (1970) Bonding, effective stresses, and strength of soils. *Journal Soil Mechanics and Foundation Division, Proceedings American Society Civil Engineers* 96:1073-1077

Arrhenius G (1963) Pelagic sediments. In: Hill MN (ed) *The Sea*. Interscience, New York 3:655-727

Aoyagi K, Kazama T (1980) Transformational changes of clay minerals, zeolites and silica minerals during diagenesis. *Sedimentology* 27:179-188

Bennett RH (1976) Clay fabric and geotechnical properties of selected submarine sediment cores from the Mississippi Delta. *Dissertation for Ph.D Texas A&M University, College Station, TX*. 269 pp

Bennett RH, Bryant WR, Keller GH (1977) Clay fabric and geotechnical properties of selected submarine sediment cores from the Mississippi delta. *NOAA Professional Paper 9, US Department of Commerce*, 86 pp

Bennett RH, Bryant WR, Keller GH (1979) Clay fabric and related pore geometry of selected submarine sediments: Mississippi delta. *Scanning Electron Microscopy I*, pp 519-524 and 424 pp (discussion)

Bennett RH, Bryant WR, Keller GH (1981) Clay fabric of selected submarine sediments: fundamental properties and models. *Journal Sedimentary Petrology* 51(1):217-232

Bennett RH, Burns JT, Clarke TL, Faris JR, Forde EB, Richards AF (1982) Piezometer probes for assessing effective stress and stability in submarine sediments. In: Saxon S and Nieuwenhuis JK (eds) *Marine Slides and Other Mass Movements*. Plenum New York, pp. 126-161

Bennett RH, Nelsen TA (1983) Seafloor Characteristics and Dynamics Affecting Geotechnical Properties at Shelf Breaks. In: Stanley DT and Moore GT (eds) *The Shelfbreak: Critical Interface on Continental Margins*. Society Economic Paleontologists and Mineralogists Special Publication 33:333-355

Bennett RH, Bryant WR, Burkett PJ, Shephard LE (1985a) Microstructure of Red Clays from the Northwest Pacific Deep Sea Basin. *International Clay Conference, Denver, CO, Association Internationale pour L'Etude des Argiles*, 23 pp

Bennett RH, Lehman L, Hulbert MH, Harvey GR, Bush SA, Forde EB, Crews P, Sawyer WB (1985b) Interrelationships of organic carbon and submarine sediment geotechnical properties. *Marine Geotechnology* 6(1):61-98

Bennett RH, Hulbert MH (1986) Clay Microstructure. *International Human Resources Development Corporation, Boston*, 161 pp

Berger WH (1978) Pelagic sedimentation, pelagic sediments. In: Fairbridge RW and Bourgenois J (eds) *Encyclopedia of Sedimentology*. Dowden, Hutchinson, and Ross, New York, pp. 544-558

Bishop AW and others (1986) Undisturbed samples of London Clay from the Ashford Common Shaft: strength-effective stress relationship. *Geotechnique* 15:1-81

Bjerrum L (1967) Engineering geology of Norwegian normally consolidated marine clays as related to settlements of buildings. *Geotechnique* 17:81-118

Bjerrum L (1972) Embankments of soft ground. *Proceedings American Society Civil Engineers, Specialty Conference on the Performance of Earth and Earth-Supported Structures* 2:1-54

Bjerrum L (1973) Problems of soil mechanics and construction of soft clays and structurally unstable soils (collapsible, expansive and others). *Proceedings 8th International Conference on Soil Mechanics and Foundation Engineering* 3:111-159

Bolt GH (1956) Physico-chemical analysis of the compressibility of pure clays. *Geotechnique* 6:86-93

Bowles FA (1968a) Electron Microscopy Investigation of the Microstructure in Sediment Samples from the Gulf of Mexico. *Dissertation for Ph.D Texas A&M University, College Station, TX*, 140 pp

Bowles FA (1968b) Microstructure of sediments: investigation with ultrathin section. *Science* 159:1236-1237

Bramlette MN (1958) Significance of coccolithophorids in calcium carbonate deposits. *Geological Society America Bulletin* 69:121-126

Brewer R (1964) *Fabric and Mineral Analysis of Soils*. John Wiley and Sons, New York, 470 pp

Broecker WS, Peng T (1982) *Tracers in the Sea*. Columbia University, New York 690 pp

Brumund WF, Callender Jr. GW (1975) Compressibility of undisturbed submarine sediments. *Proceedings Civil Engineers Oceans/iii. American Society Civil Engineers* 1:363-379

Brumund WF, Jonas E, Ladd CC (1976) Estimating in situ maximum past (preconsolidation) pressure of saturated clays from results of laboratory consolidometer tests. *Transportation Research Board Special Report* 163:4-12

Bryant WR, Bennett R, Katherman C (1981) Shear strength, consolidation, porosity, and permeability of oceanic sediments. In: Emiliani C (ed) *The Sea 7: The Oceanic Lithosphere*. John Wiley and Sons, New York, pp. 1555-1616

Bryant WR, Cernock P, Morelock J (1967) Shear strength and consolidation characteristics of marine sediments, Gulf of Mexico. In: Richards A (ed) *Marine Geotechnique*. University of Illinois Press, Urbana, pp 41-62

Bryant WR, Hottman W, Trabant P (1975) Permeability of unconsolidated and consolidated marine sediments, Gulf of Mexico. *Marine Geotechnology* 1:1-14

Bryant WR, Wallin CS (1968) Stability and Geotechnical characteristics of marine sediments, Gulf of Mexico. *Transactions Gulf Coast Association Geological Societies* 18:334-356

Bryant WR, Bennett RH, Shephard LE, Burkett PJ (1985) Identification of aeolian argillites in the red clays of the Northwest Pacific. *International Clay Conference, Denver, CO, Association Internationale pour L'Etude des Argiles*, 32 pp

Buchanan PN (1964) Effect of temperature and absorbed water on permeability and consolidation characteristics of sodium and calcium montmorillonite. *Dissertation for Ph.D Texas A&M University*, 140 pp

Burmister BM (1951) The application of controlled test methods in consolidation testing. *Consolidation Testing of Soils*. Amer-

ican Society Testing Materials Special Technical Publication 126:83-91

Cabrera JG, Smalley JI (1971) Engineering behavior and structure of compacted clay, discussion and reply. *Journal Soil Mechanics and Foundation Division, Proceedings American Society Civil Engineers*, pp. 802-803

Calvert SE (1977) Mineralogy of silica phases in deep-sea cherts and porcellanites. *Philosophical Transactions Royal Society London A286:239-252*

Casagrande A (1932) The structure of clay and its importance in foundation engineering. *Contribution Soil Mechanics*, Boston Society Civil Engineers (1940), 72 pp, and *Journal Boston Society Civil Engineers* 19 (April 1932)

Casagrande A (1936) The determination of the preconsolidation load and its practical significance. *Proceedings first International Conference Soil Mechanics and Foundation Engineers*, Cambridge 3:60-64

Clague DA, Jarrard RD (1973) Tertiary Pacific plate motion deduced from the Hawaiian-Emperor chain. *Geological Society American Bulletin* 84:1135-1154

Cohen AL, Marlow DP, Garner GE (1968) A rapid critical point method using fluorocarbons ("freons") as intermediate and transitional fluids. *Journal Microscopy* 7:331-342

Cooling LF, Skempton AW (1942) A laboratory study of London clay. *Journal Institute Civil Engineering* 27:251-256

Correns CW (1937) Scientific results of German Atlantic expedition in the exploration ship "Meteor." *Deutsche Atl Exp Meteor* 1925-1927, 340 pp

Correns CW (1939) Pelagic sediments in the North Atlantic Ocean: recent marine sediments. *Symposium Society Economic Paleontologists and Mineralogists Special Publication* 4:373-399

Dadey KA (1983) Stress history of unlithified marine sediment in the northwest Pacific. M.S. Thesis, University of Rhode Island, 157 pp

Darwin C (1946) An account of this fine dust which often falls on vessels in the Atlantic Ocean. *Geological Society London Quarterly Journal* 2:26-30

Delfflache AP, Bryant WR (1970) Compressional behavior of high void ratio marine sediments. *Second Annual Offshore Technology Conference Preprints* 1:47-64

Delfflache AP, Bryant WR, Cernock P (1971) Determination of compressibility of marine sediments from compressional wave velocity measurements. *Third Annual Offshore Technology Conference Preprints* 1:33-42

Dietz RS (1941) Clay minerals in recent marine sediments. *Resume American Minerals*, University of Illinois, 27 pp

Emiliani C, Milliman JD (1966) Deep-sea sediments and their geological record. *Earth-Science Reviews* 1:105-132

Foster RH, De PK (1971) Optical and electron microscopic investigation of shear induced structures in lightly consolidated (soft) and heavily consolidated (hard) kaolinite. *Clays and Clay Minerals* 19:31-47

Fukushima K, Kohyama N, Fukami A (1980) In-Situ observations of clay minerals hydrated and intercalated with liquid chemicals using film-sealed environmental cells. *Reading Text for 38th Electron Microscopy Society America Meeting and Pacific Regional Congress*

Geotechnical Consortium (1985) Geotechnical properties of Northwest Pacific pelagic clays. *Deep Sea Drilling Project Leg 86, Hole 576A*. In: Heath GR, Burckle LH and others *Initial Reports of the Deep Sea Drilling Project*, US Government Printing Office, Washington, DC 86:723-758

Gillott JE (1969) Study of the fabric of fine-grained sediments with the scanning electron microscope. *Journal Sedimentary Petrology* 39:90-105

Glossary of Geology (1972) Gray M and others (eds) *American Geological Institute*, Washington, DC, 805 pp

Glossary of Oceanographic Terms (1966) Baker Jr BB, and others (eds) 2nd edition *Special Publication SP-35*, US Naval Oceanographic Office, Washington, DC, 204 pp

Goldschmidt VM (1926) *Undersokelser over ler-sedimenter Nordisk-jordbrugsforskning* 4:7:434-445

Griffin JJ, Windom H, Goldbert ED (1968) The distribution of clay minerals in the world ocean. *Deep Sea Research* 15:433-459

Grim RE, Dietz RS, Bradley WF (1949) Clay mineral composition of some sediments from the Pacific Ocean off the California coast and Gulf of California. *Geological Society America Bulletin* 60:785-1808

Hamilton EL (1964) Consolidation characteristics and related properties of sediments from experimental Mohole (Guadeloupe site). *Journal Geophysical Research* 69:4257-4269

Hayat MA, Zirkin BR (1973) Critical point drying method. In: Hayat MA (ed) *Principles and Techniques of Electron Microscopy, Biological Applications III* pp 297-313

Heath GR (1969) Mineralogy of Cenozoic deep-sea sediments from the Equatorial Pacific Ocean. *Geological Society America Bulletin* 80:1992-2018

Heath GR, Pisias NG (1979) A method for the quantitative estimation of clay minerals in North Pacific deep-sea sediments. *Clays and Clay Minerals* 27(3):175-184

Heath GR, Burckle LH, and others (1985) *Initial Reports of the Deep Sea Drilling Project*, US Government Printing Office, Washington, DC 86:804

Heath GR, Kovar RB, Lopez C, Campi GL (1985) Elemental composition of Cenozoic pelagic clays from the deep sea drilling project sites 576 and 578, Western North Pacific. In: Heath GR, Burckle LH and others *Initial Reports of the Deep Sea Drilling Project*, US Government Printing Office, Washington, DC 86:605-646

Hein JR, Yeh HW, Alexander E (1979) Origin of iron-rich montmorillonite from the manganese nodule belt of the North Equatorial Pacific. *Clay and Clay Minerals* 27(3):185-194

Hoffert M (1980) Les "Argiles rouges des grands fonds" dans le Pacifique Centre Est. Authigenese, transport, diagenese. *Sci Geol Mem* 61:1-231

Houston WN, Mitchell JK (1969) Property interrelationships in sensitive clays. *Journal Soil Mechanics and Foundation Division, Proceedings American Society Civil Engineers* 95:1037-1062

Hurley PM, Hart SR, Pinson WH, Fairbairn HW (1959) Authigenic versus detrital illite in sediments. *Geological Society America Bulletin* 70:1622

Hurley PM, Heezen BC, Pinson WH, Fairbairn HW (1963) K-Ar age values of pelagic sediments of the North Atlantic. *Geochimica ET Cosmochimica Acta* 24:393

Ingles OG (1968) Soil chemistry relevant to the engineering behavior of soils, in: I. K. Lee (ed) *Soil Mechanics, Selected Topics*. Butterworths, London, pp 1-57

Janecek TR, Rea DK (1983) Eolian deposition in the Northwest Pacific Ocean: Cenozoic history at atmospheric circulation. *Geological Society America Bulletin* 94:730-738

Jarrard RD, Clague DA (1977) Implications of Pacific Island and seamount ages for the origin of volcanic chains. *Reviews Geophysics and Space Physics* 15:57-76

Keller GH, Bennett RH (1973) Sediment mass physical properties—Panama Basin and Northeastern Equatorial Pacific. In: van Andel TjH, Heath GR and others. *Initial Reports of the Deep Sea Drilling Project 16*, US Government Printing Office, Washington, DC, pp 499-512

Kenney TC (1964) Sea level movement and the geologic histories of the post-glacial marine soils at Boston, Nicolet, Ottawa and

Oslo. *Geotechnique* 14:203-230

Kruyt HO (ed) (1952) *Colloid Science, Irreversible Systems*. Elsevier, Amsterdam, 1, 554 p

Lambe TW (1951) *Soil Testing for Engineers*. John Wiley and Sons, New York, 165 pp

Lambe TW (1953) The structure of inorganic soil. Separate 315. *American Society Civil Engineers Proceedings* 79:1-49

Lambe TW (1958a) The engineering behavior of compacted clay. *Journal Soil Mechanics and Foundation Division, American Society Civil Engineers* 84(SM2):1655-1-1655-35

Lambe TW (1958b) The structure of compacted clay. *American Society Civil Engineers Proceedings*, Separate 1654, and *Journal Soil Mechanics and Foundation Division* 84:1-34

Lambe TW, Whitman RV (1969) *Soil Mechanics*. John Wiley & Sons, Inc., New York, 553 pp

Lee HJ (1984) State of the art: laboratory determination of the strength of marine soils. *American Society Testing Materials Symposium Laboratory In Situ Determination Strength Marine Soils*, San Diego

Leinen M (1985) Quartz content of Northwest Pacific Hole 576A and implications for Cenozoic aeolian transport. In: Heath GR, Burckle LH and others *Initial Reports of the Deep Sea Drilling Project 86*, US Government Printing Office, Washington, DC, pp 581-588

Leinen M, Heath GR (1981) Sedimentary indicators of atmospheric circulation in the Northern Hemisphere during the Cenozoic. *Paleogeography, Paleoclimatology, Paleoecology* 36:1-211

Leinen M, King TW (1985) Mineralogy of North Pacific sediments from North Pacific candidate sites. In: Shephard LE (ed) *Subseabed Disposal Program Annual Report: Site Assessment*. Sandia National Laboratories pp 113-140

Lener A, McCave IN (1983) Eolian components in Cretaceous and Tertiary North Atlantic sediments. *Journal Sedimentary Petrology* 53(3):811-832

Lenotre N, Chamley H, Hoffert M (1985) Clay stratigraphy at Deep Sea Drilling Project Sites 576 and 578, Leg 86 (Western North Pacific). In: Heath GR, Burckle LH and others. *Initial Reports of the Deep Sea Drilling Project*, US Government Printing Office, Washington, DC 86:571-579

Leonards GA, Ramich BK (1959) Time effects in the consolidation of clays, papers on soils. 1959 Meeting American Society Testing Materials 254:116-130

Leonards GA, Altschaeffl AG (1964) Compressibility of clay. *Journal Soil Mechanics Foundation Division, American Society Civil Engineers Proceedings Paper* 4049 90(SM5):133-135

Lerman A (1979) *Geochemical processes—water and sediment environments*. Wiley Interscience, New York, 481 pp

Lowe III, J (1974) New concepts in consolidation and settlement analysis. *Journal Geotechnical Engineering Division, American Society Civil Engineers Proceedings Paper* 10623, 100(GT6):574-612

Lyle M (1979) The Formation and Growth of Ferromanganese Oxides on Nazca Plate. Dissertation for Ph.D., Oregon State University, Corvallis, Oregon, 172 pp

Means RE, Parcher JV (1963) *Physical Properties of Soils*. Merrill CE, Columbus, 362 pp

Mehmel M (1939) Application of X-ray methods to the investigation of recent sediments. In: Trask (ed) *Recent Marine Sediments*, pp 616-630

Mitchell JK, Houston WN (1969) Causes of clay sensitivity. *Journal Soil Mechanics and Foundation Division Proceedings American Society Civil Engineers* 95:845-871

Mitchell JK, Singh A, Campanella RG (1969) Bonding, effective stresses, and strength of soils. *Journal Soil Mechanics and Foundation Division Proceedings, American Society Civil Engineers* 95:1219-1246

Mitchell JK, Singh A, Campanella RG (1971) Bonding, effective stresses, and strength of soils. *Journal Soil Mechanics and Foundation Division Proceedings, American Society Civil Engineers* 97:478

Murray J, Renard AF (1891) Report on deep-sea deposits based on the specimens collected during the voyage of HMS Challenger in the years 1872 to 1876. In: *Rep. Voyage "Challenger,"* Longmans, London, 525 pp

O'Brien NR (1971) Fabric of kaolinite and illite floccules. *Clays and Clay Minerals* 19:353-359

Olsen H and others (1986) Piston core properties and disturbance effect. *Journal Geotechnical Engineering, American Society Civil Engineering* 112(6):608-625

Olson RE, Mesri G (1970) Mechanisms controlling compressibility of clays. *Journal Soil Mechanics and Foundation Division, Proceedings American Society Civil Engineers* 96:1863-1878

Perry Jr. EA, Hower J (1970) Burial diagenesis of Gulf Coast pelitic sediments. *Clays and Clay Minerals* 18:165-177

Perry Jr. EA, Hower J (1972) Late-stage dehydration in deeply buried pelitic sediments. *American Association Petroleum Geologists Bulletin* 56:2013-2021

Prospero JM (1981) Eolian transport to the world ocean. In: Emiliani C (ed) *The Oceanic Lithosphere*. John Wiley and Sons, New York, pp 801-874

Pusch R (1966) Quick clay microstructure. *Engineering Geology* 1:433-443

Pusch R (1967) A technique for investigation of clay microstructure. *Journal Microscopic Paris* 6:966-986

Pusch R (1968) A technique for investigation of clay microstructure. *Swedish Geotechnical Inst. Proc. Special Report*, Stockholm (24)963-986

Rateev MA, Gorbunova ZN, Lisitzin AP, Nosov GL (1969) The distributing clay minerals in the oceans. *Journal Sedimentology* 13:31-43

Rea DK, Janecek TR (1982) Late Cenozoic changes in atmospheric circulation deduced from North Pacific eolian sediments. *Marine Geology* 49:149-167

Revelle R (1936) Marine bottom samples collected in the Pacific Ocean by the CARNEGIE on its 7th cruise. Dissertation for Ph.D University of California, 317 pp

Rey RW, Goldberg ED (1958) Quartz content of pelagic sediments of the Pacific Ocean. *Tellus* 10:153-159

Richards AF, Hamilton EL (1967) Investigations of deep-sea sediment cores. III. Consolidation. In: Richards A (ed) *Marine Geotechnique*, University of Illinois, Urbana, Illinois, pp 93-102

Reich V, Von Rad U (1979) Silica diagenesis in the Atlantic Ocean: diagenetic potential and transformation. In: Talwani M, Hay W, and Ryan WBF (eds) *Deep Drilling Results in the Atlantic Ocean: Continental Margins and Paleoenvironment*, Maurice Ewing Series 3. American Geophysical Union, Washington, DC, pp 315-340

Rosenqvist ITH (1959) Physico-chemical properties of soils: soil-water systems. *Journal Soil Mechanics and Foundation Division Proceedings American Society Civil Engineers* 85:31-53

Rosenqvist ITH (1962) The influence of physico-chemical factors upon the mechanical properties of clays. *Ninth National Conference on Clays and Clay Minerals* 9:12-27

Schmertmann JH (1955) The undisturbed consolidation behavior of soils. *Transactions American Society Division Engineering* 120:1201-1227

Schoonmaker J, Mackenzie FT, Manghnani M, Schneider RC, Kim D, Weiner A, To J (1985) Mineralogy and diagenesis: their effect on acoustic and electrical properties of pelagic clays. Deep Sea Drilling Project Leg 86. In: Heath GR, Burckle LH and others. *Initial Reports of the Deep Sea Drilling Project*, US Government Printing Office, Washington, DC 86:549-570

Shephard LE, Bryant WR (1980) Consolidation characteristics of Japan Trench sediments. In: Scientific Party. Initial Reports of the Deep Sea Drilling Project, US Government Printing Office, Washington, DC 56/57:1201–1205 Pt 2

Shephard LE, Bryant WR (1983) Geotechnical properties of lower trench slope sediments. *Journal Tectonophysics Special Issue on Convergence and Subduction*, pp 279–312

Shephard LE, Bryant WR, Chiou WA (1981) Geotechnical properties of Middle America Trench sediments. Deep Sea Drilling Project Leg 66. In: Watkins JS, Moore JC and others. Initial Reports of the Deep Sea Drilling Project, US Government Printing Office, Washington, DC 66:475–504

Singh S (1970) Bonding, effective stresses, and strengths of soils. *Journal Soil Mechanics and Foundation Division, Proceedings American Society Civil Engineers* 96:1469–1473

Skepton AW (1970) The consolidation of clays by gravitational compaction. *Quarterly Journal Geological Society, London* 125:373–411

Smart P (1967a) Soil structure, mechanical properties and electron microscopy. Ph.D Thesis University of Cambridge, 160 pp

Smart P (1967b) Particle arrangements in kaolin. *Fifteenth Conference on Clays and Clay Minerals* 15:241–254

Starakhow NM (1967) Principles of Lithogenesis. Oliver VI and Boyd, London, 246 pp

Sverdrup HV, Johnson MW, Fleming RH (1942) The Oceans. Prentice-Hall, Englewood Cliffs, NJ, 1087 pp

Taylor DW (1948) Fundamentals of Soil Mechanics. John Wiley and Sons, New York, 700 pp

Taylor E, Bryant WR (1985) Geotechnical properties of sediments from the Middle America Trench and Slope. In: von Huene R, Aubouin J and others. Initial Reports of the Deep Sea Drilling Project, US Government Printing Office, Washington, DC 84:745–766

Terzaghi K (1925) Principles of soil mechanics settlement and consolidation of clay. *Engineering News-Record*, pp 874–878

Terzaghi K (1956) Varieties of submarine slope failures. Eighth Proceeding Conference Soil Mechanics and Foundation Engineers, Texas, pp 1–41

Theissen DA (1942) Wechselsetige absorption von kolloiden. *Z. Electrochem* 48:675

Torrance KJ (1970) Causes of clay sensitivity. *Journal Soil Mechanics and Foundation Division Proceedings American Society Civil Engineers* 96:360–361

Trabant PK, Bryant WR, Bouma AH (1975) Consolidation characteristics of sediments from Leg 31 of the Deep Sea Drilling Project. In: Karig DE, Ingle Jr. JC and others. Initial Reports of the Deep Sea Drilling Project, US Government Printing Office, Washington, DC 31:569–572

Updike RG, Oscarson RL (1986) An atlas of the facies—micro fabrics of the Bootlegger Cove Formation using the Scanning Electron Microscope. US Geological Survey Open File Report 87–60, 18 pp

von Olphen H (1963) An Introduction to Clay Colloid Chemistry. Interscience Publishers, John Wiley and Sons, New York, 1

von Rad U, Riech V, Rosch H (1978) Silica diagenesis in continental margin sediments off northwest Africa. In: Lancelot Y, Serbold E and others. Initial Report of the Deep Sea Drilling Project, US Government Printing Office, Washington, DC 41:000–000

Walker GR (1981) Geotechnical Properties of deep sea sediments in the Northwestern Pacific Ocean. MS thesis, University Rhode Island, Providence

Warner DL (1964) An analysis of the influence of the physical-chemical factors upon the consolidation of fine-grained clastic sediments. Dissertation for Ph.D., University of California, Berkeley

Welton JE (1984) SEM Petrology Atlas American Association Petroleum Geologists, 184 pp. American Association Petroleum Geologists Methods in Exploration Series No. 4, 237 pp

Windom HL (1969) Atmospheric dust records in permanent snow fields: implications to marine sedimentation. *Geological Society America Bulletin* 80:761–782

Windom DL (1976) Lithogenous material in marine sediments. In: Riley JP, Chester J (eds) *Chemical Oceanography* 2nd edition, Academic Press, London 5:105–135

Winterkorn HF (1948) Physico-chemical properties of soils. *Proceedings 2nd International Conference Soil Mechanics Foundation Engineering*, Rotterdam pp 23–29

Yaalon DH (1962) Mineral composition of the average shale. *Clay Minerals Bulletin* 5:31–36

Yariv S, Cruss H (1979) *Geochemistry of colloid systems*. Springer-Verlag, Berlin, 450 pp

Znidarcic D, Schiffman RL (1983) Constant rate of deformation consolidation testing. Technical Report, Department Civil Engineering, University CO, Boulder, 280 pp

Manuscript received 12 January 1988; revision received 16 August 1988.

Geo-Marine Letters

An International Journal of Marine Geology

CONTENTS VOLUME 8 1988

Editor-in-Chief

Arnold H. Bouma

Department of Geology and Geophysics, Louisiana State University, Baton Rouge, Louisiana 70803-4101, USA

Editorial Board

Neal E. Barnes

Missouri City, Texas, USA

David A. Cacchione

U.S. Geological Survey, Menlo Park, California, USA

Robert M. Carter

James Cook University of North Queensland, Townsville, Australia

James M. Coleman

Louisiana State University, Baton Rouge, Louisiana, USA

Joseph R. Curran

Scripps Institution of Oceanography, La Jolla, California, USA

Alberto G. de Figueiredo

Lab. Geologia Marinha, Universidade Federal Fluminense, Niteroi, Brazil

Larry J. Doyle

University of South Florida, St. Petersburg, Florida, USA

Robert W. Embley

OSU Hatfield Marine Science Center, Newport, Oregon, USA

Burg W. Flemming

Institut für Meeresgeologie und Meeresbiologie, Wilhelmshaven, West Germany

Helios S. Glibidenko

Sakhalin Complex Scientific Research Institute, Yuzhno-Sakhalinsk, Sakhalin, USSR

Gary H. Greene

U.S. Geological Survey, Menlo Park, California, USA

Liu Guang-Ding

National Ocean Bureau, Beijing, People's Republic of China

Anthony D. Heathershaw

Admiralty Research Establishment, Dorset, UK

Hans-Rudi Katz

Lower Hutt, New Zealand

Keith A. Kvenvolden

U.S. Geological Survey, Menlo Park, California, USA

Andrés Maldonado

Instituto de Ciencias del Mar C.S.I.C., Barcelona, Spain

Yossi Mart

National Oceanographic Institute, Haifa, Israel

S. Dijn Nio

Comparative Sedimentology Division, State University of Utrecht, Utrecht, The Netherlands

Harold D. Palmer

MRJ, Inc., Oakton, Virginia, USA

David J. W. Piper

Bedford Institute of Oceanography, Dartmouth, Nova Scotia, Canada

David B. Prior

Louisiana State University, Baton Rouge, Louisiana, USA

Richard Rezak

Texas A & M University, College Station, Texas, USA

Nahum Schneidermann

Chevron Overseas Petroleum, Inc., San Ramon, California, USA

Roger M. Slatt

Arco Oil and Gas Co., Plano, Texas, USA

Daniel J. Stanley

Smithsonian Institution, Washington, D.C., USA

Donald L. Tiffin

Vancouver, British Columbia, Canada

Friedrich Werner

Geologisch-Palaeontologisches Institut, Universität Kiel, Kiel, West Germany

L. Donelson Wright

Virginia Institute of Marine Science, Gloucester Point, Virginia, USA



Springer International

The exclusive copyright for all languages and countries, including the right for photomechanical and any other reproductions, also in microform, is transferred to the publisher.

The use of registered names, trademarks, etc. in this publication does not imply, even in the absence of a specific statement, that such names are exempt from the relevant protective laws and regulations and therefore free for general use.

Printed in the United States of America
© 1988 by Springer-Verlag New York Inc.

CONTENTS—VOLUME 8

Number 1 1988

W. C. Schwab, H. J. Lee, R. E. Kayen, P. J. Quintero, G. B. Tate	
Erosion and Slope Instability on Horizon Guyot, Mid-Pacific Mountains	1
D. A. Cacchione, W. C. Schwab, M. Noble, G. Tate	
Internal Tides and Sediment Movement on Horizon Guyot, Mid-Pacific Mountains	11
A. Cramp, M. Collins	
A Late Pleistocene-Holocene Sapropelic Layer in the Northwest Aegean Sea, Eastern Mediterranean	19
F. E. Groussset, J. L. Joron, P. E. Biscaye, C. Latouche, M. Treuil, N. Maillet, J. C. Faugères, E. Gonthier	
Mediterranean Outflow through the Strait of Gibraltar since 18,000 Years B.P.: Mineralogical and Geochemical Arguments	25
J. Hardisty	
Measurement of Shallow Water Wave Direction for Longshore Sediment Transport	35
P. Quevauviller	
Equilibrium Conditions for Curved Shape Bays with Application to an Ancient Coast	41
A. Molina-Cruz, A. Ayala-López	
Influence of the Hydrothermal Vents on the Distribution of Benthic Foraminifera from the Guaymas Basin, Mexico	49
R. A. Kostaschuk, G. M. MacDonald	
Multitrack Surveying of Large Bedforms	57

Number 2 1988

Special Issue: Sedimentary Development of the Louisiana Continental Shelf Related to Sea Level Cycles

J. M. Coleman, H. H. Roberts	
Part I—Sedimentary Sequences	63
J. M. Coleman, H. H. Roberts	
Part II—Seismic Response	109

(Volume Contents continued on next page)

CONTENTS—VOLUME 8 (continued)

Number 3 1988

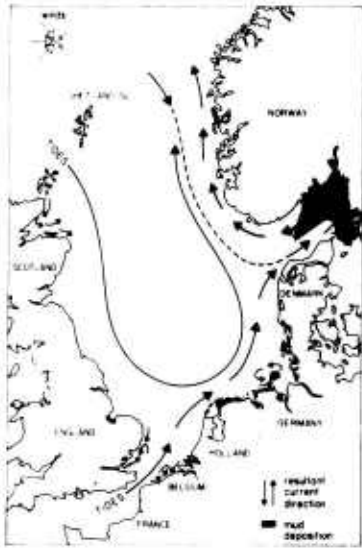
H. G. Greene, N. F. Exon	
Acoustic Stratigraphy and Hydrothermal Activity within Epi Submarine Caldera, Vanuatu, New Hebrides Arc	121
E. Uchupi, W. C. Schwab, R. D. Ballard, J. L. Cheminee, J. Francheteau, R. Hekinian, D. K. Blackman, H. Sigurdsson	
An Angus/Argo Study of the Neovolcanic Zone along the East Pacific Rise from the Clipperton Fracture Zone to 12°N	131
J. B. Colwell, N. F. Exon	
Quaternary Hemipelagic Sedimentation in the Basins Flanking the Solomon Islands Volcanic Arc	139
F. Trincardi, W. R. Normark	
Sediment Waves on the Tiber Prodelta Slope: Interaction of Deltaic Sedimentation and Currents along the Shelf	149
S. J. Culver, C. A. Brunner, C. A. Nittrouer	
Observations of a Fast Burst of the Deep Western Boundary Undercurrent and Sediment Transport in South Wilmington Canyon from DSRV <i>Alvin</i>	159
S. Reynolds, D. S. Gorsline	
Some Enigmatic Depressions of the Arguello Slope, California	167
V. Kodagali	
Influence of Regional and Local Topography on the Distribution of Polymetallic Nodules in Central Indian Ocean Basin	173
K. A. Kvenvolden	
Hydrocarbon Gas in Sediment of the Southern Pacific Ocean	179

Number 4 1988

Special Issue: Origin, Physical, and Mineralogical Nature of Red Clays: The Pacific Ocean Basin as a Model	
Instructions to Authors	vi
W. R. Bryant, R. H. Bennett	
Origin, Physical, and Mineralogical Nature of Red Clays: The Pacific Ocean Basin as a Model	189
Volume Contents	

Environmental Sciences

W. Salomons, B. L. Bayne, E. K. Duursma, U. Förstner (Eds.)



Pollution of the North Sea

An Assessment

1988. 237 figures. Approx. 600 pages. Hard cover DM 198,-. ISBN 3-540-19288-3

Contents: The North Sea System: Physics, Chemistry, Biology: The Hydrography and Hydrographic Balances of the North Sea. Suspended Matter and Sediment Transport. Geobiological Effects on the Mobility of Contaminants in Marine Sediments. The Nature and Functioning of Salt Marshes, Estuaries, Fjords. The Water-Air Interface. The Ecosystem. Fishery Resources. Natural Events. – Input and Behavior of Pollutants: The Scheldt Estuary. The Rhine-Meuse Estuary. The Estuaries of the Humber and Thames. The Estuaries of the Ems, Weser and Elbe. Dredged Materials. Sewage Sludge Disposal in the North Sea. Waste Incineration. Inputs from the Atmosphere. Occurrence and Fate of Organic Micropollutants in the North Sea. Occurrence and Fate of Heavy Metals in the North Sea. North Sea Nutrients and Eutrophication. – Impacts on Selected Areas and by Human Activities: The German Bight. Impact of Pollution on the Wadden Sea. The Impact of Anthropogenic Activities on the Coastal Wetlands of the North Sea. Fjords. Impact of Sewage Sludge. Impact of Contaminants Mobilized from Sediments upon Disposal. Oil Exploration and Production and Oil Spills. Fishery Effects. Ecological Impacts During the Completion of the Eastern Scheldt Project. – Biological Impacts and Monitoring: Accumulation (of Contaminants) by Fish. Accumulation by Birds. Accumulation and Body Distribution of Xenobiotics in Marine Mammals. Effects on Invertebrates. Effects of Pollutants on Fish. Ecotoxicology: Biological Effects Measurements on Molluscs and Their Use in Impact Assessment. Mesocosms. The Role of Biological Monitoring. Model-Monitoring Relationships.

W. Salomons, Institute of Soil Fertility, Haren, The Netherlands; U. Förstner, TU of Hamburg-Harburg, Fed. Republic of Germany (Eds.)

Chemistry and Biology of Solid Waste

Dredged Material and Mine Tailings

1988. 83 figures, 59 tables. X, 305 pages. Hard cover DM 139,-. ISBN 3-540-18231-4

Environmental Management of Solid Waste

Dredged Material and Mine Tailings

1988. 118 figures. X, 396 pages. Hard cover DM 168,-. ISBN 3-540-18232-2

Dredged Material and Mine Tailings are two of the same thing once they are deposited on land: they must be safeguarded, wash-out must be prevented, and they must be protected by a plant cover. This comprehensive treatise covers both important aspects of their management: In **Chemistry and Biology of Solid Waste** the principles and assessment are scientifically studied and discussed, while **Environmental Management of Solid Waste** turns to the practical applications, such as prediction, restoration and management. Previously, dredged material was a commodity, it could be sold as soil, e.g. to gardeners. In the meantime, dredged material from the North Sea (e.g. the Rotterdam or Amsterdam harbor) must be treated as hazardous waste. Many environmentalists, managers and companies do not know how to solve the inherent problems. This new work deals with the chemical, physical and biological principles; the biological and geochemical assessment; the prediction of effects and treatment; and finally, with the restoration and revegetation. It is written by many leading scientists in the various fields, and will prove invaluable for scientists, managers and politicians who are concerned with the present environmental situation.

U. Seeliger, L. D. de Lacerda,
S. R. Patchineelam (Eds.)

Metals in Coastal Environments of Latin America

1988. 106 figures. XV, 297 pages.
Hard cover DM 84,-.
ISBN 3-540-16945-8

For the first time a state-of-the-art of present metal pollution along the coastline of Latin America is provided. This collection of papers from a conference held in August 1986 in Rio de Janeiro, Brazil, is designed to inform readers of recent advances in an important, interdisciplinary field. Primary focus is on: – Metal Surveys – Metals in Sediments – Metals in Biota – Metal Transport and Cycles – Metal Monitoring.

This book fills a long-standing gap in the literature and will be of prime interest to researchers, students and professionals in geology, biology and chemistry.

Springer-Verlag Berlin Heidelberg New York London Paris Tokyo Hong Kong

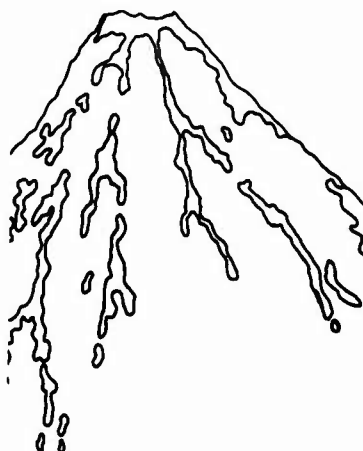
Heidelberger Platz 3, D-1000 Berlin 33 · 175 Fifth Ave., New York, NY 10010, USA · 28, Lurke Street, Bedford MK40 3HU, England ·
26, rue des Carmes, F-75005 Paris · 37-3, Hongo 3-chome, Bunkyo-ku, Tokyo 113, Japan · Citicorp Centre, Room 1603,
18 Whitfield Road, Causeway Bay, Hong Kong

tm.87164/1

Springer



Announcing a New Series



IAVCEI Proceedings in Volcanology

This new proceedings series of the International Association of Volcanology and Chemistry of the Earth's Interior (IAVCEI) reflects the vigorous growth of volcanological research in recent years and an increasing tendency for this new work to be presented at specialist symposia and conferences. Publication of the proceedings of these meetings as special issues of the bimonthly *Bulletin of Volcanology* (formerly *Bulletin Volcanologique*) is not possible if the newly reorganized Bulletin is to maintain its record of rapid publication. Thus IAVCEI Proceedings in Volcanology was conceived as a companion series devoted to timely publication of new research on a single theme of current interest. In contrast to the Bulletin, volumes will be separate entities and will be published at irregular intervals depending on demand. The Proceedings will cover the same range of volcanological, geochemical, and geophysical topics dealt with by the Bulletin. IAVCEI News, SEAN information on current volcanic eruptions, and the Bulletin of Volcanic Eruption will continue to appear in the *Bulletin of Volcanology*.

The aim is to maintain a high standard for the Proceedings by choosing only those topics likely to have a wide international appeal and by maintaining strict reviewing procedures in collaboration with convenors of high scientific standing. Convenors will be identified clearly as the editors of particular volumes.

Subscribers to *Bulletin of Volcanology* are offered a 20% discount on all volumes in this NEW series!

Volume 1

J. H. Latter, Geophysics Division, Wellington, New Zealand (Ed.)

Volcanic Hazards: Assessment and Monitoring

1988. 273 figures. Approx. 630 pages. Hard cover in preparation.

ISBN 19337-5

Volcanic Hazards are of great contemporary environmental concern. This book consists of two parts, the first dealing mainly with Hazard Assessment, and the second mostly with Monitoring. Special attention is devoted to the question of how surveillance of both active and inactive volcanoes can be carried out in different parts of the world.

Contents: Hazards Assessment: Volcanic Winter? Climatic Effects of the Largest Volcanic Eruptions. - Prediction of Volcanic Hazards on the Basis of the Study of Dynamics of Volcanic Activity, Kamchatka. - Study Models for Volcanic Hazards in the Lesser Antilles. - The Evolution of La Grande Découverte (La Soufrière) Volcano, Guadeloupe (F. W. I.). - Volcan Popocatépetl: Recent Eruptive History, and Potential Hazards and Risks in Future Eruptions. - Use of Computer-Generated Movies to Present Volcanic Hazards. - Mt. Etna (Sicily): Volcanic Hazard Assessment. - The 1982-83 Eruption of Galunggung (Indonesia): A Case Study of Volcanic Hazards with Particular Relevance to Air Navigation. - Some Notes on False Alarms of Volcanic Activity, and Mud Flows. - Explosive Volcanic Activity Generated from Within Advancing Silicic Lava Flows. - The May 1915 Eruptions of Lassen Peak, California: Characteristics of Events Occurring on May 19. - Discrimination Between Debris Avalanches and Other Volcanic Deposits. - The 1984 Collapse and Debris Avalanche Deposits of Ontake Volcano, Central Japan. - Monitoring: General. - Thermal Infrared. - Chemical. - Gravity. - Seismic. - Infrasonic. - Triangulation and Tilt. - Subject Index.

Springer-Verlag
Berlin Heidelberg New York London
Paris Tokyo Hong Kong
Heidelberger Platz 3, D-1000 Berlin 33 · 175 Fifth
Ave., New York, NY 10010, USA
28, Luton Street, Bedford MK40 3HU, England
26 rue des Carmes, F-75005 Paris
37-3, Hongo 3-chome, Bunkyo-ku, Tokyo 113, Japan
Citicorp Centre, Room 1603, 18 Whitfield Road,
Causeway Bay, Hong Kong

ISSN 0008-3602

Springer

